# GENOME-WIDE GENE EXPRESSION PROFILING OF THE ANGELMAN SYNDROME MOUSE WITH *UBE3A* MUTATION: FROM GENOTYPE TO PHENOTYPE

**LOW JUAN HSUEN DAREN**

School of Biological Sciences

A thesis submitted to the Nanyang Technological University in partial fulfillment of the requirement for the degree of Doctor of Philosophy

2012

# Acknowledgment

I am heartily thankful to my supervisor Associate Professor Ken-Shiung Chen from School of Biological Sciences, Nanyang Technological University, whose encouragement, scientific guidance and support enabled me to develop an understanding of the subject.

I would wish to thank my fellow colleagues for their inspiration and assistance from the initial to the final level. The unity of the lab had made working pleasurable. In particular, Madam Xin Lixia had provided premium assistance in the mouse work described in this project.

I am grateful towards the involvement of my Thesis Advisory Committee (TAC) and Head of Department in this project including Associate Professor Peter Dröge, Assistant Professor I-Hsin Su, Associate Professor Zhiwei Feng and Assistant Professor Jiming Li. Their unobligated advice is invaluable.

Lastly, I am indebted to the Nanyang Technological University, School of Biological Sciences, for this PhD candidature opportunity and for the research scholarship award.

# Table of Content

# List of Tables:

# List of Figures:

# Abbreviations

| | |
|---|---|
| α-MSH | Alpha-Melanocyte Stimulating Hormone |
| ANOVA | Analysis of variance |
| AS | Angelman syndrome |
| AS-IC | Angelman syndrome imprinting centre |
| ATS | Antisense transcript |
| bp | Base pairs |
| BP | Breakpoint |
| C-terminal | carboxyl-terminus |
| °C | Degree Celsius |
| cAMP | Cyclic adenosine monophosphate |
| cDNA | Complementary DNA |
| ChIP | Chromatin immunoprecipitation |
| CMV | Cytomegalovirus |
| $C_T$ | Cycle threshold |
| DNA | Deoxyribonucleic acid |
| Drd2 | Dopamine receptor D2 |
| DTT | Dithiothreitol |
| EDTA | Ethylenediaminetetraacetic acid |
| EEG | Electroencephalogram |
| Epha6 | Ephrin type-A receptor 6 |
| Fgf7 | Fibroblast growth factor 7 |
| Gabra5 | Gamma-aminobutyric acid (GABA) A receptor, alpha 5 |
| Glra1 | Glycine receptor, alpha 1 |
| HBS | HEPES-buffered saline solution |
| HECT | homologous to the E6-AP carboxyl terminus |
| HERC2 | HECT domain and RCC1-like domain-containing protein 2 |
| HSP70 | Heat Shock Protein 70 |
| HPV | Human papillomavirus |
| HRP | Horseradish peroxidase |
| IACUC | Institutional animal care and use committee |
| IC | Imprinting centre |
| iPSC | Induced pluripotent stem cell |
| kDa | Kilo Dalton |
| kb | Kilo bases |
| Mc1r | Melanocortin-1 receptor |
| MIM | Mendelian inheritance in man |
| MITF | Microphthalmia-associated transcription factor |
| mRNA | Messenger RNA |
| N-terminal | amino-terminus |

| | |
|---|---|
| Nr4a2 | nuclear receptor subfamily 4, group A, member 2 |
| OCA2 | oculocutaneous albinism II |
| PBS | Phosphate buffered saline |
| PCR | Polymerase chain reaction |
| qRT-PCR | Quantitative reverse transcription real time PCR |
| RMA | Robust Multichip Average |
| RNA | Ribonucleic acid |
| RNAi | RNA interference |
| RT-PCR | Reverse transcription PCR |
| SDS-PAGE | Sodium dodecyl sulfate polyacrylamide gel electrophoresis |
| shRNA | Small hairpin RNA |
| Slc5a7 | Solute carrier family 5 (choline transporter), member 7 |
| SP1 | Sp1 transcription factor |
| TE | Tris EDTA |
| TBST | Tris Buffered Saline Tween-20 |
| UBE3A | Ubiquitin protein ligase E3A |
| $UBE3A^{(m-/p+)}$ | Maternal inherited knockout of UBE3A |
| UPD | Uniparental disomy |
| UPS | Ubiquitin-proteasome system |
| UV | Ultra violet |

## Summary

***Background:*** Angelman syndrome (AS) is an inheritable neurodevelopmental disorder resulting from the loss of function of the ubiquitin E3A ligase (UBE3A). Clinical features of the disorder include severe mental retardation, motor incoordination and perpetual happy disposition. Associated features of AS include hypopigmentation and seizures. Despite many targets and interacting partners of UBE3A being identified, the detailed pathogenesis of the disorder, as well as how the lack of functional UBE3A upsets cellular homeostasis, remains vague.

**The aim of this project is to characterize the gene expression profile of the AS mouse model by performing a genome-wide microarray screening to identify differentially expressed genes and to unravel potential genotype-phenotype correlationship mechanisms.**

***Results:*** Sixty-four differentially expressed genes (7 up-regulated and 57 down-regulated) in the AS mouse cerebellum were identified, which subsequent pathway analysis showed their involvement in 3 major networks including cell signaling, nervous system development and cell death. Representative genes (*Fgf7*, *Glra1*, *Mc1r*, *Nr4a2*, *Slc5a7*, *Epha6*) from each network were selected based on their functional relevance to AS and validated for their differential expression using

qRT-PCR. The validation was extended towards the protein level using Western blot for Nr4a2 and Mc1r. Both showed reduction in their respective protein level in the mutant AS mouse. To confirm that the effects of Ube3a on *Mc1r* and *Nr4a2* are a direct consequence of lack of Ube3a expression, an *Ube3a* shRNA knockdown system was created in the P19 cell line, and lower *Mc1r* and *Nr4a2* expression was observed in the *Ube3a* knockdown cells. Conversely Ube3a overexpression in the P19 cell results in an increase in the *Mc1r* and *Nr4a2* mRNA levels. To determine the mechanism by which Ube3a can affect the cellular level of *Mc1r*, we hypothesized that Ube3a is associated with the regulation of the *Mc1r* promoter. To test this hypothesis, a *MC1R* promoter luciferase-reporter plasmid was constructed and subsequently used to demonstrate that UBE3A is able to induce *MC1R* promoter activity in a dosage dependent manner. Impaired ubiquitin ligase function in UBE3A did not have a dramatic effect on this transactivation. Using the chromatin immunoprecipitation assay, UBE3A was shown to be physically bound to the *MC1R* minimal promoter, a region that is highly homologous between the human and mouse. This region contains a conserved E box element and an adjacent human SP1 site. Deletion of this E box/SP1 site along the *MC1R* minimal promoter abolished the effect of UBE3A on the promoter activity. Since MC1R is widely studied for its role in the upstream regulation of pigment production and is down-regulated in the AS mice, the AS mice was subsequently checked for the putative pigmentation dysregulation. The dorsal skin of the AS mice appeared fairer when

compared to their wildtype littermates. This difference in hypopigmentation is more apparent in the footpad, where the pigments are less dense and sparse; their wildtype littermates had concentrated pigments that are more intense. Immunohistology staining revealed that Mc1r is normally expressed between the epidermis and dermis region, predominately around the hair follicles. This expression was dramatically decreased in the *Ube3a*$^{(-/-)}$ mice.

***Conclusion:*** Understanding the unique transcriptome profile of the AS mouse is important to understand the pathogenesis of the disorder, such as in the case of hypopigmentation. These molecular data can also provide certain relief towards the current controversy of the mechanism causing the hypopigmentation trait in AS patients. Altogether the results gathered in this report will contribute to the repertoire of knowledge known about Angelman syndrome, by revealing genes affected in the absence of functional Ube3a and provide candidates genes for future genotype-phenotype correlation study.

# Chapter I: Introduction

**1.1: Angelman syndrome**

**1.2: Genetics of Angelman syndrome**

**1.3: Epigenetic regulation of Angelman syndrome**

**1.4: *UBE3A*: The Angelman syndrome causative gene**

**1.5: UBE3A in the brain**

**1.6: Hypopigmentation in Angelman syndrome**

Understanding biological processes has been the ultimate aim of many researches in molecular biology. The complexity of these processes makes it discernible that the malfunction in any of its component can upset cellular homeostasis, which may potentially lead to the onset of diseases. This is even more apparent for heritable disorders, such as the Angelman syndrome (AS; MIM: 105830). In this report, we characterize the cellular transcriptome of the AS mouse model in the genome-wide level, and investigate the molecular basis for the manifestation of some of the AS phenotype.

AS is an example of a human genetic disorder directly involved in the ubiquitin-dependent proteolytic pathway. The causative gene is an ubiquitin E3 ligase (*UBE3A*), which is part of the ubiquitin proteasome system (UPS) (1,2). Lying along the human chromosome 15q11-13, *UBE3A* is often found to be deleted or mutated in AS patients and hence affecting the regulation of protein degradation via UPS. Since UPS is closely implicated in many neuro-diseases such as Alzhimer's disease, Parkinson's disease and AS, the study of *UBE3A* and AS will not only unravel the cellular and global function of UBE3A, but also how perturbation of the UPS can cause the onset of various diseases (3). In addition, AS represents the first case of a genetic disorder caused by the distinct imprinted expression of a gene product, i.e. *UBE3A* (4). *UBE3A* is found to be imprinted in the human and mouse brain, such that only the maternally inherited allele is

expressed whereas the paternally inherited allele is silent (4). This sort of imprinting effect is mediated by epigenetic modification such as histone modifications including DNA methylation and RNA interference (e.g. non-coding RNAs) (5,6). Finally, scientific research on AS can contribute towards the treatment or better management for the patients.

## 1.1: Angelman Syndrome

AS is a neuro-genetic disorder affecting 1 in 10,000-20,000 in the United States/Europe, and 1 in 40,000 newborns in Western Australia (7-9). Consistent characteristics among AS patients include mental retardation, developmental delay, lack of speech, and walking/balance disorders (10). Most patients also exhibit seizures, as well as other associated features (20%-80%), such as hypopigmentation, when compared to their family (11-13). Clinical diagnosis is based on a set of consensus physical and behavioral features drawn up over the years, though all of the features need not be present for the diagnosis to be made (Table 1) (10). Preliminary diagnosis is often made when the typical behaviors are recognized. AS usually goes undetected during birth and infancy since the developmental features are not obvious at these stages. The most common age that AS diagnosed is when the child is between two and five years of age, when the features are most evident. Generally, acquiring AS is not life threatening, however individuals with AS require life-long care.

AS primarily affects brain functions that results in many neurophysiological features. First discovered in 1965 by a pediatrician, Dr Harry Angelman, who described the normal skull structure in AS patients using X-ray but suggested

cortical-subcortical atrophy (14). With the development of technology, electroencephalogram (EEG) was gradually employed to diagnose AS in infants, children and adults (15-19). Electrophysiological testing on the AS cerebellum revealed abnormal recordings that show three distinctive high-amplitude rhythmic patterns (20). Magnetic resonance imaging (MRI) shows white matter changes and suggested dysmyelination or demyelination (21). The dysfunction in the AS brain can be reflected in the patients' phenotypes, including seizures that last throughout life, movement incoordination and mental retardation (10). These phenotypes are recapitulated in the AS mouse models. AS mice have a small cerebellum and showed long term potentiation impairment with abnormal dendritic spine morphology and number (See Section 1.4) (22). Other than the neurological pathogenesis, there are other non-neuronal features frequently observed in AS such as hypopigmentation (See Section 1.7) (23).

Besides general medical relief for its epileptic seizures, there are currently no therapeutic treatments for AS. The latest therapeutic trial involved introducing betanine and folic acid as a form of dietary supplementation to patients (n=48), aiming to promote a global increase in DNA methylation that may reduce the expression of the UBE3A antisense RNA, a negative regulator of the AS causative UBE3A gene, thereby increasing UBE3A expression on the paternal allele. However there were no statistically significant improvements between the treated

and untreated AS patient (24). In a separate trial, AS mice were introduced to levodopa-carbidopa. Levodopa is a dopamine precursor that will be converted to dopamine in the brain, and has been a common treatment in managing Parkinson's disease. Mice treated with levodopa-carbidopa show improvement in their motor function and behavioral tests (25). Pharmacological interventions in controlling mood and sleeping disorder in AS have been only partially effective (26). Other gene therapy plans include strategies to "superactivate" UBE3A and/or repress the silencing mechanisms of UBE3A (25).

**Table 1: Consensus Clinical Features of Angelman Syndrome**

| Feature Frequency | Diagnostic Criteria |
|---|---|
| **Consistent Feature (100%)** | • Developmental delay<br>• Movement or balance disorder, usually ataxia of gait, and/or tremulous movement of limbs. Movement disorder can be mild. May not appear as frank ataxia but can be forward lurching, unsteadiness, clumsiness, or quick, jerky motions<br>• Behavioral uniqueness: any combination of frequent laughter/smiling; apparent happy demeanor; easily excitable personality, often with uplifted hand-flapping, or waving movements; hypermotoric behavior<br>• Speech impairment |
| **Frequent Feature ( ≥80%)** | • Delayed, disproportionate growth in head circumference, usually resulting in microcephaly by age 2 years.<br>• Seizures, onset usually <3 years of age. Seizure severity usually decreases with age but the seizure disorder lasts throughout adulthood<br>• Abnormal EEG, with a characteristic pattern The EEG abnormalities can occur in the first 2 years of life and can precede clinical features, and are often not correlated to clinical seizure events |
| **Associated Feature (20%-80%)** | • Cranial facial abnormalities (e.g. flat occiput, occipital groove, prognathia, wide mouth, wide-spaced teeth)<br>• Protruding and thrusting tongue; suck/swallowing disorders<br>• Feeding problems and/or truncal hypotonia during infancy<br>• Frequent drooling<br>• Excessive chewing/mouthing behaviors<br>• Strabismus<br>• Hypopigmentation (when compared to family members)<br>• Hyperreflexia<br>• Increased sensitivity to heat<br>• Abnormal sleep-wake cycles<br>• Abnormal food related behaviors<br>• Obesity (in the older child)<br>• Scoliosis<br>• Constipation |

Adapted and modified from Williams et al. 2006 [10]

## 1.2: Genetics of Angelman syndrome

AS patients develop the disorder through either one of the following five mechanisms (Figure 1):

Type I: large interstitial deletion of chromosome 15q11-q13

Type II: paternal uniparental disomy (UPD) of chromosome 15

Type III: imprinting defects (in particular along chromosome 15q)

Type IV: *UBE3A* mutation (an imprinted gene located along chromosome 15)

Type V: unknown mechanism(s)

Type I large interstitial deletion of chromosome 15 represents approximately 70% of the AS cohort. Many cytogenetics studies have mapped the region to the chromosome 15q11-q13 (2,27). Such deletion tends to happen at specific "hotspots" or breakpoint (BP) clusters in proximal 15q (28). These group of patients exhibit the most dramatic clinical phenotype, most likely due to the effects of multiple genes deletions (29). They show highest incidence of severe seizures (90%) and hypopigmentation (90%).

Approximately 2% of the AS cases results from paternal uniparental disomy (UPD), such that patients inherited both chromosome 15 from their father (Type II) (2,30).

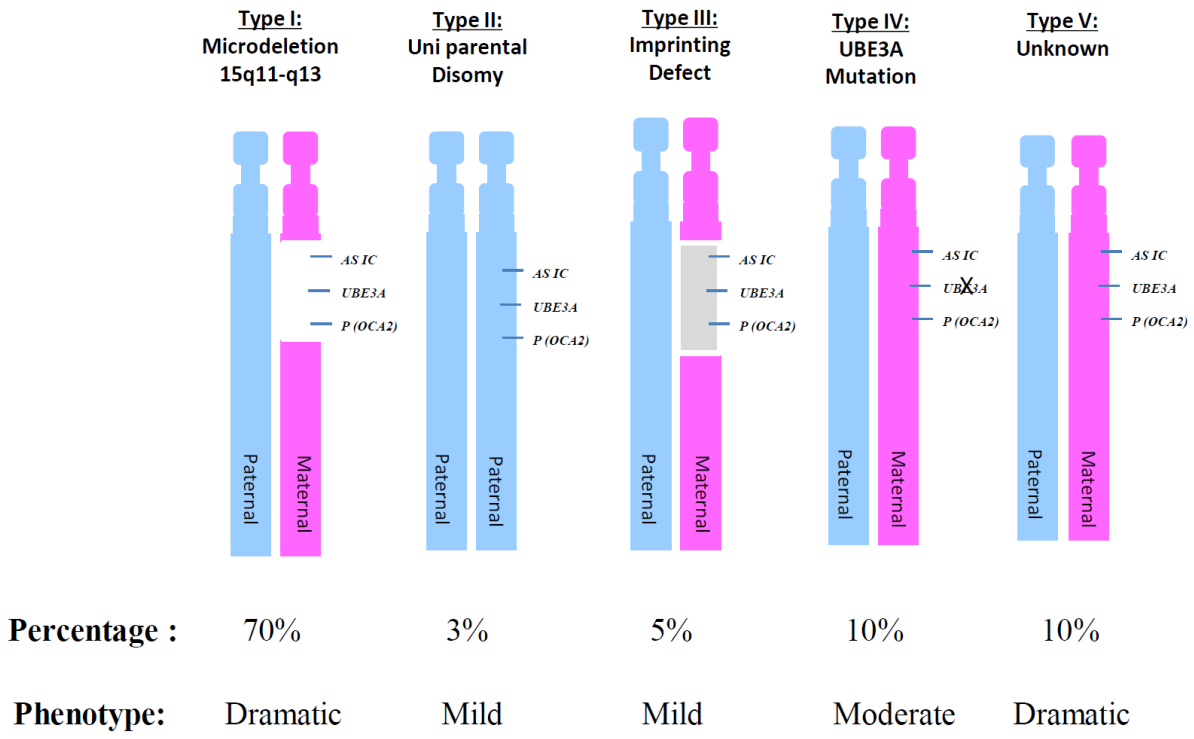


**Figure 1. The five AS pathogenic genotype**

The five AS pathogenic genotype observed in patients, including the large interstitial deletion of 15q11-q13 (type I); paternal uniparental disomy of chromosome 15 (type II); imprinting defect (type III); mutation in the E3 ubiquitin ligase, UBE3A (type IV); and unknown etiology (type V). All the above, except type V, involves the loss of functional UBE3A. All classical patients exhibit four cardinal feature including (1) severe developmental delay and/or mental retardation, (2) speech impairment, (3) movement/balance disorder and (4) easily excitable personality and unusual happy disposition that is unique to AS. The percentage from each genotype of the AS cohort is indicated including their respective relative degree of clinical manifestation.

The loss of maternal chromosome 15 results in the loss of gene expression from the maternal inherited allele. The phenotypes exhibited in this group are usually mild.

Type III imprinting defect patients form approximately 3% of the total AS cases (2,31). Imprinting in human chromosome 15q11-q13 is determined by a bipartite imprinting center located at the *SNURF-SNRPN* locus near the *UBE3A* gene (32,33). This imprinting center (IC) is now commonly known as AS-IC, which is responsible for the proper epigenetic chromatin modifications, including both DNA and histone methylation, for allele specific gene expression. The current proposed function of this AS-IC is suggested to control the switch from paternal to maternal imprint during oogenesis (34,35). Type III patients are less severely affected clinically and have indistinguishable phenotype as type II patients.

One can also acquire AS through a single gene mutation in *UBE3A*, representing 10% of the AS patient cohort (2). Over the years, mapping of the AS critical gene was considered difficult due to the rare reports of familial AS that provide a means for linkage analysis. This is probably due to the fact that AS patients do not often produce offspring. Subsequently, more reports have been progressively published identifying a spectrum of mutations in *UBE3A* from AS patients, in which most of them are sporadic (36,37). A majority of the mutations are nonsense mutations that cause premature termination during translation (29). The site of the mutation is

often located towards the C-terminal of UBE3A and less frequently towards the N terminal (29,36-38). This group of patients have a phenotype severity that falls between those of type I and type II/III.

The last group of AS patients (Type V) has unknown aetiology, which leads to much speculation on the causative mechanism. This includes mutation of *UBE3A* in the non-coding regions, or that *UBE3A* is inactivated through an alternative method. It was also suggested that malfunction in other genes working in the similar ubiquitin pathway can also cause AS, or mutation in genes other than *UBE3A* along chr15q11-q13 is responsible.

The phenotypic profiles of AS are often variable even within the same type (29,39-43). However, type I patients show the most dramatic manifestation, probably due to the multiple genes deleted along 15q11-q13 (29). Type I AS patients a have high incidence of severe early onset seizures, microcephaly and hypopigmentation, along with the classic features of AS including motor disability (29). Patients with *UBE3A* mutations show a moderate degree of the classic phenotype, with occasional occurrence of features like hypopigmentation (29,44). On the other hand, patients with UPD (Type II) or imprinting defects (Type III) showed the mildest degree of severity, most likely due to occasional incomplete penetrance (29,39).

The genetic clinical diagnosis of AS is a complex multistep process (Figure 2). When a patient is suspected of AS, blood sample from the patient will first be sent for DNA methylation analysis. A normal DNA methylation profile will suggest that the patient carries *UBE3A* mutations, thus narrowing down for further UBE3A sequence analysis. Conversely, if the patient carries chromosomal 15 deletion, UPD or imprinting defect, their DNA methylation profile will be abnormal. The samples will then be subjected to further screening to differentiate the latter mechanisms. The next step is typically to perform FISH (fluorescent in situ hybridization) chromosomal test to detect for chromosomal 15q11-13 deletion, a mechanism in which majority of the AS patient acquires. An alternative to FISH will be to conduct the array-based comparative genomic hybridization (CGH). If the test appears negative, subsequent test will involve the analysis of parental blood for DNA marker identification to identify potential UPD present in the patient. If this test is negative, the patient is presumed to have an imprinting defect, where further testing is done to check for deletion near the imprinting centre. Recently, Wang and colleagues developed a simplified method to detect and discriminate between deletion and non-deletion AS patients based on a single-step methylation-specific PCR and quantitative melting curve analysis of the *SNRPN* gene (45). In this assay, samples were bi-sulfite treated which converts un-methylated cytosines into uracil, whereas methylated cytosines are protected from this conversion. Normal maternal inherited allele is DNA methylated and hence the DNA is

protected against the effect of the bi-sulphite treatment. On the other hand, the paternal allele is not methylated and bi-sulphite treatment will converts the cytosine to uracil on the DNA, resulting in a lower GC content as compared to the maternal allele. Subsequent PCR and melting curve analysis will produce 2 peaks, representing the paternal allele at lower melting condition and the maternal allele at higher melting conditions. This enables the distinction between the parental alleles. The method also enables the distinguish between deletion with non-deletion genotype based on the amplitude (peak) of the melting curve. Deletion Angelman syndrome patient will produce one single peak contributed by the paternal allele. Conversely, non-deletion patient will also produce one single peak but will have larger amplitude (peak). The larger amplitude from the single peak is contributed by the maternal allele that has imprinting defects which now bears an epigenotype similar to the paternal allele, or in other case uniparental disomy whereby the patient sample contain two copies of paternal allele.

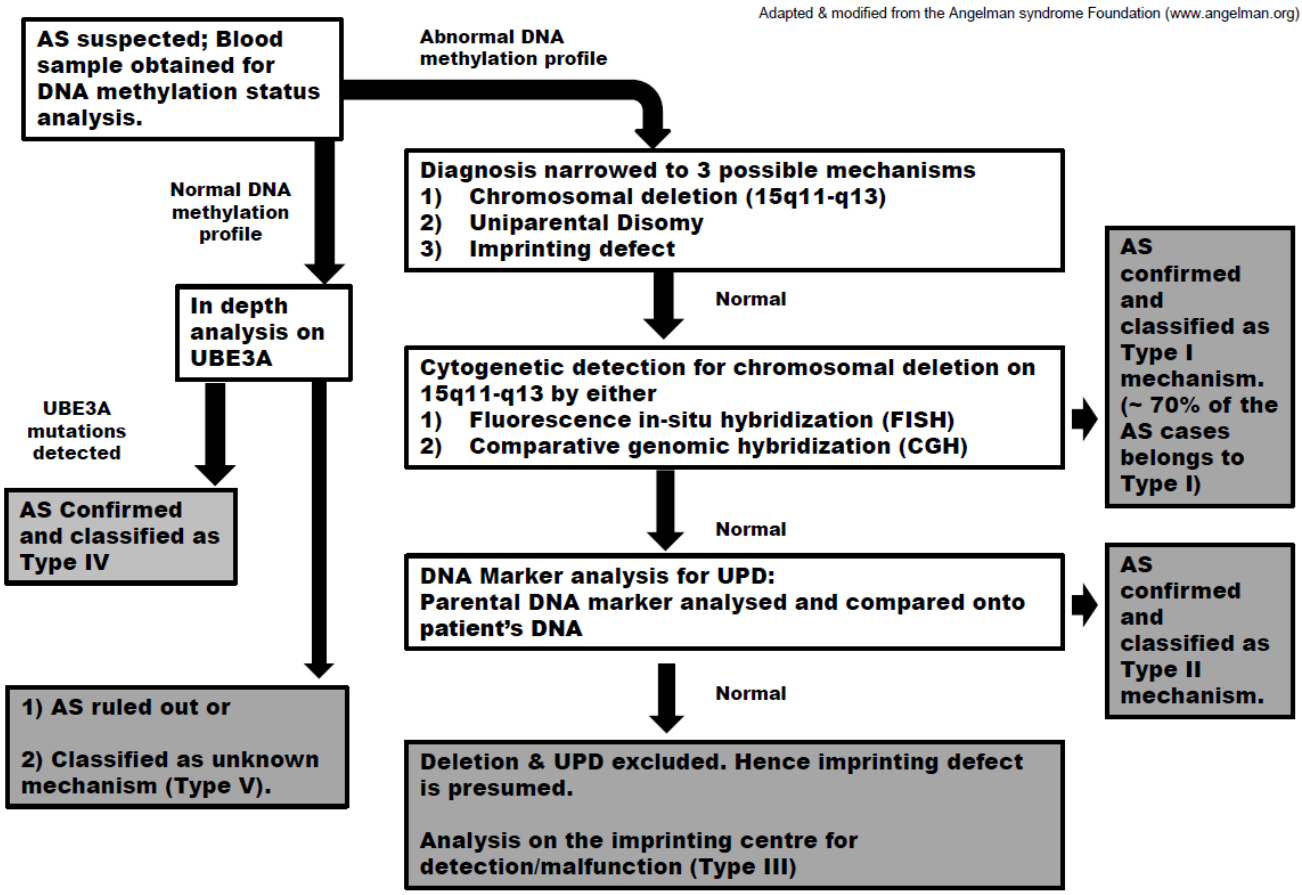


**Figure 2. AS diagnostic test pathway**

## 1.3: Epigenetic regulation of AS

AS critical region has always been an interesting locus for the study of epigenetic regulation, in particular imprinting (46). The AS region on human chromosome 15q11-q13 contains many genes that are subjected to genomic imprinting, which marks the parental origin of chromosomes and results in allele-specific differences in DNA and histone methylation and transcriptional expression (47). In this locus, most genes, including *NDN* (Necdin), *MAGEL2* (MAGE-like protein 2) and *SNURF-SNRPN* (small ribonucleoprotein N) are expressed from the paternal inherited allele (46). On the other hand, genes such as *UBE3A* (ubiquitin protein ligase E3A) and *ATP10A* (P-type ATPase) are preferentially expressed from the allele inherited maternally (Figure 3) (4,22,48,49).

Despite lack of understanding in the mechanisms governing the establishment and maintenance of imprinting, there has been much progress in identifying crucial regulatory elements including regions of differential DNA methylation. Genomic imprinting is controlled by its associated imprinting centre. In AS, the imprinting centre (AS-IC) is suggested to be 35-40 kb upstream of SNRPN exon 1 (32,33). This imprinted domain is conserved along the mouse chromosome 7C and is currently believed to mediate a switch from paternal to maternal imprint during

oogenesis (34,50). Further studies have narrow down the AS-IC to a 880 bp region (51). This location was defined from the study of microdeletions in multiplex families with AS that has imprinting defects. However, due to the fact that only 20% of AS patients with imprinting defects shows deletion/mutation in this region, this putative minimal AS-IC is still under investigation (52). This further portrays the complexity of the imprinting regulation, and the actual mechanism is currently still ambiguous.

In addition to the AS-IC, the region is also governed by non-coding antisense RNA. In recent years, there has been increasing interest in gene regulation by non-coding RNA, which has been considered one of the most important aspects of epigenetic regulation. The non-coding RNA associated with AS is the *UBE3A* antisense transcript (*UBE3A-ATS*). The *UBE3A-ATS* is a long non-coding antisense RNA (~ 460 kb) that is expressed upstream of *SNURF-SNRPN* and overlaps *IPW* and *UBE3A* (Figure 3) (53). The murine counterpart also expresses similar large non-coding *Ube3a-ATS* RNA (~ 1000 kb) (6,54). Since *UBE3A* is the causative gene for AS and its maternal specific expression in the brain is of genuine interest in AS studies, the *UBE3A-ATS* is an important aspect to consider when deciphering the pathogenesis of AS. The *UBE3A-ATS* is expressed from the paternal inherited allele in the human brain and undergoes extensive splicing that serve as a host for many types of small nucleolar RNA (snoRNA) upon processing of the host

transcript (53,55-57). RNA-FISH experiments indicate that *UBE3A-ATS* is not detectable in fibroblast or neuronal precursor (NT2) cells, suggesting its allele-specific *UBE3A* expression is regulated in the brain (58). Inferred from other imprinted genes (e.g. *Xist*, *Kcnq1*), the proposed mechanism of such silencing includes degradation of the message RNA that it is regulating, transcriptional interference by competing for RNA polymerase occupancy, as well as chromatin modification (59-63). However, the validity of these mechanisms has yet to be proven.

The latest research areas studying the *UBE3A* imprinting mechanisms in human patients have been performed on the induced pluripotent stem cell (iPSC) lines established from the AS patients (64). This study shows that *UBE3A* imprinting is present in the iPSC-derived neurons of both AS deletion patients as well as the control individuals. It was demonstrated in mice using high resolution single nucleotide polymorphism (SNPs) genotyping that only the 3' end of UBE3A is imprinted whereas the 5' end of the gene is biallelically expressed (65). This results in a speculative model such that the "partial" histone modification affects the transcriptional elongation of *UBE3A* through premature abortion, yielding a truncated messenger RNA (66). Another model of the mechanism of how *UBE3A-ATS* affects *UBE3A* expression is the "collision model". This model assumes that transcription can only occur in one direction at a single time. Hence, during the

transcription of the *UBE3A* sense strand, the RNA polymerase (RNAPII) will collide and competed off their template by the incoming RNAPII complex transcribing the *UBE3A-ATS* in the other direction (66,67). These two interesting models currently awaits experimental validation.

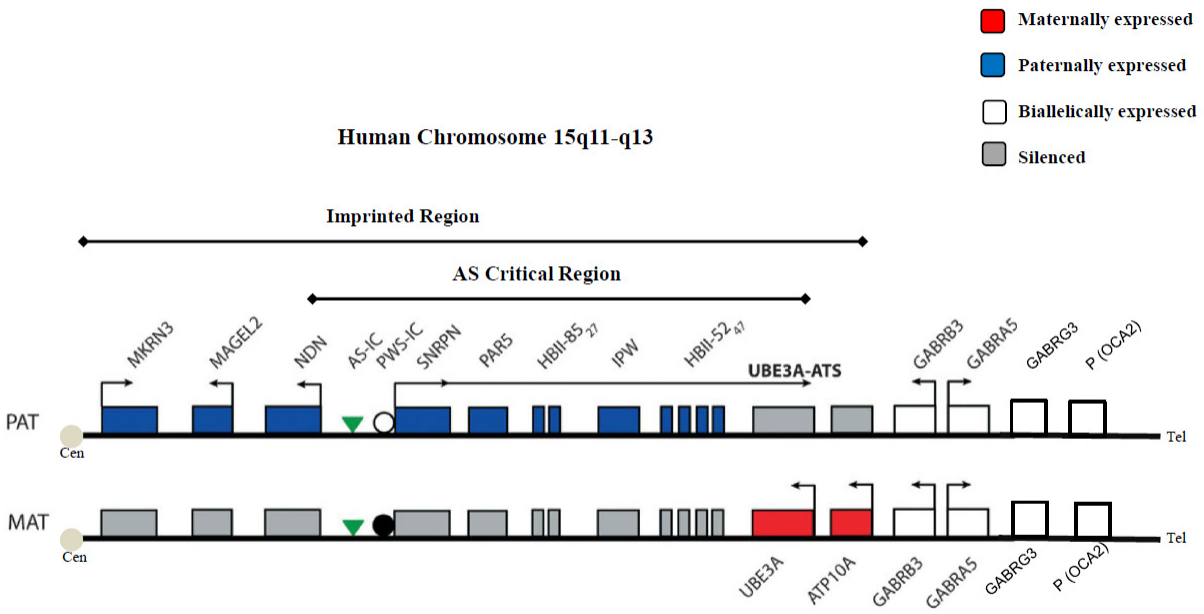


Adapted and modified from Lalande et al., 2007. [47]

**Figure 3. Human chromosome 15q11-q13 AS/PWS imprinting map**

Human chromosome 15q11-q13 AS/PWS imprinting map depicting the allele-specific gene expression in the brain. Blue boxes indicate the paternally expressed genes. Red filled boxes indicate the maternal expressed genes. The AS imprinting center (AS-IC) is represented by a triangle. UBE3A-antisense (UBE3A-ATS) transcripts expression initiates from the exon 1 of the *SNURF-SNRPN* gene from the paternal allele. This entire region is syntenic to the mouse chromosome 7.

## 1.4: Animal Models of AS

Development of AS animal models has provided invaluable platform to study the disorder. Currently several AS transgene/knockout mouse lines has been generated, including mice with *Ube3a* knockout/mutations, mice with large deletion along 15q11-q13, as well as mice with deletion along the AS imprinting centre. More recently, the development of AS model using drosophila has created another alternative method to study AS. Table 2 summarizes the various available AS animal models.

There are currently two reported AS mice model carrying *Ube3a* knockout/mutation, which represents the most basic scenario of AS. The first *Ube3a* knockout mouse was generated by targeting the knockout of *Ube3a* exon 2 (GenBank accession number U82122) that also creates a frame-shift and inactivates all protein isoforms (22). Obvious phenotypes of the maternal inherited knockout ($Ube3a^{m-/p+}$) include hypo-activity, a smaller cerebellum and the mice are physically lighter and reduced in size as compared to their wildtype littermates. Fine testing also show impaired motor coordination, hippocampal learning long-term potentiation deficits, as well as abnormal dendritic spine development. Even more recently, this group of mice was found to have a decreased number of

dopaminergic neuron in the substantia nigra region of the brain, attributing the motor dysfunction observed in the *Ube3a*$^{m-/p+}$ mice to the abnormality in the nigrostriatal pathway (68). This mouse model is used for the experiments described in this project. The second type of AS mice carrying *Ube3a* mutation was generated by knocking out *Ube3a* exon 15 and 16 (69). The mice were reported to show abnormal electrocorticographic pattern in the hippocampus and cerebellar Pukinje cells. Similarly, the mutant mice also have consistent impairment in motor function and learning abilities.

The other group of AS mouse model involves microdeletions of the AS critical region on mouse chromosome 7C, including *Ube3a* (70). This group of mice will represent type I AS patient that has microdeletion along human chromosome 15q11-q13. Interestingly, the mice with maternal inheritance of the deletion did not show obvious abnormalities and were fully viable and fertile. Only upon careful experimental analysis will the mice show mild neurological and behavioral phenotype. In another recent AS mouse model generated through targeting a large maternal deletion from *Ube3a* to *Gabrb3*, no apparent defects were observed other than spontaneous seizure activity and abnormal EEG. Behavioral analysis indicates that these AS mice show motor, learning and memory impairment similar to the AS mice with *Ube3a* mutations (71).

In 2006, Wu and colleagues generated two mouse model representing an abnormality comparable to a defective AS imprinting centre (72). The first model involves an insertion mutation 13 kb upstream of *Snrpn* exon 1 through homologous recombination gene targeting. When transmitted maternally, the mouse recapitulate the major features observed in the AS patient with deletion on the AS-IC region. This includes the lack of DNA methylation at the maternal *Snrpn* promoter, similar to the paternal epigenotype, leading to expression activation. This characteristic is still present after many generations; hence they can be passed through both maternal and paternal germ line and transmitted. The second mouse model involves the deletion of a large (80 kb) chromosomal fragment extending from the site of the first model. This results in a similar imprinting defect with variable penetrance.

The AS animal model has recently been extended to the Drosophila (73,74). These AS flies carry null *Dube3a* mutations and revealed a range of abnormalities including impaired olfactory associative memory, atypical climbing behavior (74). Recently, it has been shown that *Dube3a*-null mutant files also have reduced dendritic branching in the sensory neurons of the peripheral nervous system (73). Thus, the AS Drosophila model provides an alternative platform to elucidate UBE3A substrates that is relevant to the disease.

## Table 2: Animal Models of Angelman Syndrome

| AS Mouse & *Drosophila* Models | Mutation | Major Phenotype | References |
|---|---|---|---|
| Ube3a knockout | Deletion of *Ube3a* exon 2 | • Motor dysfunction<br>• Inducible seizures<br>• Impaired long-term potentiation<br>• Small cerebellum | 22 |
| Ube3a knockout | Deletion of Ube3a exon 15 & 16 | • Motor dysfunction<br>• Impaired spatial learning<br>• Abnormal EEG recording | 69 |
| Imprinting defect | AS Imprinting centre mutation | • Methylation disruption<br>• Inducible seizure<br>• Small cerebellum | Chen et al. (unpublished data) |
| Microdeletion | Deletion of mouse chr 7 region syntenic to human chr 15q11-q13 | • No apparent abnormalities<br>• Motor/learning ability not studied | 70 |
| Microdeletion | Deletion of mouse chr 7 from *Ube3a* to *Gabra3* | • Spontaneous seizures<br>• Abnormal EEG<br>• Impaired motor/learning/ memory | 71 |
| Dube3a null | Dube3a null | • Abnormal locomotive behavior<br>• Impaired long-term memory | 73 |
| dUBE3A null | Deletion of exon 1 | • Decreased dendritic branching<br>• Retarded growth of terminal dendritic processes. | 74 |

## 1.5: *UBE3A*: The AS Causative Gene

UBE3A (also known as E6AP), is an ubiquitin E3 ligase functioning as part of the ubiquitin proteosomal degradation system (UPS) which targets specific proteins for degradation. Originally identified for its role in ubiquitinating p53 during cervical oncogenesis, the steady progression in the identification of other UBE3A substrate interacting partner have provide a clearer perception on the role of UBE3A in biological processes. UBE3A is perceived as a bifunctional molecule that can act as an E3 ligase, and as a coactivator for nuclear steroid receptors (1,75). Linkage analysis had demonstrated that *UBE3A* mutation/s alone can result in the development of AS, spurring great interest in the function and regulation of UBE3A, as well as how it contributes to the pathogenesis of the disease (2).

UBE3A contributes to cellular protein turnover by targeting their degradation through the UPS (1). UPS has been implicated in many neuro-degenerative diseases such as Alzheimer's, Parkinson's diseases and AS (3). This UPS is achieved by highly regulated tagging of target protein with the protein ubiquitin, starting off with the activation of ubiquitin by an activating enzyme (E1) that creates a high energy thioester intermediate, E1-S-Ubiquitin (76). This intermediate causes a conformation change in E1, which promotes association with the ubiquitin

carrier protein (E2) and subsequently transferring of the ubiquitin from E1 to E2, forming the E2-S-Ubiquitin intermediate. Finally, the substrate specific E3 ligase, such as UBE3A, interacts with both the specific target protein and the E2-ubiquitin and transfers the ubiquitin to the target protein. In mammals, there are only two known E1 ligases and a dozens of known E2 ligases. On the other hand, there are hundreds of E3 ligases, supposedly to achieve target specificity. In recent years, increasing attention has been focusing on the UPS in the neuronal synapses for the roles in feedback control of transcription, as well as modulating synaptic development/elimination and neurotransmission strength (25,77,78).

Many protein targets of UBE3A have been identified. UBE3A was first identified for its association with p53 in the presence of the human papillomavirus (HPV) E6 protein (1). This leads to the subsequent ubiquitinization of p53 by UBE3A, resulting in cancer progression. Some reports show that the HPV E6 protein is required for the p53-UBE3A association, whereas other groups demonstrate that UBE3A is a regular target for p53 (1,22,79-81). This conflict has yet to be resolved. Other targets of UBE3A, as well as its interacting partners have also been gradually unraveled and summarized in Table 3 (1,75,82-97). The substrates for UBE3A have been implicated in many cellular processes, including cell cycle progression and cell signaling. Identification of UBE3A interacting partners that show non-degradation consequences, but associated with transcriptional regulation, clearly illustrates the multifunctional role of UBE3A.

## Table 3. Interaction/Target proteins of UBE3A

| Interacting/Target Protein | Type of Protein | Implications | References |
|---|---|---|---|
| Ring1B | Ubiquitin Ligase | Nucleosomal histone modifications | 83 |
| Arc | Synaptic protein | Regulation of proper internalization of AMPA subtype glutamate receptors | 84 |
| Prx1 | Antioxidant peroxidases | Intracellular oxidative signal transduction pathways | 85 |
| p27 | cyclin-dependent kinase inhibitor | Cell cycle alterations. | 86 |
| PML | Tummor suppressor | Growth inhibition, senescence and apoptosis | 87 |
| alpha-synuclein | Synuclein protein | Pathology of Lewy bodies and Parkinson's diease. | 88 |
| HSP70 | Heat Shock Protein | Protein quality control | 89 |
| annexin A1 | Ca2+ & Phospholipid -binding protein | Diverse function related to annexin A1 including cell death signaling, carcinogenesis | 90 |
| TSC2 | tumor suppressor protein | Oncogenesis | 91 |

| | | | |
|---|---|---|---|
| Hepatitis C virus (HCV) core protein | viral nucleocapsid | Viral nucleocapsid degradation | 92 |
| Pbl/ECT2 | Rho-GEF protein | Cytokinesis | 93 |
| HHR23A | yeast DNA repair Rad23 homologues | DNA repair and cell cycle progression | 97 |
| UBE3A | Ubiquitin E3 Ligase | Self degradation | 94 |
| Androgen receptor (AR)/ Progesterone receptor (PR) | Nuclear hormone receptor | Transcriptional coactivator of AR/PR | 75 |
| UbcH7 & UbcH8 | E2 ubiquitin-conjugating enzymes | UPS | 95 |
| p53 | Oncogene | Cervical oncogenesis. | 98 |
| HPV-16 E6 | Viral E6 protein | Cervical oncogenesis | 1 |

The human UBE3A and its murine homolog are 99% identical at the amino acid level. There are currently three known UBE3A protein isoforms differing only at their extreme amino-terminal (98). The functional difference among the isoforms has not yet been investigated. All isoforms contain a HECT (homologous to the E6-AP carboxyl terminus) domain at the C-terminal, first described by Scheffner and colleagues (Figure 4) (1). This HECT domain is highly conserved among many E3 enzymes with E3 ligase activity (99). The 100 amino acids along the C-terminal are essential for the acceptance and transfer of ubiquitin to target proteins. Mutagenesis analysis reveals that change of the cysteine residue at the 883$^{rd}$ amino acid to a serine or alanine can abolish all ligase activity of the enzyme (Figure 4) (100). It was demonstrated that UBE3A has self-ubiquitination ability which may provide a means of regulatory mechanism to control the amount of intracellular UBE3A (101).

In addition to the HECT domain, UBE3A also contains an activation domain at its N-terminal that is responsible for its intrinsic coactivation function for steroid hormone receptors, including progesterone receptor (PR), estrogen receptor (ER) and androgen receptor (AR) (Figure 4) (75). Two LXXLL consensus motifs can be found along this activation domain that mediates the interaction between UBE3A and steroid hormone receptors. Transfection experiments using various *UBE3A* deletion constructs showed that the coactivation ability of UBE3A only requires the activation domain and is independent of the HECT domain and its associated

ligase properties (75). In the same study, UBE3A has also been demonstrated to coactivate the transcriptional factor SP1. Chromatin immunoprecipitation (ChIP) assay has revealed that UBE3A is recruited to the promoter region of the AR responsive gene PSA, as well as the ER responsive gene in vivo and regulates hormone-dependent gene expression (80). More recently, the E-box response element on the human telomerase reverse transcriptase (*hTERT*) promoter was found to recruit UBE3A for transactivation activity (102).

In most tissues, UBE3A is biallelically expressed. However, it is imprinted in a selected population of brain cells, in particular within the cerebellum and hippocampus, such that only the allele inherited maternally is expressed (4). On the other hand, the allele inherited paternally is silenced. Hence, inheriting a maternal *UBE3A* mutation/deletion in the brain may result in complete abolition of UBE3A function, as well as potential UBE3A haploinsufficiency in other tissues. The consequences of such occurrence will be a serious perturbation of cellular homeostasis in the brain, as well as in the peripheral tissues, that will contribute to the development of neurological abnormalities and other phenotypic characteristic of AS.

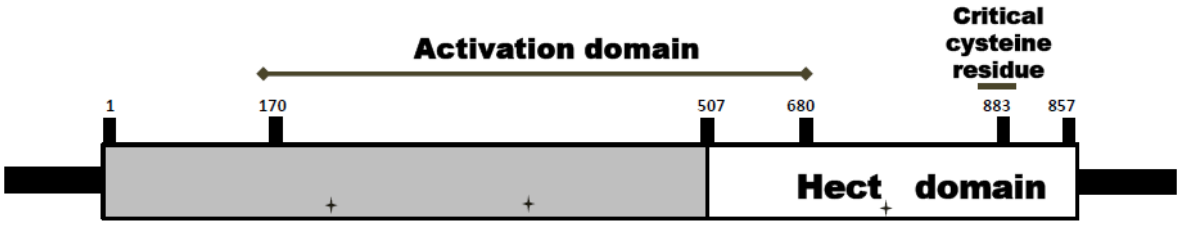


Adapted and modified from Ramamoorthy et al., 2008 [99]

**Figure 4. Schematic diagram illustrating the functional protein domain of UBE3A**

Schematic diagram illustrating the functional protein domain of UBE3A: Well characterized domain of UBE3A includes the HECT domain at the carboxyl terminal with a critical cysteine residue that confers the ubiquitin ligase activity of UBE3A. The activation domain resides towards the amino terminal which is responsible for coactivation of nuclear hormone receptor. Three nuclear boxes containing the receptor interacting LXXLL motif (designated with "+") are dispersed throughout the protein, such that two are located in the amino terminus and the third resides within the carboxyl terminal of UBE3A.

## 1.6: *UBE3A* in the brain

Understanding the cellular and global function of UBE3A in the brain has been the main focus of much research in AS. Increasing reports on UBE3A functions in the brain demonstrate its fundamental role in regulating neuronal homeostasis including synaptic transmission, learning and memory (synaptic plasticity), as well as neuro-motor utility.

The contributions of UBE3A in the synapse are substantial (25). In cultured hippocampal neurons, Ube3a was detected in the nucleus and pre/post synaptic compartments (77). It was observed that the cellular architecture of the *Ube3a*$^{(m-/p+)}$ mouse brain is normal but the size, density and morphology of the dendritic spines are apparently abnormal (77). This suggest that UBE3A locally regulates the synaptic regions most possibly by the turnover of its target protein through ubiquitin mediated degradation, and most likely regulating transcription in the nucleus (77). A similar observation in the *dUBE3A* null mutant shows reduced dendritic branching of the sensory neurons and retarded growth of the terminal dendriti (74). On the other hand, overexpression of dUBE3A in flies also resulted in decreased dendritic branching, strongly suggesting that balanced amount of UBE3A are critical for normal dendritic patterning (74). It is likely that UBE3A exerts its effects at the synapse through degradation of specific target proteins,

regulating synaptic function. Recently, it has been shown that experience-driven neuronal activity was shown to induce *Ube3a* transcription which then controls the degradation of a synaptic protein called *Arc*, which promotes the internalization of glutamate receptor AMPA subtypes at the synapse (83).

The fact that lack of functional UBE3A leads to the impairment of learning and memory in the brain is well documented, suggesting the possible correlationship between UBE3A and synaptic plasticity. It was shown that experience-dependent maturation of the neocortex is perturbed in *Ube3a*$^{(m-/p+)}$ mice (103). A similar report also showed that the maternal Ube3a is required in the experience-dependent development of the mouse visual system and ocular dominance plasticity was drastically affected in the *Ube3a*$^{(m-/p+)}$ mice (104). Interestingly, participation of Ube3a in neuronal plasticity does not directly affect new-born progenitor cells in the hippocampus, but has an impact during development. Using specific markers that label cell proliferation, cell survival and neuron production, it was shown that none of these aspects were affected in newborn hippocampal progentitor cells in the *Ube3a*$^{(m-/p+)}$ mice. Instead, the population of the surviving new progenitor cells that appear positive to neuronal markers were apparently reduced (105). Since new neurons are generated and integrated into the existing neural circuit in the hippocampus to provide enhanced plasticity, the finding infers that lack of Ube3a impairs hippocampal plasticity and neurogenesis (106).

The motor dysfunction as a result of maternal UBE3A deficiency in the cerebellum can be considered one of the most obvious phenotypes observed in AS patients and *Ube3a* mutant mice. Other than the classical rotarod test to analyze gross cerebellar defects, in which maternal Ube3a deficient mice appeared to be underperforming, new methods to quantify the cerebellar motor system defects had been evaluated (22). Using fluid consumption rhythms and licking behavior/number observations, the *Ube3a*$^{(m-/p+)}$ mice showed significant differences as compared to the wildtype control (107). Interestingly, *Ube3a* expression was quantified to be dramatically decreased during aging of the mammalian cortex across the lifespan in human, monkey and cats (108). This appeared to be consistent with the loss of agility in aging, as well as with age-related neurodegenerative disorder and longevity. The recent finding on the loss of dopaminergic neurons in the substantia nigra region of the brain in the *Ube3a*$^{(m-/p+)}$ mice is another important aspect contributing to motor dysfunction (68). On the other hand, the search for a solution to reverse the neurological deficit as a result of Ube3a deficiency had been elegantly demonstrated through the reduction of α-CaMKII inhibitory phosphorylation (109). It seemed that the identification of the global gene expression disruption caused by UBE3A malfunction must first be addressed, in order to understand the pathogenesis in greater detail.

## 1.7: Angelman Syndrome and the Hypopigmentation Trait

Although AS is considered a neurological disorder, there are non-neuronal phenotypes associated with the disease (10). Hypopigmentation in the skin is one of the features observed in peripheral tissues of AS patients, in which patients have light skin tone when compared to their family members (23). Most of the type I (large deletion) AS patients show hypopigmentation (90%), whereas only up to 20-50% of the rest of the non-deletion patients (type II-IV) manifest this feature (29). Hence pigment dysregulation in AS represents another unique area to decipher genotype-phenotype correlations.

In general, cutaneous pigment, or melanin, is synthesized and stored in granules/melanosome of the melanocytes and then transferred to neighbouring keratinocytes on the epidermis (110). The exact mechanism of pigment production is complex and governed through multigenic regulation of more than 120 genes (111). However, several key players had been identified including the *P* gene (*OCA2*) and the melanocortin-1-receptor (*MC1R*) (112,113). The major determinant of mammalian pigmentation is the ratio of the two predominant forms of mammalian melanin, i.e. black/brown eumelanin and yellow/red pheomelanin (114). This ratio is dependent on melanocortin-1-receptor (MC1R), a G-protein-coupled receptor present in plasma membrane of melanocytes functioning in the

upstream regulation of melanin synthesis (112,115). The natural ligand for this receptor is the α-melanocyte stimulating hormone (α-MSH) synthesized by the neighbouring keratinocytes (116). Upon activation by α-MSH, MC1R induces an increase in intracellular cAMP and subsequently activates protein kinase A (PKA) and the phosphorylation of cAMP-responsive element-binding protein. This leads to the activation of genes encoding enzymes that are important for the production of black/brown eumelanin, such as the microphthalmia transcription factor (MITF) (117). However, competitive binding by an antagonist agouti-signaling peptide blocks MC1R activation, as well as stabilizing the inactive conformation of the receptor that leads to the activation for the production of the yellow/red pheomelanin (118). It was also shown that the *Mc1r* mRNA level increases in cells treated with the natural agonist, α-MSH (119). Mutations and polymorphisms that reduce *MC1R* expression or functions affect the receptor performance and result in the switch and overproduction of pheomelanin, which is inferred to cause fair skin in carriers (MIM: 155555) (120).

Hypopigmentation in the skin is considered an associated feature of AS (up to 20-80%) in a consensus clinical diagnostics criteria report (10). The great majority of type I patients that carry a microdeletion along the maternally inherited chromosome 15q11-q13 exhibit hypopigmentation (29). The cause of their pigment dysregulation is attributed to the hemizygosity of the oculocutaneous albinism II gene (*OCA2*) that lies adjacent to *UBE3A* along human chromosome 15 (121). In

addition, a few type I AS patients were reported to contain mutation along the paternal *OCA2* in addition to the loss of maternal *OCA2* through the microdeletion resulting in a nearly complete loss of OCA2 function through this compound mutation (122,123). The occurrence of such compound mutation in the *OCA2* might not be representative of the entire type I AS population where 90% exhibit hypopigmentation. *OCA2* encodes an integral membrane protein that regulates the pH of the melanosome compartment which contains melanin (113). It is also believed to be involved in stabilizing complexes for black/brown melanin down-stream production. Disruption of *OCA2* alone causes recessive oculocutaneous albinism type II (MIM: 203200). The attribution of OCA2 towards causing AS hypopigmentation currently does not account for the fact that up to 50 % of other AS patients (type II-IV) with *UBE3A* mutations, imprinting defects and UPD, also show to a certain extent the hypopigmentation traits (44). These patients have supposedly intact *OCA2* in both alleles and the genotype-phenotype correlation for the hypopigmentation trait for these patients is currently unresolved.

# Chapter II: Project Goal

**To determine the gene expression profile of AS mice in order to better understand the molecular mechanism/s and genotype-phenotype correlationship of AS.**

***Specific Aims***

1. To perform genome-wide expression profiling of the AS mouse using microarray to determine differential gene expression.
2. To validate the dysregulation of *Mc1r* in AS mice identified through microarray study.
3. To identify the mechanism on how UBE3A can affect *MC1R* expression.
4. To reconcile the current controversy in the AS hypopigmentation trait.

# Chapter III: Materials and Methods

**3.1: Ethics Statement/Mouse Strains:** All animal work was maintained, performed and approved by the NTU School of Biological Sciences Animal Facility based on guidelines from the Institutional Animal Care and Use Committee (IACUC). *Ube3a*$^{m-/p+}$ mice were obtained from The Jackson Laboratory (stock number 004477).

**3.2: Genomic DNA extraction from mouse tail:** Mouse tail was digested overnight at 55$^{o}$C in 500µl of NTES buffer (50mM Tris pH 7.5, 50mM ethylenediaminetetraacetic acid (EDTA) pH 8.0, 100 mM NaCl, 5 mM ditiothreitol (DTT), 0.5 mM spermidine, 2% sodium dodecyl sulfate (SDS) and proteinase K. Phenol was added to the digested tail and rocked for 30 min followed by centrifugation at 13,000g for 15 min. The aqueous layer was isolated and phenol:chloroform:isoamyl alcohol (25:24:1) was added. After 30 min of rocking, the sample was centrifuged for 15 min at 13,000g. The top aqueous layer was isolated and equal amount of chloroform was added and rocked for 30 min. The sample was then centrifuged at 13,000 g for 15 min and the top layer was transferred into a new tube. Genomic DNA was then precipitated using 500 µl of isopropanol and the thread like DNA was spooled out and dissolved in 200 µl of TE buffer overnight at 37$^{o}$C. The concentration of the DNA was determined using the Nanodrop Spectrophotometer. All DNA samples were found to have a 260/280 OD ratio between 1.8 and 2.0.

**3.3: Genotyping of the AS mouse:** Genomic DNA (10 µg) was used as template for PCR genotyping of the mouse using Faststart Taq Polymerase (Roche, Indianapolis, IN, USA) and three sets of specific primers (forward primer: 5'-gctcaaggttgtatgccttggtgct-3', reverse primer 1: 5'-agttctcaaggtaagctgagcttgc-3', reverse primer 2: 5'-tgcatcgcattgtctgagtaggtgtc-3'). PCR cycling conditions include denaturation at 94$^{o}$C for 3 min and 35 cycles of 94 $^{o}$C for 30 secs, 68 $^{o}$C for 1 min and 72 $^{o}$C for 1 min and a final extention at 72 $^{o}$C for 2 min. The PCR product was then resolved on 1% Agarose gel to identify the 700 bps fragment corresponding to the wildtype allele or the 320 bp fragment corresponding to the mutant allele.

**3.4: Total RNA extraction:** Tissues (cerebellum & dorsal skin)/Cells were lysed homogenized in 1 ml of Trizol reagent (Invitrogen, Carlsbad, CA, USA). The samples were then incubated at room temperature for 5 min to allow complete dissociation of nucleoprotein complexes. Subsequently, chloroform (0.2 ml) was added and shaked vigourously and incubated for 3 min at room temperature. The sample was then centrifuged at 12, 000 g in 4$^{o}$C for 15 min. The top layer was transferred to a new tube and 0.5 ml of isopropanol was added to precipitate the RNA for 10 min at room temperature. The sample was then centrifuged at 4 $^{o}$C for 10 min at 12, 000 g and the supernatant was discarded. The pellet was then washed in 1 ml of 75% ethanol and centrifuged for 5 min at 7, 500 g. The wash ethanol was

discarded and then the air-dried RNA pellet was dissolved in DEPC treated water. The samples were then heated at 55$^{o}$C for 10 min. The RNA concentration was determined using the Nanodrop Spectrophotometer and all samples were observed to have a 260/280 ratio between 1.6 and 2.0.

**3.5: Microarray Sample Preparation and Hybridization:** One microgram of starting total RNA from the cerebellum of wildtype and *Ube3a*$^{m-/p+}$ mice were each used for the Affymetrix GeneChip Mouse Exon Array analysis. Samples were processed according to Affymetrix GeneChip Whole Transcript Sense Target Labeling Assay (Affymetrix, Santa Clara, CA, USA; Figure 6). Target preparation and hybridization were performed using a pre-commercial version of the GeneChip WT cDNA Synthesis Kit, WT cDNA amplification kit, and WT Terminal Labeling kit (Affymetrix).

**3.6: Microarray Analysis & Statistics:** A total of 4 biological replicates from each of wildtype and *Ube3a*$^{m-/p+}$ mice were included in the final analysis to detect differential gene expression derived from Partek Genomic Suite (Partek Inc, St Louis, MO). The Affymetrix generated CEL files containing raw data were subjected to Robust Multi-Chip Average (RMA) normalization, background subtraction and summarization. One way ANOVA was subsequently performed to detect p-values for the respective gene expression fold changes. The criteria for a

gene to be considered differentially expressed were set at $p \leq 0.05$ and a minimal fold change of 1.5 folds. Gene ontology and network/pathway analysis were performed using the Ingenuity pathways analysis software (Ingenuity System, Redwood City, CA, USA) that is integrated within the Partek Genomic Suite software. Quality control analysis was performed using the Affymetrix Expression Console software with reference to the Affymetrix quality control white papers.

**3.7: Semi Quantitative Reverse Transcription PCR:** Two micrograms of total RNA from each sample was treated with RQ1 DNase (Promega, Madison, WI, USA) and then reverse transcribed using Superscript (Invitrogen). Subsequently, 1 µl of the cDNA template generated was used for each PCR reaction using Faststart Taq Polymerase (Roche), and cycling conditions were 95$^{o}$C for 10 min, then 30-35 cycles of 30 sec at 95$^{o}$C, 30 sec at 60$^{o}$C, and 30 sec at 72 $^{o}$C, followed by a final extension of 10 mins at 72$^{o}$C.

**3.8: qRT-PCR (Microarray Validation):** qRT-PCR was performed using 1µl of cDNA template described above. A 25 µl reaction containing iTaq SYBR Green Supermix with ROX (BioRad, Hercules, CA, USA) was prepared according to the manufacturer's suggestion, and PCR amplified using the ABI 7500 system (Applied Biosystem, Carlsbad, CA, USA). Cycling conditions were 10 min at 50$^{o}$C, 10 min at 95$^{o}$C, then 45 cycles of 30 sec at 95$^{o}$C, 30 sec at 60$^{o}$C, and 32 sec at 72

$^{o}$C. The experiment was performed in three biological replicates. The $C_T$ value for each gene was determined in the linear phase of the amplification for each gene, and normalized to $C_T$ value of *G3pdh* to obtain the $\Delta C_{T.}$ The fold change for each gene was obtain using $2^{-(\text{mean Wildtype } \Delta CT - \text{mean } Ube3a(\text{m-/p+}) \ \Delta CT)}$. A Student's t-test was performed on the $\Delta C_T$ for each gene to obtain a p-value for differential expression.

**3.9: Western Blot:** Six week old female mouse cerebellum was homogenized in lysis buffer (30 mM Tris, 7M Urea, 2M Thiourea, 4% CHAPS, pH 8.5, protease inhibitor). P19 cells were lysed in lysis buffer (0.1M Tris-HCl, pH 7.4, 150mM NaCl, 1mM EDTA, 2mM $MgCl_2$, 1% Triton X-100, 15% glycerol, 2mg/ml phenlymethylsulfonyl fluoride and protease inhibitor). Ten micrograms of total protein was separated in SDS-PAGE. The protein separated in poly-acrylamide gel was then transferred onto PVDF membrane at 4$^{o}$C. For quantitative analysis purposes, the membrane was then incubated in Ponceau S Staining Solution (Sigma Aldrich, St. Louis, MO, USA) for 5 min to reversibly stain and check for equal loading of total protein and homogenous transfer efficiency. The membrane was then blocked in 5 % milk to prevent non-specific binding. Western blotting anti-body detection was performed using 1 µg of primary anti-Ube3a (Bethyl Laboratories, Montgomery, TX, USA), anti-Mc1r and anti-Nr4a2 antibodies (Santa Cruz Biotechnology, Santa Cruz, CA, USA) incubated overnight at 4$^{o}$C and

detected by chemiluminescent horseradish peroxidase (HRP) conjugated secondary antibody.

**3.10: *Ube3a* shRNA Expressing Vector Construct:** A pair of complementary single stranded 19-mer( 5'-ctt-cgt-atg-gat-aac-aat-g-3') oligo-nulcleotide which correspond to exon 5 of *Ube3a* (Genbank Number: NM_011668.2) was synthesized and contained a flanking *Bgl*II and *Hind*III restriction site. The targeted exon 5 corresponds to the exon 2 that was deleted in the mouse previously described (22). Three micrograms from each of the complementary single stranded oligonucleotide was mixed into a 50 µl annealing reaction containing the annealing buffer (100 mM NaCL and 50 mM HEPES pH 7.4). The mixture was subjected to step-down cooling annealing by incubating at 90 $^{o}$C for 4 min, then at 70 $^{o}$C for 10 min, then 37 $^{o}$C for 20 min and finally 10 $^{o}$C. The created double stranded oligo-nucleotide was then cloned into the Bglll/ HindIII linearised pSUPER.puro vector (Oligoengine, Seattle, WA, USA) by overnight ligation using the T4 DNA ligase (Promega). This construct will be referred to as pUbe3aKD hereafter.

**3.11: Ube3a Overexpressing Vector Construct:** *Ube3a* coding region was amplified from p3003 pGEM E6-AP (Addgene, Cambridge, MA, USA) using forward primer: 5'-gat-cta-ggt-acc-tat-ggc-cac-agc-ttg-taa-aag-3' and reverse primer: 5'-act-gat-gga-tcc-tta-cag-cat-gcc-aaa-tcc-3'. The 2559 base pair PCR

product was then cloned into pcDNA/HisMaxB vector (Invitrogen) between the *Kpn*I and *Bam*HI restriction site. In order to track the transfection/expression efficiency, a 1368 base pair fragment containing the internal ribosomal entry site (IRES)-eGFP fusion was amplified from pIGCN21 vector (NCI Frederick, Frederick, MD, USA) using forward primer: 5'-gat-cta-gga-tcc-gcc-aag-cta-tcg-aat-tcc-gc-3' and reverse primer: 5'-act-gat-gcg-gcc-gct-tat-gca-gaa-ttc-gaa-gct-tga-gc-3' and cloned between the *Bam*HI and *Not*I site of the pcDNA/HisMaxB vector. This vector will be referred to as pUbe3aOE hereafter.

**3.12: Cell Culture and Transfection:** Mouse embryonic carcinoma derived P19 cells (ATCC number: CRL- 1825; Manasaas, MA, USA) were cultured in alpha minimum essential medium supplemented with 7.5 % bovine calf serum and 2.5% fetal bovine serum. The mouse derived skin melanoma B16-F0 cells (ATCC number: CRL-6475) were propagated in Dulbecco's Modified Eagle's Medium with 10% fetal calf serum. Respective cells were transfected with respective plasmids using Lipofectamine 2000 reagent (Invitrogen). Briefly, the Lipofectamine 2000 was diluted in serum free medium and incubated for 5 mins before addition of the diluted DNA. The cloudy mixture is incubated for 20 min before adding into the cell culture. Alternatively, transfection was also executed using the calcium phosphate method previously described (124). The transfection was performed by mixing the DNA with 0.125 M of $CaCl_2$ and subsequently

adding the mixture into an equal amount of 2 X HBS ( 274 mM of NaCl, 10 mM of KCl, 1.4 mM of $Na_2HPO_4.7H_2O$, 15 mM Dextrose, 42 mM of HEPES and then adjusting the pH to 7.12 using NaOH). The mixture is incubated for 20 mins before adding into the cell culture. Both transfection methods achieved ≥80% efficiency based on separate independent transfection with a GFP expressing plasmid. The cells were harvested 24 hours later.

**3.13: qRT-PCR (Knockdown/Overexpression):** Total RNA was extracted using Trizol regent (Invitrogen) according to manufacturer's protocol. To determine the relative amount of *Mc1r*, *Nr4a2* and *Ube3a* transcript, 1 µg of total RNA was DNase treated, reversed transcribed and amplified using qRT-PCR as described above using similar conditions. The qRT-PCR was performed in triplicates using three independent shRNA transfections. Fold change and statistics calculation were performed as described above.

**3.14: Construction of the human *MC1R* promoter-luciferase reporter plasmid:** Human *MC1R* promoter was amplified from the genomic DNA of human HEK293T cells using forward primer: 5'-cccgccttgggctcccaaag-3' and reverse primer: 5'-agtcctgtccaggaagcagg-3'. Cycling conditions were 95$^{o}$C for 10 min, then 35 cycles of 30 sec at 95$^{o}$C, 30 sec at 60$^{o}$C, and 30 sec at 72 $^{o}$C, followed by a final extension of 10 min at 72$^{o}$C. The PCR product of the promoter was then

cloned into the *Kpn*I and *Xho*I site of a luciferase reporter plasmid pGL3 basic (Promega). This construct will be referred to as pMC1RP.

**3.15: Construction of the human *MC1R* promoter-luciferase reporter with the deletion of the E box/SP1 site:** The fragment of the 5' region of the *MC1R* promoter from the E box/ SP1 site was amplified from pMC1RP using primers (Forward: 5'-cccgccttgggctcccaaag-3'; Reverse: 5'-ccgggggcgtgagcaccca-3') and cloned into the *Kpn*I/*Nhe*I site of pGL3–basic plasmid. Subsequently, the 3' downstream region from the E box/SP1 was amplified from pMC1RP using primer set (Forward: 5'-tcagtgggaggggctctgag-3'; Reverse: 5'-agtcctgtccaggaagcagg-3') and cloned into the *Nhe*I/*Xho*I site to create pMC1RPDel.

**3.16: Construction of the E box/SP1-CMV promoter luciferase reporter plasmid:** To construct a CMV promoter driving a luciferase reporter, the CMV promoter was amplified (Forward primer: 5'-gttgacattgattattgactag-3'; Reverse primer: 5'-gagctctgcttatatagacctc-3') from the pcDNA4/Hismax B plasmid (Invitrogen) and cloned into the *Bgl*II/*Hind*III site of pGL3-basic plasmid to create pGL3CMV. To insert one E box/SP1 response element into pGL3CMV, a pair of 13 oligonucleotide (Forward: 5'-catgtggccgccc-3'; Reverse: 5'-gggcggccacatg-3') corresponding to the E box/SP1 site of the human *MC1R* minimal promoter was annealed to form double stranded DNA using annealing buffer (100 mM NaCl and

50 mM HEPES) and cloned into the *Kpn*I and *Nhe*I site of the pGL3 basic plasmid to create pEBSP1. To insert two E box/SP1 response elements into pGL3CMV, a pair of oligonucleotide (Forward: 5' catgtggccgcccgactgacatgtggccgccc-3'; Reverse: gggcggccacatgtcagtcgggcggccacatg-3') containing two sets of E box/SP1 response element was annealed and cloned into the *Sma*I/*Xho*I site of the pGL3CMV to create pEBSP2. To create a similar construct (pEBSP3) with three E box/SP1 site response elements, the first pair of oligonucleotides that was used to construct pEBSP1 was annealed and cloned into the *Kpn*I/*Nhe*I site of pEBSP2 plasmid.

**3.17: Construction of UBE3A-C883A expressing plasmid:** *UBE3A-C883A* was PCR amplified from the GST E6-AP C883A plasmid (Addgene plasmid 13465) using forward primer: 5'-tatggaagcctgcacgaatg-3' and reverse primer: 5'-ttacagcatgccaaatcc-3' and cycling conditions: 95$^{o}$C for 10 min, then 30-35 cycles of 30 sec at 95$^{o}$C, 30 sec at 60$^{o}$C, and 30 sec at 72 $^{o}$C, followed by a final extension of 10 min at 72$^{o}$C. The PCR product was subsequently cloned into the *Kpn*I and *Bam*HI site of the pcDNA/HismaxB vector (Invitrogen).

**3.18: Luciferase Assay:** Mouse derived embryonic carcinoma P19 cells or skin melanoma B16 cells (4 X $10^5$) were seeded one a 6-well plate one day prior to transfection. The cells were then transfected with respective constructs using the

calcium phosphate method described above (124). To normalize the luciferase data for transfection efficiency, cells were also co-transfected with the 1.0 µg of pSV-β-Galactosidase plasmid (Promega). Cells were harvested a day later, washed with 1 X ice cold PBS and then lysed in 1 X reporter lysis buffer (Promega). The cells/lysate were scraped, then centrifuged to remove cellular debris. The cell lysate (20 µl) was then mixed with 100 µl of Luciferase Assay Reagent and immediately measured the light produce on the $20/20^n$ Luminometer (Turner Biosystem). β-Galactosidase assay was then performed using the β-Galactosidase Enzyme Assay System (Promega) by incubating equal amount of cell lysate with the Assay 2 X Buffer (200 m,M sodium phosphate buffer (pH 7.3), 2 mM $MgCl_2$, 100mM β-mercaptoethanol, 1.33mg/ml ONPG) until the solution turns light yellow in colour. The reaction was then quenched by adding 1.5 volume of sodium carbonate. The amount of β-Galactosidase activity was then measured by reading the absorbance at 420 nm using the Nanodrop spectrophotometer. Each set of experiments was performed in biological triplicates and the luciferase intensity was subjected to Student's t-test statistical analysis to determine the P-value.

**3.19: Chromatin Immunoprecipitation (ChIP) Assay:** Mouse derived embryonic carcinoma P19 cells and skin melanoma B16 cells (1 X $10^6$) were crossed linked using formaldehyde to a final concentration of 0.75% for 10 mins at room temperature and quenched by adding glycine at 125 mM final concentration. The

cells were lysed in SDS lysis buffer (50 mM Tris-HCl pH 8, 10 mM EDTA and 1% SDS) and sonicated. The sonicated lysate was then diluted in ChIP dilution buffer (0.07% SDS, 1.1% Triton X-100, 1.2 mM EDTA, 163.7 mM Tris HCl pH 8.1, 167 mM NaCl and protease inhibitor) and pre-cleared with Recombinant Protein G Agarose (Invitrogen) for 1 hour at 4$^{o}$C. The supernatant was collected and incubated overnight with rotation at 4$^{o}$C with anti-Ube3a antibody (Bethyl Laboratories) and subsequently incubated with Recombinant Protein G Agarose for 1 hour at 4$^{o}$C. The beads were collected, washed with one wash of low salt wash buffer (Tris-HCl 20 mM ph8.1, 2 mM EDTA, 0.1 % SDS, 150 mM NaCl and 1% triton), one wash of high salt wash buffer (Tris-HCl 20 mM ph8.1, 2 mM EDTA, 0.1 % SDS, 500 mM NaCl and 1% triton), one wash of LiCl wash buffer (Tris-HCl 10 mM pH 8.1, 0.25 M LiCl, 1% NP40, 1% deoxycholate and 1 mM EDTA), and two washes of TE buffer (10 mM Tris-HCl pH 8 and 1 mM EDTA), and finally eluted with elution buffer (1% SDS and 0.1M $NaHCO_3$). Reverse cross-linking was performed by adding 5 M NaCl and then heated at 65$^{o}$C for 4 hours. The DNA was then recovered using phenol-chloroform extraction and ethanol precipitation and PCR amplified using forward primer: 5'-ctcggtgctgcctctgcc-3' and reverse primer: 5'-aactcatccctggagcccc-3'.

**3.20: Immunohistochemistry:** Dorsal skin of six week old wildtype and *Ube3a*$^{(-/-)}$ mice was removed, placed into a cryomolds, then covered with cryo-embedding

media OCT and frozen immediately. The frozen tissue block was then transferred to a crytome cryostat and was left to equilibrate to the temperature of the cryotome cryostat. The tissue block was then sectioned to a thickness of 5 µm and placed onto a glass slide. The skin sections were fixed in ethanol at -20$^{o}$C for 30 minutes, subsequently washed 3 times in PBS and then blocked in 10% serum for 2 hours at room temperature. The sections were then incubated overnight at 4$^{o}$C with primary anti-Mc1r antibody (Santa Cruz) and then washed twice in TBST for 5 min each time with agitation. To eliminate endogenous peroxidase activity, the sections were then treated with 0.3% hydrogen peroxide for 15 minutes, then washed in TBS for 5 min for 3 times and then finally incubate with secondary HRP conjugated anti-goat antibody for 1 hour at room temperature. Chromogen detection of the antibody was perform with 3,3' Diaminobenzidine (Sigma Aldrich) for half an hour.

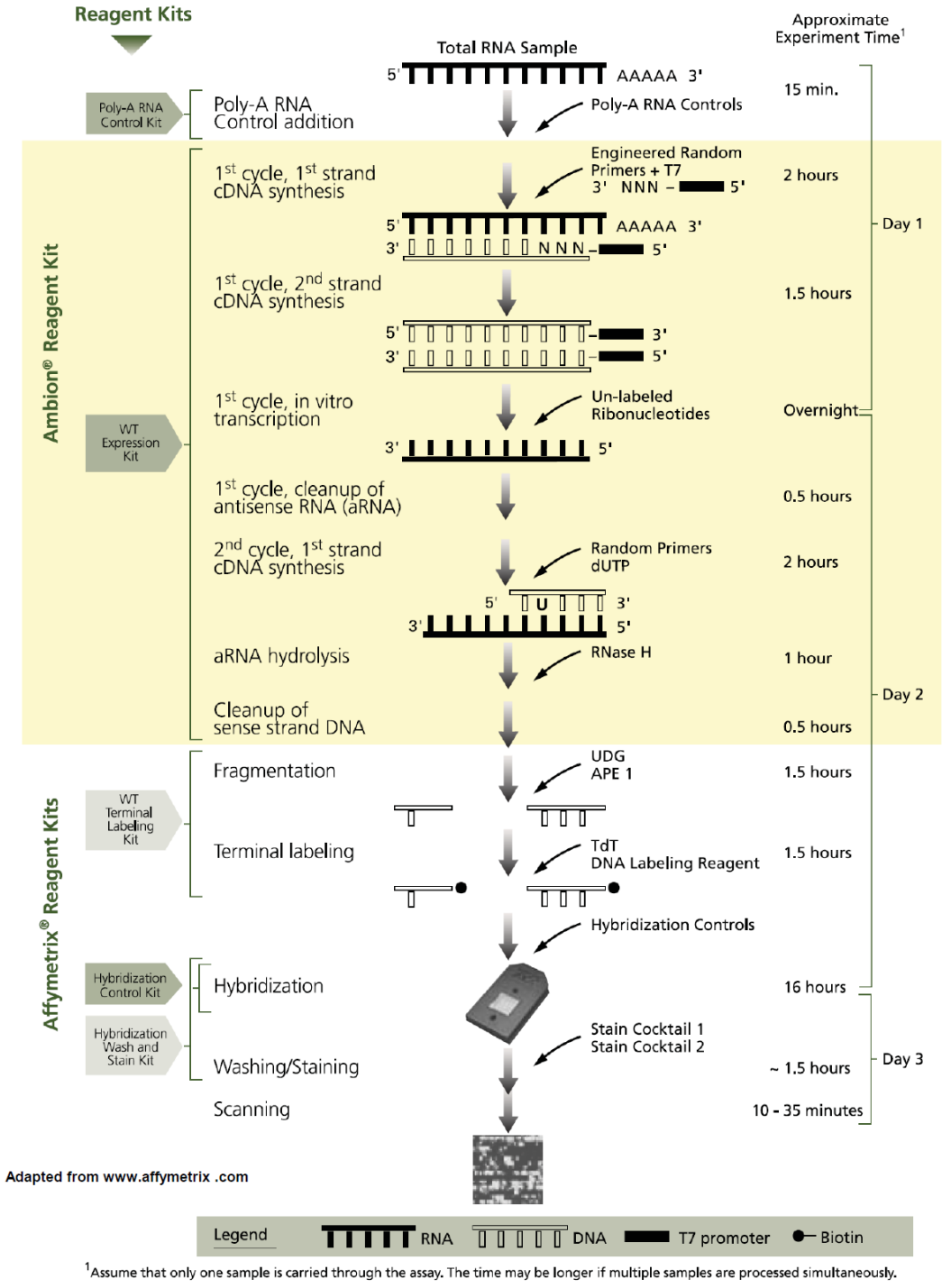


[1]Assume that only one sample is carried through the assay. The time may be longer if multiple samples are processed simultaneously.

**Figure 5: Workflow of the GeneChip® WT Terminal Labeling and Hybridization**

# Chapter IV: Results

**4.1:** **Genome-wide gene profiling microarray analysis of the AS *Ube3a*$^{m-/p+}$ mouse cerebellum**

**4.2:** **Pathway analysis identifies 3 major networks involved in the AS *Ube3a*$^{m-/p+}$ mouse cerebellum differentially expressed genes**

**4.3:** **Microarray differential gene expression validation**

**4.4:** ***Ube3a* knockdown using RNAi results in reduced M*c1r/Nr4a2* levels**

**4.5:** **Ube3a overexpression results in an elevated *Mc1r* and *Nr4a2* expression**

**4.6:** **Up-regulation of *MC1R* promoter by UBE3A is dosage dependent and is independent of its E3 ligase activity**

**4.7:** **Ube3a is associated with the *Mc1r* promoter**

**4.8:** **UBE3A up-regulates *MC1R* promoter via an E-box/SP1 element dependent mechanism**

**4.9:** **MC1R expression in the dorsal skin of AS Ube3a-null mice**

**4.10:** **Hypopigmentation is observed in *Ube3a*$^{(-/-)}$ mice**

## 4.1: Genome-wide gene profiling microarray analysis of the AS *Ube3a*$^{m-/p+}$ mouse cerebellum

We are interested in characterizing the transcriptome profile of the AS *Ube3a*$^{m-/p+}$ mice to identify genes that are affected in the absence of functional Ube3a. Hence, we checked for differential gene expression between the wildtype and *Ube3a*$^{m-/p+}$ mice cerebellum. A genome-wide microarray analysis was performed using the Affymetrix GeneChip Mouse Exon array on 4 biological replicates from each group. Genes are considered to be differentially expressed if they show a fold change of at least 1.5-fold and $p \leq 0.05$ based on Student's t-test (4).

The gene expression profiles between the two groups were analyzed using the Affymetrix microarray Core Probeset, which is based on highly confident supporting evidence from RefSeq and Genbank full length mRNAs. A total of 64 differentially expressed genes (7 up-regulated & 57 down-regulated) were identified and were statistically significant (Table 4). Most of the down-regulated genes in the *Ube3a*$^{m-/p+}$ mice appear to encode for receptors involving neurogenic functions, such as neurotransmitter receptors (e.g. *Glra1/3, Chrna4 and Drd2*). Another heavily represented group of genes that were down-regulated involves transcription regulation, functioning in neurogenesis and other physiological aspects (e.g. *Mc1r*, *Nr4a2*).

## Table 4: Microarray Gene Expression Analysis (Core Probeset): Wildtype (*Ube3a*$^{m+/p+}$) VS *Ube3a* knockout ( *Ube3a*$^{m-/p+}$ ) mice

| No | Affymetrix Transcript ID | NCBI Accession No | Gene Symbol | Gene Name | p-Value | Fold Change |
|---|---|---|---|---|---|---|
| **Up-Regulation in mutant** | | | | | | |
| 1 | 6880900 | NM_008008 | Fgf7 | fibroblast growth factor 7/ | 0.022 | 2.091 |
| 2 | 6927341 | NM_080445 | B3galt6 | UDP-Gal:betaGal beta 1,3-galactosyltransferase | 0.036 | 1.907 |
| 3 | 6817951 | AK029771 | 9330180L21Rik | RIKEN cDNA 9330180L21 | 0.015 | 1.750 |
| 4 | 6985703 | NM_026758 | Mphosph6 | M phase phosphoprotein 6 | 0.039 | 1.701 |
| 5 | 6786954 | AK085965 | 2010316F05Rik | RIKEN cDNA 2010316F05 | 0.027 | 1.587 |
| 6 | 6935555 | NM_019647 | Rpl21 | ribosomal protein L21 | 0.032 | 1.542 |
| 7 | 6935197 | NM_001038703 | Gpr146 | G protein-coupled receptor 146 | 0.035 | 1.541 |
| **Down-Regulation in mutant** | | | | | | |
| 8 | 6992946 | NM_178676 | Entpd3 | ectonucleoside triphosphate diphosphohydrolase 3 | 0.008 | -1.501 |
| 9 | 6976233 | NM_080438 | Glra3 | glycine receptor, alpha 3 subunit | 0.045 | -1.502 |
| 10 | 6967109 | NM_013643 | Ptpn5 | protein tyrosine phosphatase, non-receptor type 5 | 0.002 | -1.507 |
| 11 | 6963197 | NM_007627 | Cckbr | cholecystokinin B receptor | 0.012 | -1.517 |
| 12 | 6786049 | NM_172496 | Cobl | cordon-bleu | 0.040 | -1.531 |
| 13 | 6898010 | NM_008604 | Mme | membrane metallo endopeptidase | 0.027 | -1.532 |
| 14 | 6925872 | NM_008154 | Gpr3 | G-protein coupled receptor 3 | 0.029 | -1.542 |
| 15 | 6846576 | NM_007938 | Epha6 | Eph receptor A6 | 0.004 | -1.555 |
| 16 | 6979704 | NM_008559 | Mc1r | melanocortin 1 receptor | 0.001 | -1.556 |
| 17 | 6942379 | NM_010717 | Limk1 | LIM-domain containing, protein kinase | 0.043 | -1.561 |
| 18 | 6870979 | BC023699 | AI790298 | expressed sequence AI790298 | 0.024 | -1.566 |
| 19 | 6819928 | NM_175498 | Pnma2 | paraneoplastic antigen MA2 | 0.044 | -1.575 |
| 20 | 6960931 | NM_001033962 | Ube3a | ubiquitin protein ligase E3A | 0.016 | -1.579 |
| 21 | 6971996 | NM_021302 | Stk32c | serine/threonine kinase 32C | 0.029 | -1.587 |
| 22 | 6764046 | BC126965 | Pcp4l1 | Purkinje cell protein 4-like 1 | 0.029 | -1.589 |
| 23 | 6819244 | NM_009947 | Cpne6 | copine VI | 0.014 | -1.601 |
| 24 | 6873187 | NM_145123 | Crtac1 | cartilage acidic protein 1 | 0.002 | -1.613 |
| 25 | 6966324 | NM_010758 | Mag | myelin-associated glycoprotein | 0.038 | -1.615 |
| 26 | 6833516 | NM_008800 | Pde1b | phosphodiesterase 1B, Ca2+-calmodulin dependent | 0.049 | -1.620 |
| 27 | 6930606 | NM_178804 | Slit2 | slit homolog 2 (Drosophila) | 0.034 | -1.622 |
| 28 | 6820282 | NM_172812 | Htr2a | 5-hydroxytryptamine (serotonin) receptor 2A | 0.010 | -1.625 |
| 29 | 6760417 | NM_021306 | Ecel1 | endothelin converting enzyme-like 1 | 0.004 | -1.631 |
| 30 | 6933072 | NM_009263 | Spp1 | secreted phosphoprotein 1 | 0.047 | -1.633 |
| 31 | 6994790 | NM_178737 | AW551984 | expressed sequence AW551984 | 0.025 | -1.634 |
| 32 | 6982725 | BC111102 | 4930431L04Rik | RIKEN cDNA 4930431L04 gene | 0.032 | -1.636 |
| 33 | 6762197 | NM_008795 | Pctk3 | PCTAIRE-motif protein kinase 3 | 0.029 | -1.638 |
| 34 | 6805200 | NM_145451 | Gpx6 | glutathione peroxidase 6 | 0.026 | -1.639 |
| 35 | 6832276 | NM_172610 | Mpped1 | metallophosphoesterase domain containing 1 | 0.017 | -1.658 |
| 36 | 6947131 | NM_028880 | Lrrtm1 | leucine rich repeat transmembrane neuronal 1 | 0.044 | -1.669 |
| 37 | 6810961 | NM_033269 | Chrm3 | cholinergic receptor, muscarinic 3 | 0.020 | -1.679 |
| 38 | 6864813 | NM_011898 | Spry4 | sprouty homolog 4 (Drosophila) | 0.022 | -1.687 |
| 39 | 6750314 | NM_177164 | A830006F12Rik | RIKEN cDNA A830006F12 gene | 0.005 | -1.698 |
| 40 | 6931001 | NM_018764 | Pcdh7 | protocadherin 7 | 0.003 | -1.725 |
| 41 | 6856133 | NM_022025 | Slc5a7 | solute carrier family 5 (choline transporter) | 0.039 | -1.738 |
| 42 | 6854467 | XM_989487 | LOC671855 | similar to Rho GDP-dissociation inhibitor 3 | 0.005 | -1.753 |
| 43 | 6901119 | NM_022565 | Ndst4 | N-deacetylase/N-sulfotransferase (heparin glucosaminyl) 4 | 0.042 | -1.762 |
| 44 | 6808279 | NM_013628 | Pcsk1 | proprotein convertase subtilisin/kexin type 1 | 0.033 | -1.765 |
| 45 | 6854844 | NM_010831 | Snf1lk | SNF1-like kinase | 0.015 | -1.775 |
| 46 | 6801807 | NM_172805 | Kcnh5 | potassium voltage-gated channel, subfamily H (eag-related) | 0.007 | -1.787 |
| 47 | 6803891 | NM_178915 | Tmem179 | transmembrane protein 179 | 0.005 | -1.788 |
| 48 | 6988976 | NM_010077 | Drd2 | dopamine receptor 2 | 0.017 | -1.794 |
| 49 | 6815027 | NM_009027 | Rasgrf2 | RAS protein-specific guanine nucleotide-releasing factor 2 | 0.044 | -1.815 |
| 50 | 6931355 | NM_011670 | Uchl1 | ubiquitin carboxy-terminal hydrolase L1 | 0.041 | -1.822 |
| 51 | 6906620 | NM_011839 | Mab21l2 | mab-21-like 2 (C. elegans) | 0.031 | -1.979 |
| 52 | 6862816 | NM_144946 | Neto1 | neuropilin (NRP) and tolloid (TLL)-like 1 | 0.016 | -1.981 |
| 53 | 6785684 | NM_010904 | Nefh | neurofilament, heavy polypeptide | 0.043 | -2.088 |
| 54 | 6894253 | NM_015730 | Chrna4 | cholinergic receptor, nicotinic, alpha polypeptide 4 | 0.004 | -2.093 |
| 55 | 6886908 | NM_013613 | Nr4a2 | nuclear receptor subfamily 4, group A, member 2 | 0.028 | -2.148 |

| | | | | | | |
|---|---|---|---|---|---|---|
| 56 | 6844649 | NM_009215 | Sst | somatostatin | 0.041 | -2.211 |
| 57 | 6796691 | NM_010234 | Fos | FBJ osteosarcoma oncogene | 0.015 | -2.242 |
| 58 | 6889978 | NM_010825 | Mrg1 | myeloid ecotropic viral integration site-related gene 1 | 0.023 | -2.334 |
| 59 | 6871062 | NM_153553 | Npas4 | neuronal PAS domain protein 4 | 0.012 | -2.479 |
| 60 | 6967593 | NM_176942 | Gabra5 | gamma-aminobutyric acid (GABA-A) receptor | 0.017 | -2.548 |
| 61 | 6943974 | NM_009311 | Tac1 | tachykinin 1 | 0.013 | -2.615 |
| 62 | 6833311 | NM_010444 | Nr4a1 | nuclear receptor subfamily 4, group A, member 1 | 0.016 | -2.741 |
| 63 | 6788423 | NM_020492 | Glra1 | glycine receptor, alpha 1 subunit | 0.031 | -4.946 |
| 64 | 6881459 | NM_029530 | 6330527O06Rik | RIKEN cDNA 6330527O06 gene | 0.010 | -6.616 |

**Table 4:**

Differentially expressed genes with a fold change $\geq 1.5$ ($p \leq 0.05$ based on Student's t-test) from *Ube3a*$^{m-/p+}$ mice compared to the wildtype littermates. List is shown in the order of the most up-regulated, to the most down-regulated gene (as shown by "-"sign).

### 4.2: Pathway analysis identifies 3 major networks involved in the AS *Ube3a*$^{m-/p+}$ mouse cerebellum differentially expressed genes

The differential expressed genes identified from the microarray analysis were subjected to pathway/network analysis to allow better interpretation on their biological roles/significance. The differentially expressed genes are implicated in 3 major pathways/networks which include cell signaling, nervous system development and cell death (Figure 6). The first network involves cell signaling and fifteen AS differentially expressed genes are associated within this network including *Fgf7* and *Nr4a2*. In the brain, Nr4a2 is an orphan nuclear receptor which supports dopaminergic neurons to survive and differentiate (Figure 6A) (125). The second network involves nervous system development/functions and twelve AS differentially expressed genes are associated with this network. These include *Epha6*, a tyrosine kinase receptor essential for axon guidance, as well as *Slc5a7* which encodes choline transporter important for proper choline uptake along the synapse (Figure 6B) (126,127). The third network involves cellular development/death in which eleven AS differentially expressed genes are associated with (Figure 6C). Among them are the *Mc1r* and *Glra1* whose cellular functions are relevant to AS.

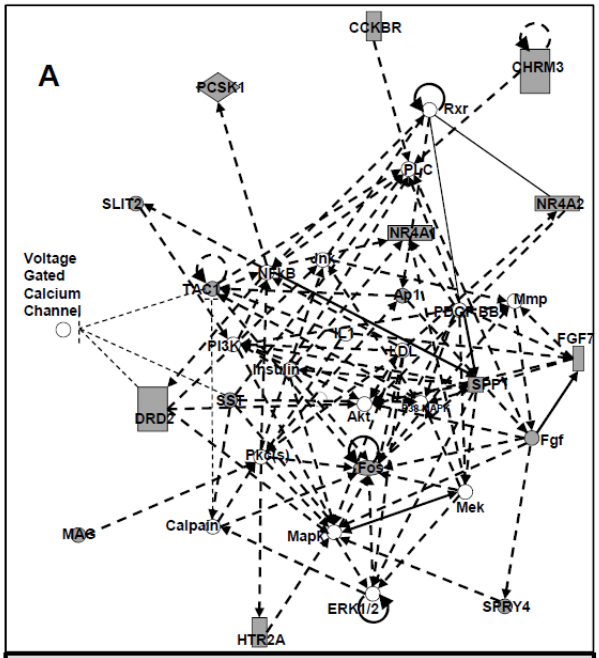


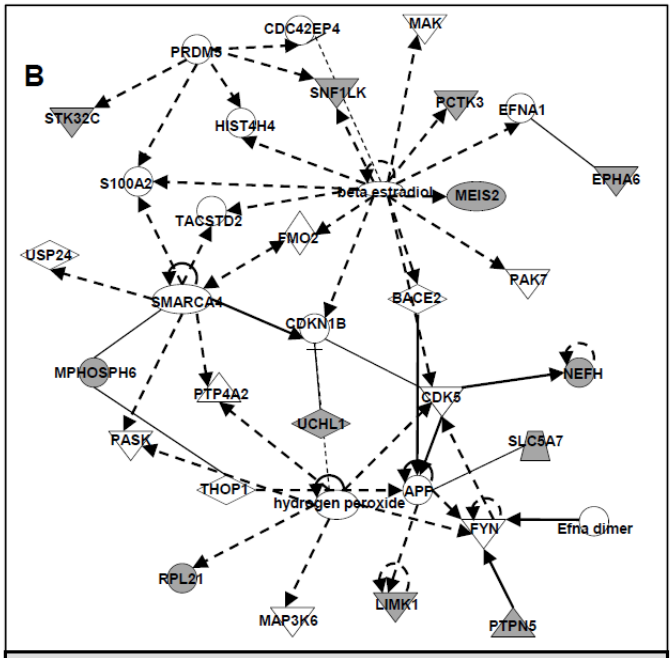


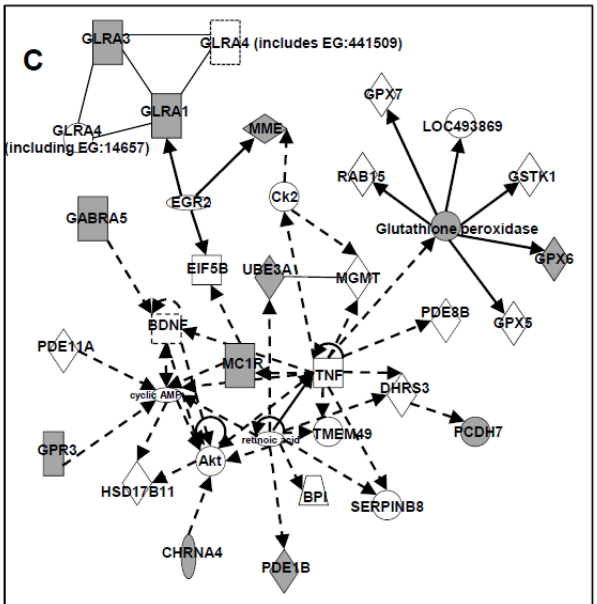


**Molecules in Network**

Akt, Ap1, Calpain, **CCKBR**, **CHRM3**, **DRD2**, ERK1/2 Fgf, **FGF7**, **FOS**, **HTR2A**, IL1 Insulin, Jnk, LDL, **MAG**, Mapk, Mek, Mmp, NfkB, **NR4A1**, **NR4A2**, P38 MAPK, **PCSK1**, PDGF BB, PI3K, Pkc(s), PLC, Rxr, **SLIT2**, **SPP1**, **SPRY4**, **SST**, **TAC1**, Voltage Gated Calcium Channel

**Top Function: Cell Signaling**

**Molecules in Network**

APP, BACE2, beta-estradiol, CDC42EP4, CDK5, CDKN1B, EFNA1, Efna dimer, **EPHA6**, FMO2, FYN, HIST4H4, hydrogen peroxide, **LIMK1**, MAK, MAP3K6, **MEIS2**, **MPHOSPH6**, **NEFH**, PAK7, PASK, **PCTK3**, PRDM5, PTP4A2, **PTPN5**, **RPL21**, S100A2, **SLC5A7**, SMARCA4, **SNF1LK**, **STK32C**, TACSTD2, THOP1, **UCHL1**, USP24

**Top Function :Nervous System Development**

**Molecules in Network**

Akt, BDNF, BPI, **CHRNA4**, Ck2, cyclic AMP, DHR53, EGR2, EIF5B, **GABRA5**, **GLRA1**, **GLRA3**, GLRA4, Glutathione Peroxidase, **GPR3**, GPX5, **GPX6**, GPX7, GSTK1, HSD17B11, LOC493869, **MC1R**, MGMT, **MME**, **PCDH7**, PDE11A, **PDE1B**, PDE8B, RAB15, retinoic acid, SERPINB8, TMEM49, TNF, **UBE3A**

**Top Function: Cell Death**

**Figure 6: Pathway analysis on differentially expressed genes**

A) Network 1 is associated with cell signaling and involves 15 of our reported differentially expressed genes (in bold). Representative genes such as *Fgf7* and *Nr4a2* are qRT-PCR validated, which are up and down-regulated in the *Ube3a*$^{m-/p+}$ mice, respectively.

B) Network 2 is associated with nervous system development and involves 12 of our reported microarray hits. *Epha6* and *Slc5a7* in this network are qRT-PCR validated showing both down-regulations in the *Ube3a*$^{m-/p+}$ mice.

C) Network 3 is associated with cell death and involves 11 genes, such as *Glra1* and *Mc1r*. Both are down-regulated in the *Ube3a*$^{m-/p+}$ mice and validated using qRT-PCR.

### 4.3: Microarray differential gene expression validation

Semi quantitative reverse transcription PCR, and qRT-PCR in biological triplicates, were employed to validate the differential expression of two representative genes from each pathway/network described above (Figure 7A, 7B). These validated genes include the fibroblast growth factor 7 (*Fgf7*), the glycine receptor alpha 1 (*Glra1*), the melanocortin-1 receptor (*Mc1r*), the nuclear receptor sub-family 4 group A member 2 (*Nr4a2*), the solute carrier family 5 member 7 (*Slc5a7*), and the ephrin type-A receptor 6 (*Epha6*), which were chosen because of their functional relevance to the AS phenotype. Other than *Fgf7* that is confirmed to be up-regulated in the AS mice, the remaining validated genes (i.e. *Glra1*, *Mc1r*, *Nr4a2*, *Slc5a7*, *Ehpa6*) were confirmed to be down-regulated. This is consistent with our prior microarray analysis data.

We then extended our differential expression validation towards the protein level for Mc1r and Nr4a2, after a recent report showed that Mc1r signaling can induce the expression of *Nr4a2* (128). To determine if down-regulation of *Mc1r* and *Nr4a2* at the mRNA level can be reflected at the protein levels, Western blot was performed comparing cerebellum total protein extract from the wildtype and *Ube3a*$^{m-/p+}$ mice. Both Mc1r and Nr4a2 protein were observed to be down-regulated in the *Ube3a*$^{m-/p+}$ mice (Figure 8A, 8B).

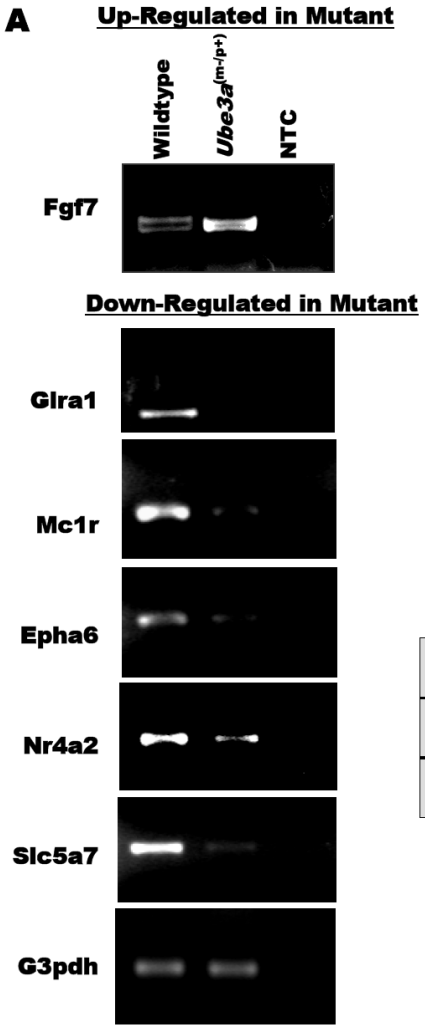


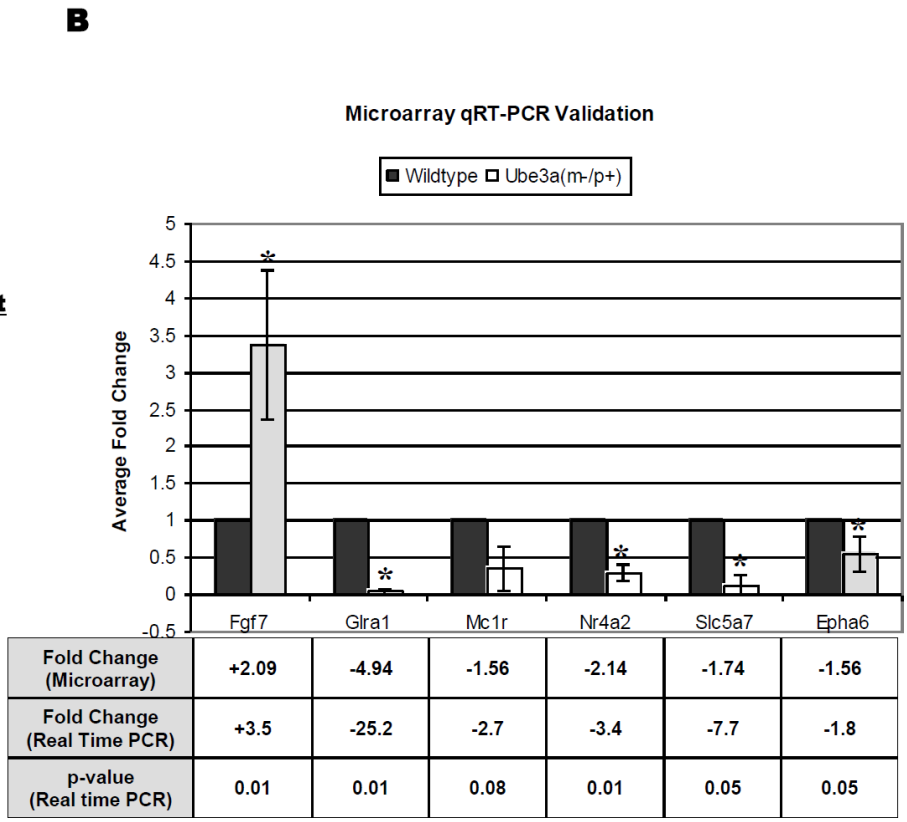


| | Fgf7 | Glra1 | Mc1r | Nr4a2 | Slc5a7 | Epha6 |
|---|---|---|---|---|---|---|
| Fold Change (Microarray) | +2.09 | -4.94 | -1.56 | -2.14 | -1.74 | -1.56 |
| Fold Change (Real Time PCR) | +3.5 | -25.2 | -2.7 | -3.4 | -7.7 | -1.8 |
| p-value (Real time PCR) | 0.01 | 0.01 | 0.08 | 0.01 | 0.05 | 0.05 |

**Figure 7: Semi quantitative reverse transcription PCR and qRT-PCR validation confirming on a selection of differentially expressed genes identified by microarray.**

(A) Semi quantitative reverse transcription PCR validation: *Fgf7* is up-regulated in *Ube3a*$^{m-/p+}$ mice, while the rest of the genes, including *Glra1, Mc1r, Nr4a2, Epha6* and *Slc5a,* are confirmed to be down-regulated. NTC: No template control.

(B) qRT-PCR validation showing the normalized mean fold change from the biological triplicates. The fold change is calculated using $2^{-(\text{mean Wildtype } \Delta CT - \text{mean } Ube3a \text{ (m-/p+) } \Delta CT)}$; "+" and "-" represents up-regulation and down-regulation of transcript, respectively; "*" indicates $p<0.05$ based on Student's t-test.

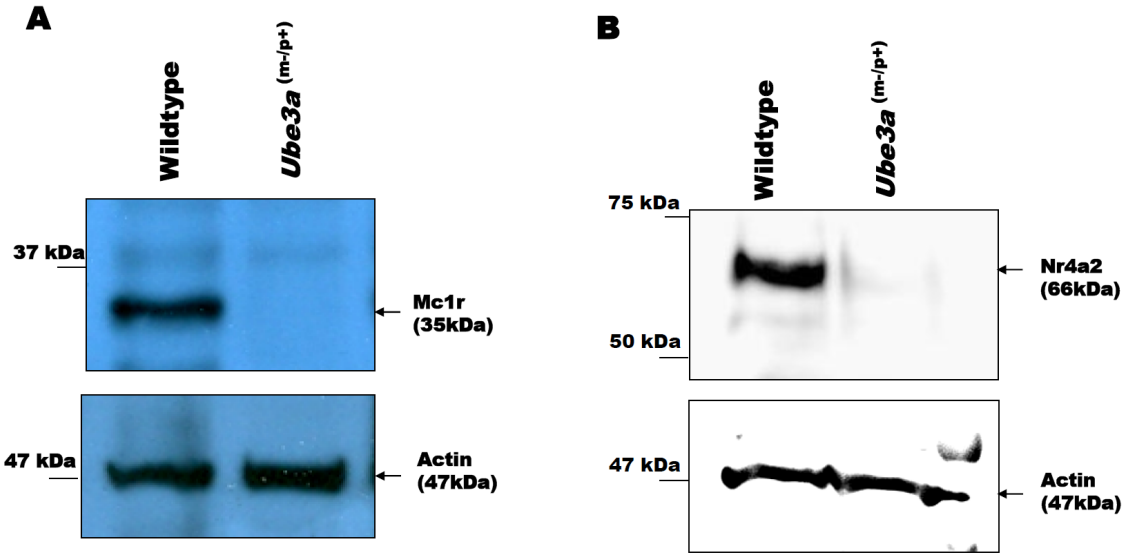


**Figure 8: Differential protein expression of Mc1r and Nr4a2 using Western blot**

Ten micrograms of total protein extracted from mouse cerebellum were analyzed by SDS PAGE using 6% acrylamide gel. Western blot analyses using antibody against Mc1r and Nr4a2 show that the 35kD Mc1r (A) and the 66kD Nr4a2 (B) protein, respectively, are down-regulated in the *Ube3a*$^{m-/p+}$ mice. Beta-actin is used as endogenous internal control in the Western blot analyses.

### 4.4: *Ube3a* knockdown using RNAi results in reduced *Mc1r/Nr4a2* levels

The possible fact that the constitutive loss of Ube3a activity during mouse development may result in an adaptive change in transcription expression in order to cope with the loss of Ube3a activity, and hence many of the transcription level changes observed may reflect an indirect, rather than direct, consequence as a result of the loss of Ube3a activity. To determine the immediate effect of loss of Ube3a activity on respective genes, an RNAi system was generated with target sequence against *Ube3a* to evaluate *Mc1r* and *Nr4a2* expression in *Ube3a* knockdown cells. P19 cells were transfected with the *Ube3a* shRNA expression plasmid and harvested after 24 hours which shows the down-regulation of *Ube3a* at both transcription and protein level. A 2-fold reduction was observed in the *Ube3a* mRNA level after knockdown (Figure 9A, 9B). In addition, Western blot analysis shows that the Ube3a protein in P19 cells was also reduced after the transfection of the *Ube3a* shRNA expression plasmid (Figure 9C). Subsequently, we checked for the relative mRNA levels of *Mc1r* and *Nr4a2* in both *Ube3a* knockdown and control cells. Both semi quantitative reverse transcription PCR and biological triplicates of qRT-PCR show that *Mc1r* and *Nr4a2* mRNA levels decreased by 8.6 and 5.3-fold respectively in the *Ube3a* knockdown cells (Figure 9A, 9B). These observations suggest that functional Ube3a is directly associated and required for *Mc1r* and *Nr4a2* gene expression.

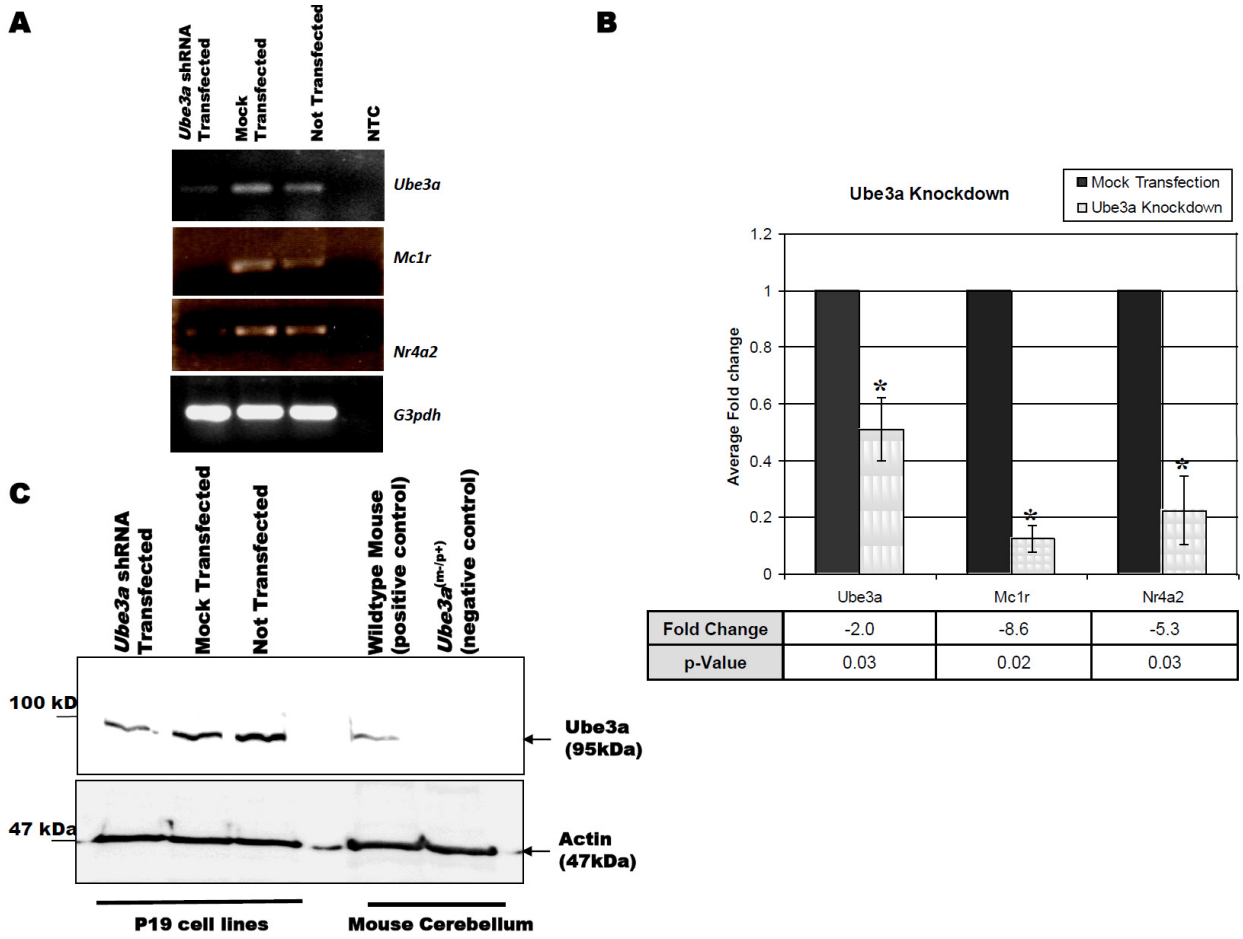


**Figure 9: Validation of down-regulation of *Mc1r* and *Nr4a2* by shRNA mediated knockdown of *Ube3a* in P19 cells.**

(A) Semi quantitative reverse transcription PCR showing the down expression of *Ube3a*, *Mc1r* and *Nr4a2* transcript in the *Ube3a* shRNA transfected cells. NTC: No template control.

(B) Biological triplicates of qRT-PCR analyses showing the normalized mean fold change. "-" represents a down-regulation in the *Ube3a* shRNA transfected cells; "*" indicates $p<0.05$ based on Student's t-test.

(C) Ten micrograms of total protein extracted from the *Ube3a* shRNA transfected and control P19 cells were analyzed by SDS PAGE using 6% acrylamide gel. Western blot analyses using antibody against Ube3a show the knockdown of the 95kD Ube3a upon transfection with the *Ube3a* shRNA plasmid (pUbe3aKD). Total protein extracted from wildtype and the $Ube3a^{m-/p+}$ mice cerebellum were used as positive and negative controls in the same Western blot analyses. Beta-actin was used as endogenous internal control in the Western blot analysis.

### 4.5: Ube3a overexpression results in an elevated *Mc1r* and *Nr4a2* expression

To further substantiate the direct role of Ube3a on *Mc1r* and *Nr4a2* expression levels, we were interested in determining if the *Mc1r* and *Nr4a2* would be affected in the event of Ube3a overexpression. Hence, we constructed an *Ube3a* expressing vector, pUbe3aOE, and transfected this plasmid into P19 cells. The cells were harvested after 24 hours later. This resulted in higher level of cellular Ube3a amount as determined by Western blot (Figure 10A). The mRNA levels of *Mc1r* and *Nr4a2* was then subsequently determined using qRT-PCR and a 5.9 and 10.9 fold increase in the mRNA levels of *Mc1r* and *Nr4a2* was observed respectively (Figure 10B).

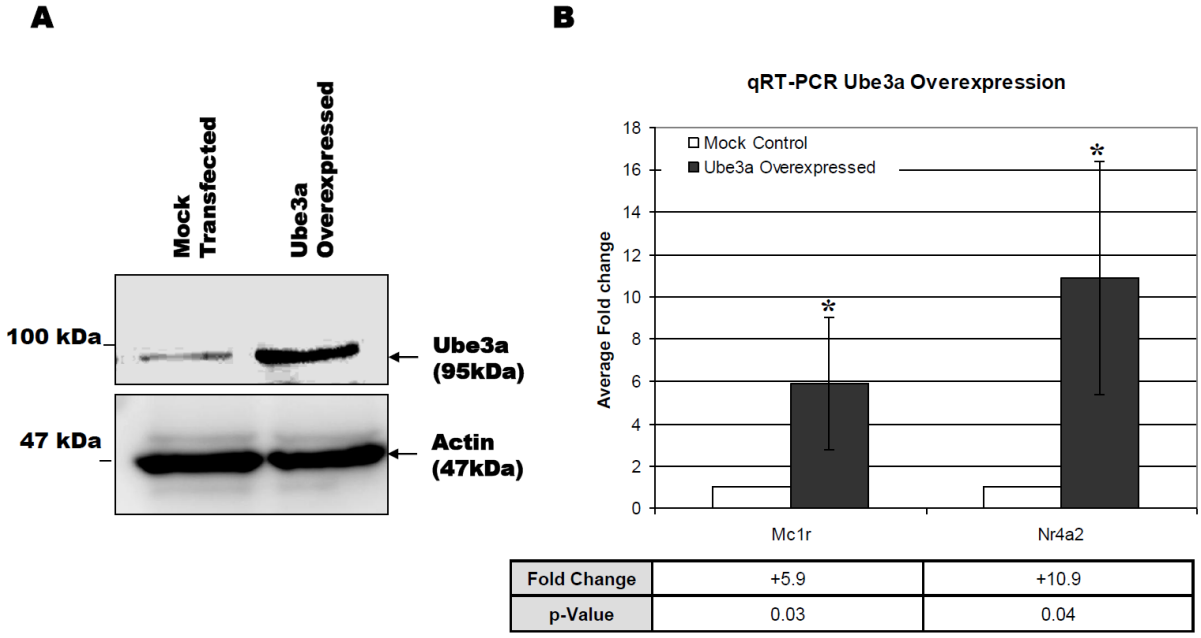


| | | |
|---|---|---|
| Fold Change | +5.9 | +10.9 |
| p-Value | 0.03 | 0.04 |

**Figure 10: Ube3a overexpression results in an up-regulation of *Mc1r* and *Nr4a2***

(A) Ten micrograms of total protein extracted from P19 cells transfected with the Ube3a expression plasmid (pUbe3aOE) and control cells were analyzed by SDS PAGE using 6% acrylamide gel. Western blot analyses using antibody against Ube3a show the increased protein level of the 95kD Ube3a upon overexpression of Ube3a. Beta-actin was used as endogenous internal control in the Western blot analysis.

(B) Biological triplicates of qRT-PCR analyses showing the normalized mean fold change of *Mc1r* and *Nr4a2* upon Ube3a overexpression in P19 cells. "+" represents an up-regulation in the *Ube3a* overexpressed cells; "*" indicates $p<0.05$ based on Student's t-test.

### 4.6: Up-regulation of *MC1R* promoter by UBE3A is dosage dependent and is independent of its E3 ligase activity

To investigate how Ube3a directly affects Mc1r expression, we hypothesized that Ube3a might exert its effect on the Mc1r promoter. Hence we constructed a *MC1R* promoter-luciferase reporter and co-transfected with 0.5, 1.0 or 1.5 µg of UBE3A expressing plasmid into P19 cells. The cells were harvested 24 hours later. P19 cells were used in this study because our above report showed that RNAi knockdown and overexpression of UBE3A has significant effect on the *Mc1r* mRNA level (129). We first performed Western blot to determine the overexpression status (Figure 11A). Subsequently, luciferase activities were then measured and then normalized with β-galactosidase activity. The relative luciferase activity was observed to increase in cells with overexpressed UBE3A as compared to the mock transfected control. This increase became more dramatic with increasing amount of UBE3A (Figure 11B). Together, these observations suggest that UBE3A is able to induce the *MC1R* promoter in a dosage dependent manner.

To determine if the ubiquitin ligase activity of UBE3A plays a role in the up-regulation of *MC1R* promoter activity, P19 cells were again co-transfected with the *MC1R* promoter-luciferase fusion construct, together with 0.5, 1.0 or 1.5 µg of UBE3A-C883A expression plasmid (Figure 11A) and harvested after 24 hours.

The UBE3A-C883A construct expresses a mutant UBE3A in which the 883th amino acid contains a cysteine to alanine mutation that negatively affects UBE3A E3 ligase (130,131). By performing subsequent luciferase assay, we found that both wildtype UBE3A and UBE3A-C883A overexpression can leads to the up-regulation of the *MC1R* promoter activity (Figure 11B). These data suggest that UBE3A can induce *MC1R* promoter activity independent of its ligase function.

In order to have a better account for the effects of UBE3A have on the *MC1R* promoter with respect to the dysregulation of melanin and pigmentation production, an identical luciferase assay was repeated in the melanoma B16 cell line. Similar results were observed in B16 cells, with UBE3A activating the *MC1R* promoter in a dosage dependent manner. The impairment of the UBE3A E3 ligase activity only modestly affected this activation (Figure 12A, B). These results suggest that the ubiquitin ligase activity of UBE3A enhances the transactivation function of UBE3A, but it is not essential for activating *MC1R* promoter activity.

To further verify that the UBE3A critical ligase residue is dispensable in the activation of *MC1R* transcriptional expression in both P19 and B16 cells, wildtype UBE3A and the mutant UBE3A-C883A were overexpressed and the *Mc1r* mRNA level was compared with those of the control using qRT-PCR after 24 hours. The *Mc1r* mRNA expression was observed to be significantly increased in cells

overexpressed with either the wildtype UBE3A or the mutant UBE3A-C883A (Figure 13A, B). One important point to note is that the magnitude of *Mc1r* up-regulation was once again observed to be higher in cells overexpressed with the wildtype UBE3A as compared to those of the mutant UBE3A-C883A. This provides additional support to the observation that UBE3A activates *MC1R* expression and its ubiquitin ligase activity is required for its full activation potential but is not essential.

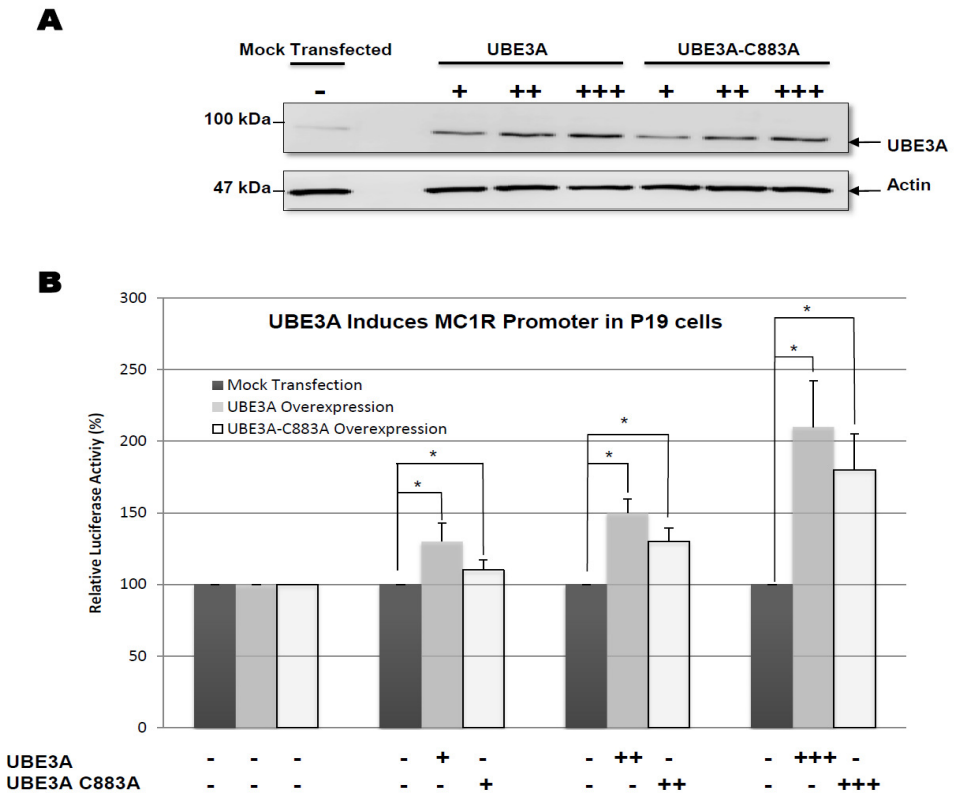


**Figure 11: UBE3A activates *MC1R* promoter in P19 cells in a dosage-dependent manner and is independent of the ubiquitin ligase function:**

(A) Total protein extracted from P19 cells transfected with 0.5 µg (+), 1.0 µg (++) and 1.5 µg (+++) of UBE3A or UBE3A-C883A expressing plasmid was analyzed by SDS-PAGE using 6% acrylamide gel to determine the overexpression status for subsequent luciferase assay. Western blot analyses using antibody against UBE3A show an increasing amount of UBE3A upon transfection of the respective amount of expressing plasmids. β-actin was used as an internal control.

(B) Relative luciferase reporter activity was determined and normalized against β-galactosidase activity in P19 cells that is co-transfected with 0.5 µg (+), 1.0 µg (++) and 1.5 µg (+++) of UBE3A or UBE3A-C883A expressing plasmid and the *MC1R* promoter-luciferase reporter plasmid. Increase luciferase activity was observed in cells with higher amounts of UBE3A when compared to the mock control. Impaired UBE3A ligase activity did not have a significant impact UBE3A ability to activate the *MC1R* promoter luciferase activity. "*" indicates $P<0.05$ based on Student's t-test when compared to the mock control.

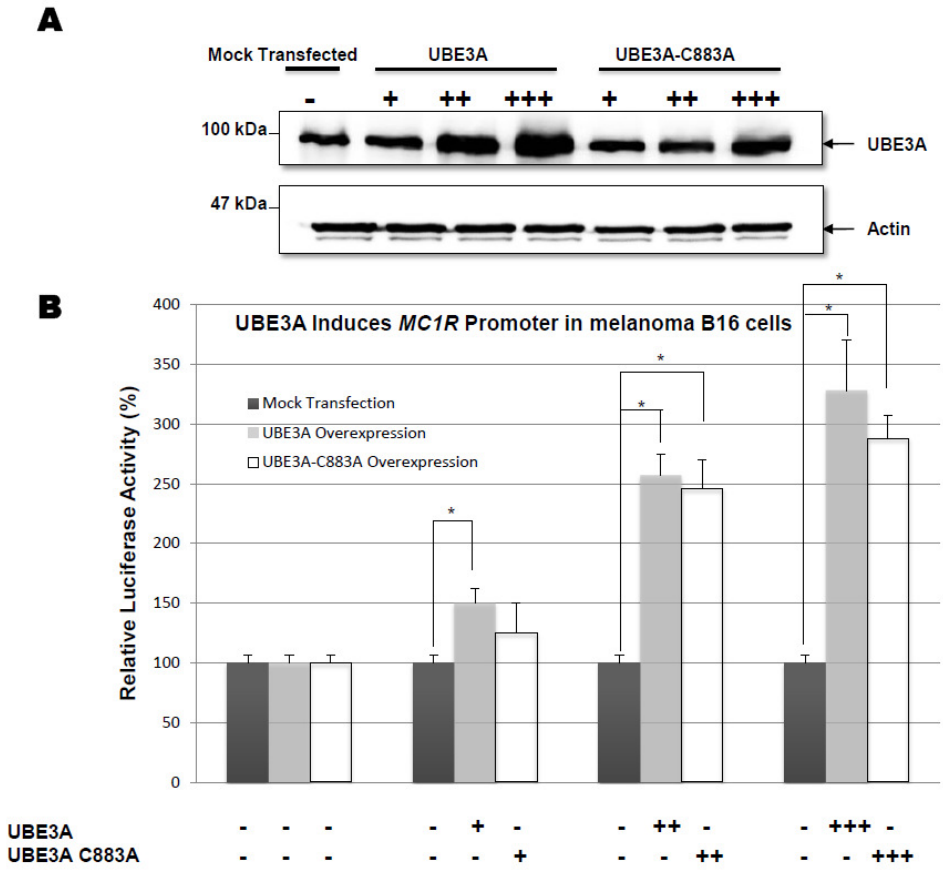


**Figure 12: UBE3A activates *MC1R* promoter in a dosage-dependent manner and is independent of the ubiquitin ligase function in the melanoma B16 cells:**

(A) To determine UBE3A overexpression status prior to subsequent luciferase assay, total protein was extracted from the melanoma B16 cells transfected with 0.5 µg (+), 1.0 µg (++) and 1.5 µg (+++) of UBE3A or UBE3A-C883A expressing plasmid, and analyzed by SDS-PAGE using 6% acrylamide gel. Western blot analyses using antibody against UBE3A show an increasing amount of UBE3A upon transfection of the respective amount of expressing plasmids. β-actin was used as an internal control.

(B) Relative luciferase reporter activity was determined and normalized against β-galactosidase activity in B16 cells that is co-transfected with 0.5 µg (+), 1.0 µg (++) and 1.5 µg (+++) of UBE3A or UBE3A-C883A expressing plasmid and the *MC1R* promoter-luciferase reporter plasmid. Increased luciferase activity was observed in cells with higher amounts of UBE3A when compared to the mock control. Impaired UBE3A ligase activity only modestly affected UBE3A ability to activate the *MC1R* promoter luciferase activity. "*" indicates $P<0.05$ based on Student's t-test when compared to the mock control.

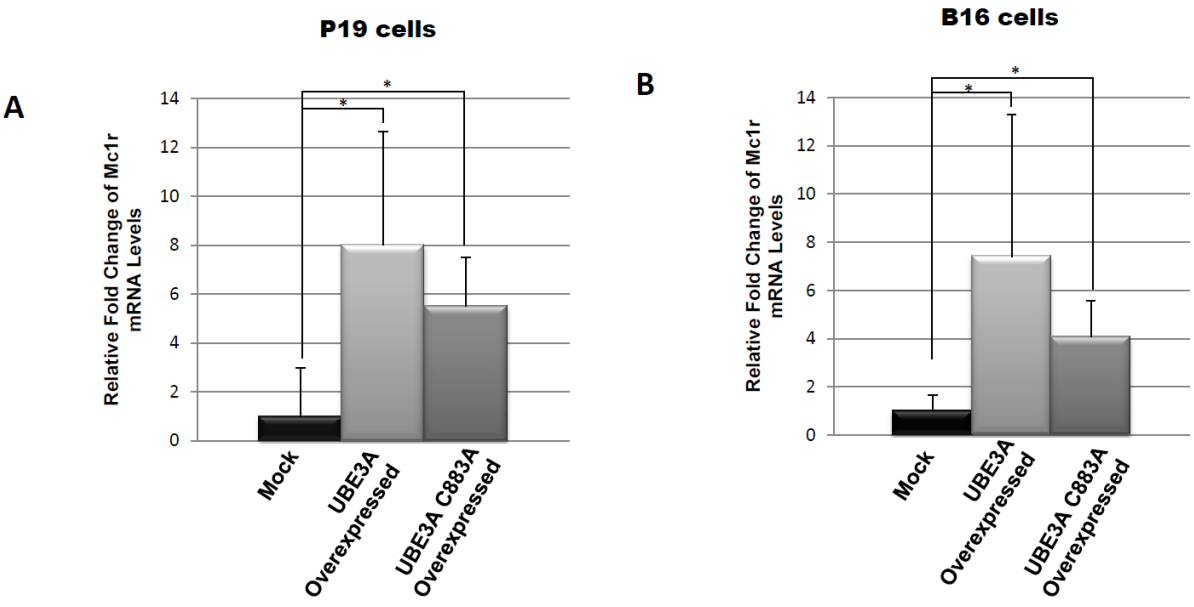


**Figure 13: UBE3A up-regulates *MC1R* mRNA level with or without its functional ubiquitin-ligase critical residue.**

The *Mc1r* mRNA level was analyzed in P19 (A) and B16 (B) cells transfected with 4 µg of wildtype UBE3A, mutant *UBE3A-C883A* expressing plasmid or the control plasmid using qRT-PCR. An up-regulation of *Mc1r* expression was observed in cells overexpressed with mutant UBE3A-C883A compared to the control cells but the up-regulation was relatively lower when compared to cells overexpressed with the wildtype UBE3A.

### 4.7: Ube3a is associated with the *Mc1r* promoter

In order to up-regulate the *MC1R* promoter activity, we hypothesized that UBE3A physically associated with the *MC1R* promoter. To identify the putative activator recognition site, we search for conserved DNA elements along the *MC1R* promoter region by a comparative genomic approach. Since both P19 and B16 cell lines used in our experiment are derived from mouse and are responsive to Ube3a levels, we compared the human and mouse *MC1R* promoter region and identified a homologous region within the human *MC1R* minimal promoter region that contains a conserved and functional E box element, as well as a human SP1 site which was previously reported to be functional as well (Figure 14A) (129,132-134). We then performed ChIP assay using anti-Ube3a antibody and showed that Ube3a can be immunoprecipitated with this highly conserved *Mc1r* promoter region in P19 and B16 cell lines (Figure 14B, C). This data shows that Ube3a, directly or via other complexes, regulates *Mc1r* expression by physically associating with the *Mc1r* promoter.

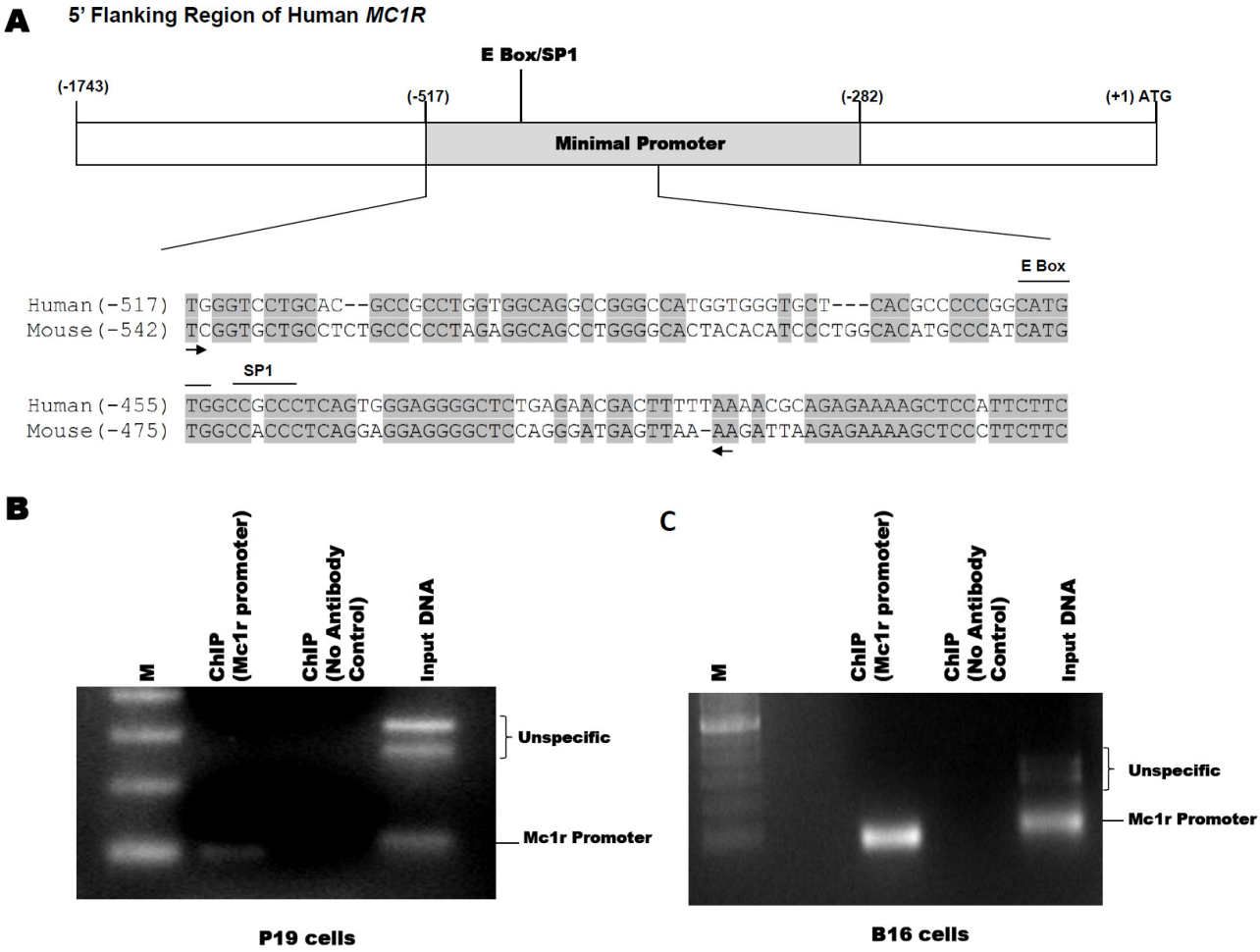


**Figure 14: Ube3a is recruited to the homologous region of the mouse and human *Mc1r* promoter.**

(A) Schematic diagram of the human *MC1R* promoter showing the previously reported minimal promoter region. Alignment of human *MC1R* minimal promoter region with 5' flanking sequence of mouse *Mc1r* transcript shows that this minimal promoter is homologous and contains a conserved E Box site and a human SP1 site.

(B) Chromatin immunoprecipitation assay using anti-Ube3a antibody demonstrating Ube3a physical association with the *Mc1r* promoter region in P19 cells.

(C) Chromatin immunoprecipitation assay using anti-Ube3a antibody demonstrating Ube3a physical association with the *Mc1r* promoter region on B16 cells.

### 4.8: UBE3A activates *MC1R* promoter via an E-box/SP1 element dependent mechanism

Since UBE3A appears to act on the *MC1R* minimal promoter, we decided to determine if the E-box/SP1 site along this region is required for activation of the promoter by UBE3A. We hypothesized that the deletion of the E-box/SP1 element will render the promoter insensitive to UBE3A stimulation. We constructed a *MC1R* promoter-luciferase fusion construct with the E-box/SP1 deleted in the minimal promoter region (pMC1RPDel). We first verified UBE3A overexpression after 24 hours post-transfection using Western blot (Figure 15A, 16A) and subsequently measured the luciferase activity upon UBE3A overexpression in both P19 and B16 cells. We found that UBE3A overexpression no longer elevated the luciferase activity in cells transfected with pMC1RPDel (Figure 15B, 16B).

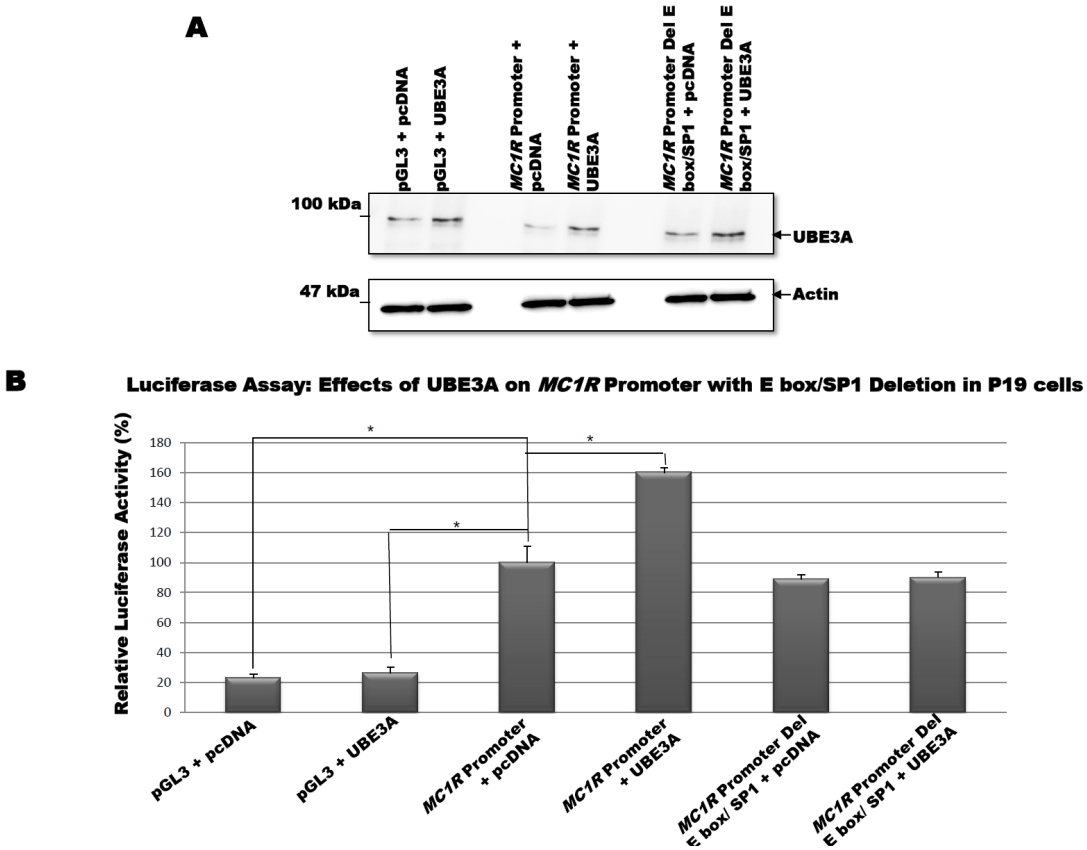


**Figure 15: The E box/SP1 site in the human *MC1R* minimal promoter is required for UBE3A transactivation in P19 cells.**

(A) Total protein extracted from P19 cells transfected with 1.0 µg of UBE3A expressing plasmid was analyzed by SDS-PAGE using 6% acrylamide gel to determine the UBE3A overexpression status for subsequent luciferase assay. Western blot analyses using anti-UBE3A antibody showed an increasing amount of UBE3A in cells transfected with the UBE3A expressing plasmids. β-actin was used as an internal control.

(B) Luciferase assay was performed to determine the functional significance of the E Box/SP1 site along the human *MC1R* minimal promoter. P19 cells were co-transfected with UBE3A expressing plasmid and wildtype *MC1R* promoter-luciferase reporter plasmid (pMC1RP) or *MC1R* promoter-luciferase reporter plasmid containing deletion of the E box/SP1 (pMC1RPDel). Subsequent relative luciferase reporter activity was measured and normalized against β-galactosidase activity, which showed that the lack of the E box/SP1 site abolishes UBE3A ability to transactivate *MC1R* promoter activity. "*" indicates $P<0.05$ based on Student's t-test when compared to the mock control.

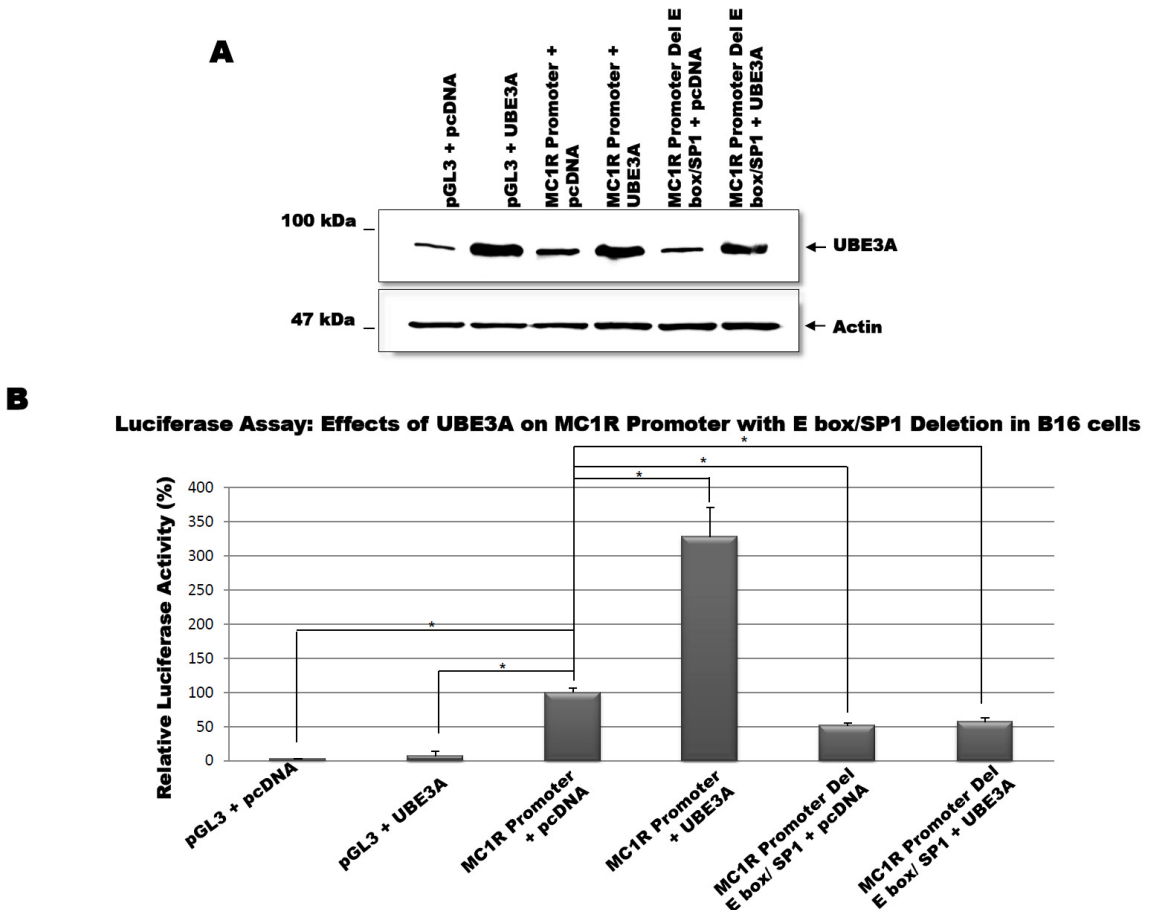


**Figure 16: The E box/SP1 site in the human *MC1R* minimal promoter is required for UBE3A transactivation in B16 cells.**

(A) Total protein extracted from B16 cells transfected with 1.0 µg of UBE3A expressing plasmid was analyzed by SDS-PAGE using 6% acrylamide gel to determine the UBE3A overexpression status for subsequent luciferase assay. Western blot analyses using anti-UBE3A antibody showed an increasing amount of UBE3A in cells transfected with the UBE3A expressing plasmids. β-actin was used as an internal control.

(B) Luciferase assay was performed to determine the functional significance of the E Box/SP1 site along the human *MC1R* minimal promoter. B16 cells were co-transfected with UBE3A expressing plasmid and wildtype MC1R promoter-luciferase reporter plasmid (pMC1RP) or MC1R promoter-luciferase reporter plasmid containing deletion of the E box/SP1 (pMC1RPDel). Subsequent relative luciferase reporter activity was measured and normalized against β-galactosidase activity, which showed that the lack of the E box/SP1 site abolishes UBE3A ability to transactivate *MC1R* promoter activity. "*" indicates $P<0.05$ based on Student's t-test when compared to the mock control.

We then determined if multiple E-box/SP1 elements will affect reporter gene activity in response to UBE3A by constructing three luciferase fusion reporters, each containing the CMV minimal promoter and either one (pEBSP1), two (pEBSP2) or three (pEBSP3) E-box/SP1 response element (Figure 17). The respective luciferase activities for each construct in UBE3A overexpressed P19 and B16 cells were then measured after 24 hours post-transfection. We found that increasing the number of the E-box/SP1 response element resulted in an increase in luciferase activity in both cell types (Figure 17A, B). Altogether, these results suggest that UBE3A modulates *MC1R* expression by exerting its effect via the E-box/SP1 site on the *MC1R* minimal promoter.

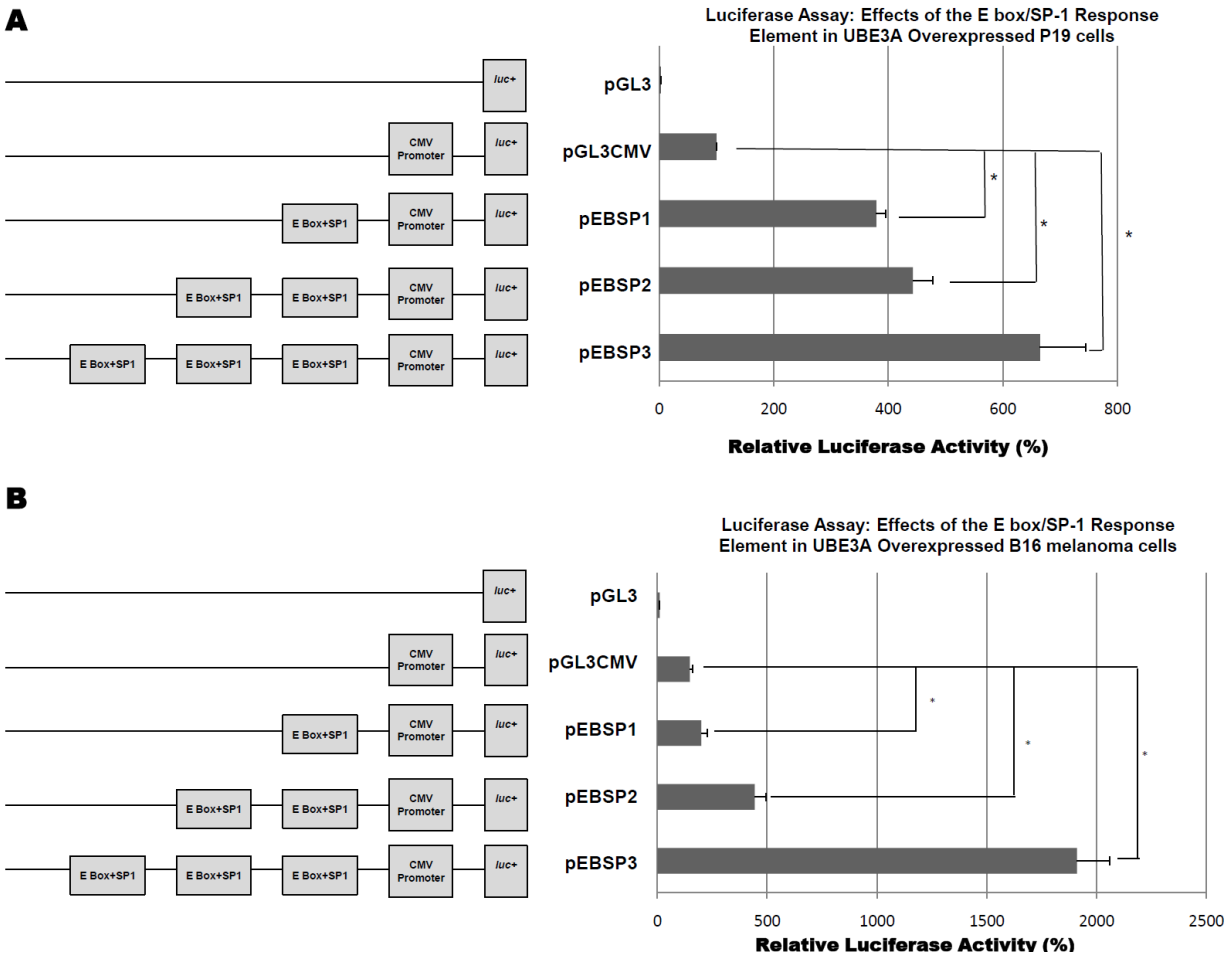


**Figure 17: Multiple E box/SP1 elements enhance the promoter-luciferase activity in UBE3A overexpressed P19 and B16 cells**

P19 and B16 cells were co-transfected with the UBE3A expressing plasmid and the CMV promoter driven luciferase reporter containing one (pEBSP1), two (pEBSP2) or three (pEBSP3) E box/SP1 element to test its functional significance. Subsequent luciferase assay was determined and normalized against β-galactosidase activity, demonstrating an elevated luciferase activity with increasing number of E box/SP1 response elements in both P19 (A) and B16 (B) cell types. "*" indicates $P<0.05$ based on Student's t-test when compared to the mock control.

### 4.9: MC1R expression in the dorsal skin of AS Ube3a-null mouse

Since MC1R is plays a paramount role in pigment regulation/production, and since UBE3A is able to activate *MC1R* promoter activity and transcription expression, we expected a reduction in Mc1r protein level in the skin of mice with Ube3a deficiency. We first preformed Western blot to determine the Mc1r level using protein extracted from the dorsal skin of the wildtype and the AS *Ube3a*$^{(-/-)}$ mice. An apparent decrease in Mc1r level was observed in the dorsal skin of the *Ube3a*$^{(-/-)}$ mice as compared to their wildtype littermates (Figure 18A). This decreased Mc1r expression in the mouse skin is consistent with those observed in the mouse cerebellum described above. To identify the localization and the loss of Mc1r expression, we then performed histological examination on the mouse dorsal skin. Mc1r expression was observed to be encompassing around hair follicles, as well as below the epidermis in the wildtype mice. The expression was however almost undetectable in the *Ube3a*$^{(-/-)}$ mice (Figure 18B).

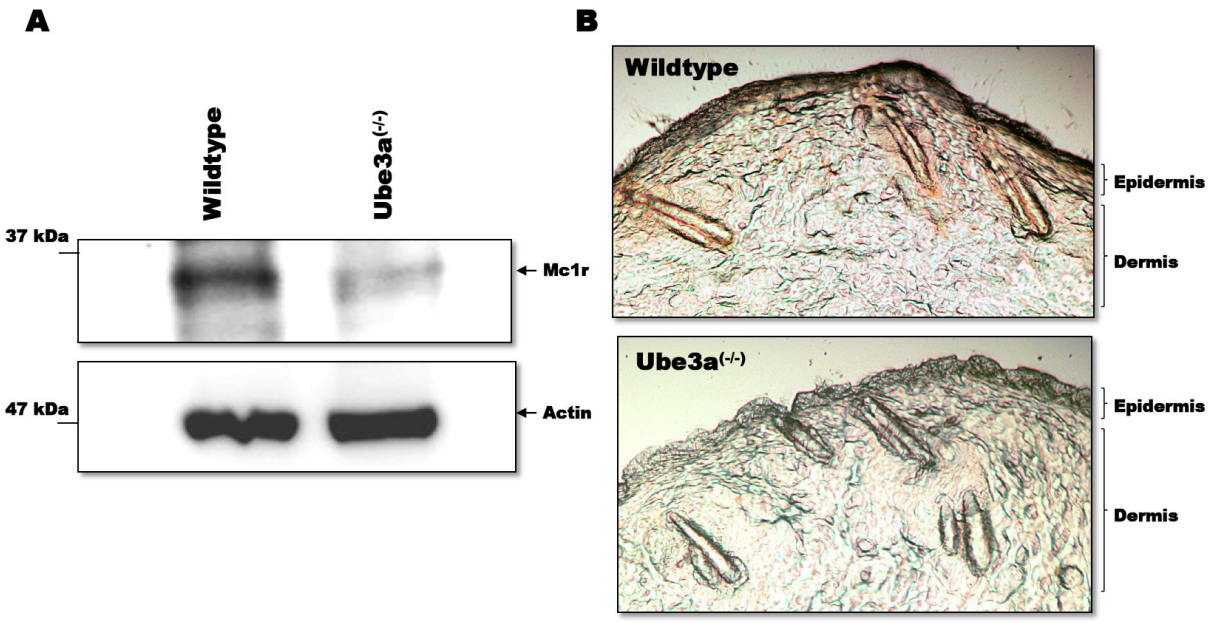


**Figure 18: Mc1r expression is dramatically decreased in the mouse skin**

(A) Total protein extracted from the dorsal skin of wildtype and *Ube3a*$^{(-/-)}$ mice were analyzed by SDS-PAGE using 8% acrylamide gel. Western blot analyses using anti-Mc1r antibody show an apparent decrease in Mc1r expression in the *Ube3a*$^{(-/-)}$ mouse skin. β-actin was used as an internal control.

(B) Wildtype and *Ube3a*$^{(-/-)}$ mouse dorsal skin were snapped frozen and sectioned for immunohistology chemical staining analyses using anti-Mc1r antibody. Subsequent detection using 3,3' Diaminobenzidine shows that Mc1r is expressed below the epidermis and mainly confined around the hair follicles in the wildtype mice and relatively low in expression in the *Ube3a*$^{(-/-)}$ mice.

### 4.10: Hypopigmentation in AS *Ube3a*-null mice

Since Mc1r expression level was significantly decreased in the *Ube3a*$^{(-/-)}$ mice, and since Mc1r is an important positive regulator of pigmentation, we assessed for any potential hypopigmentation in the dorsal skin of the *Ube3a*$^{(-/-)}$ mice that was previously not reported. We observed that *Ube3a*$^{(-/-)}$ mice appeared fairer in the dorsal skin when compared to their wildtype littermates (Figure 19A). Since a previous report showed that skin pigment is more pronounced on non-hairy regions of the mouse, such as the footpads, we also checked for any pigment difference in the AS mouse footpad (135). We observed that *Ube3a*$^{(-/-)}$ mice exhibited speckle-like pigment on the footpad, whereas their wild-type littermates showed more concentrated and denser pigment (Figure 19B). These observations further reinforces the idea that Ube3a deficiency can lead to low Mc1r expression that is associated with and results in the hypopigmentation phenotype.

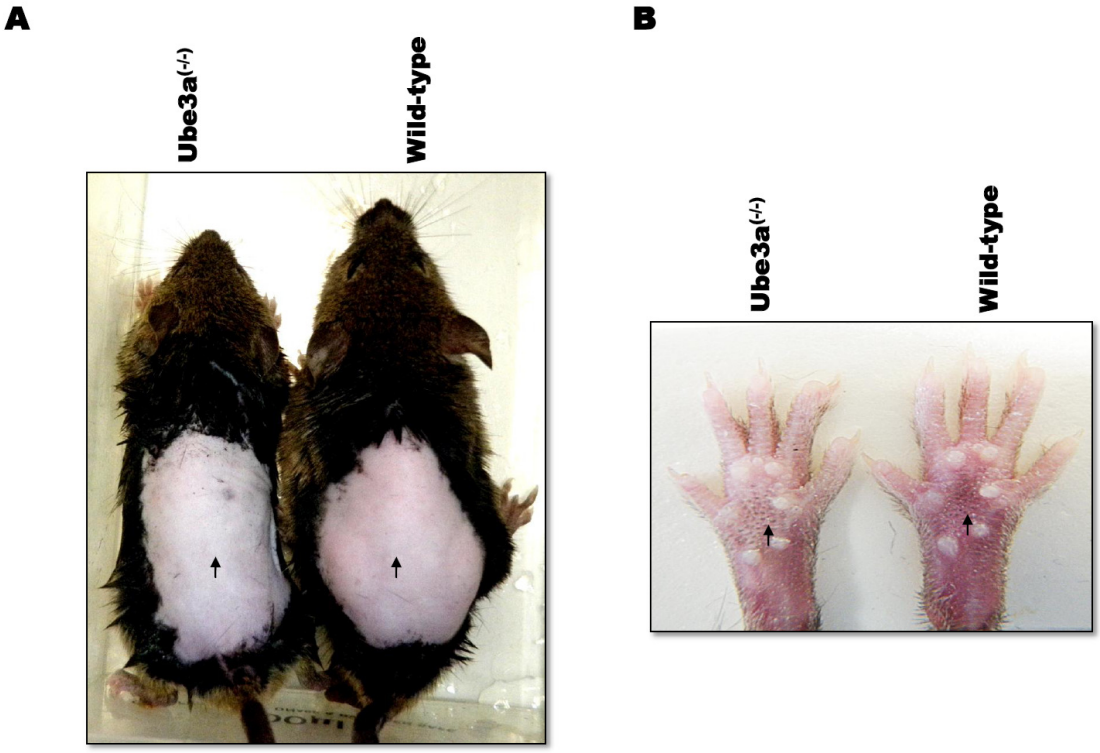


**Figure 19: Hypopigmentation is observed in the *Ube3a*$^{(-/-)}$ mouse dorsal skin and footpad**

(A) *Ube3a*$^{(-/-)}$ mice exhibit relative fairer skin tone around the dorsal region when compared to their wild-type littermates.

(B) Since the mouse footpad region contains more skin melanocytes as compared to other hairy regions of the mouse, the wildtype and *Ube3a*$^{(-/-)}$ mice were observed for their relative pigmentation. In the *Ube3a*$^{(-/-)}$ mice, pigments in the footpad regions appeared sparse and speckle-like whereas those in the wildtype appeared stronger and more concentrated.

# Chapter V: Discussion

**5.1: Interpretation of the gene expression profile of the Angelman syndrome mouse: What does it disclose?**

**5.2: The current controversy of hypopigmentation in Angelman syndrome:**

**5.3: Novel transcriptional regulation target of UBE3A: The Melanocortin-1-Receptor (*MC1R*)**

**5.4: UBE3A: The multi-functional role**

# 5.1: Interpretation of the Gene Expression Profile of the Angelman Syndrome Mouse Brain: What does it disclose?

Lack of functional maternal Ube3a expression in imprinted brain tissue can result in an accumulation of target proteins which are meant to be degraded via the UPS, and/or a dysregulation of genes expression due to the lack of the coactivation ability of Ube3a. These consequence may attribute towards the development of AS. Therefore studying the gene expression profile of the AS mice will provide useful insights into the molecular mechanisms of AS.

A genome-wide microarray transcriptome analysis was performed to detect differential gene expression between wildtype and *Ube3a*$^{(m-/p+)}$ mouse cerebellum. The mouse cerebellum was used because electrophysiology recordings reveal abnormal oscillatory activity in the AS mice (69). In addition, most AS patients show motor incoordination and these motor movements are controlled by the cerebellum. It has previously been shown that the parental-specific expression of the imprinted *Ube3a* in the human and mouse cerebellum is unique (4). Interestingly this imprinting characteristic is not observed in the chicken, highlighting the evolution of *UBE3A* imprinting in mammalian vertebrates (136).

The AS *Ube3a*$^{(m-/p+)}$ mouse gene profile reveals several neurotransmitter receptors that are differentially expressed. This includes the Glycine receptor (*Glra1*), Gamma-aminobutyric acid receptor (*Gabra5*) and the Dopamine receptor (*Drd2*). It was previously shown that the *UBE3A*$^{YFP}$ fusion protein localizes at the pre/post synaptic regions of cultured hippocampal neurons and may directly regulate the development and/or synaptic functions (77). There has always been great focus on the utility of UBE3A in neuronal synapse and how it can undermine synaptic functions. Proper neuro-signal transduction and normal motor/neuronal functions could be affected as a result of the down-regulation of these neurotransmitter receptors. For example, mutations in *Glra1* result in hyperekplexia. Patients show provocative exaggerated startle reactions upon stimulus, for example clapping or making other noises. Sudden muscle stiffness and 'drop seizures' were also observed in these patients and was first described by Kirstein and Silfverskiold in 1958 (137). These symptoms show overlapping phenotype to AS, suggesting that the cause of some of the AS phenotype, seizure for example, might be associated with lack of *Glra1* expression. It is currently unclear why *Gabra5* located adjacent to *Ube3a* in mouse (7c) and human (15q12), is down-regulated in *Ube3a* deficient mouse. Other than direct or indirect mechanisms associated with the loss of the coactivator and/or ubiquitin ligase functions of Ube3a, it is possible that either a chromatin structure alteration or the loss of a positive regulatory element caused by *Ube3a* knockout may lead to down-regulation of *Gabra5*. A similar effect is

observed in the *Mecp2* deficient mouse model affecting the up-regulation of *Irak1*expression (138,139).

Another heavily represented group of differentially expressed genes involve neuro-developmental genes, such as the Nr4a subfamily receptors. The Nr4a subfamily receptors, Nr4a1 (Nurr77), Nr4a2 (Nurr1) and Nr4a3 (NOR-1) are orphan receptors, widely known for their close ligand binding site. The down-regulation of the Nr4a2 in AS mice was confirmed by qRT-PCR and Western blot, suggesting an important role in the pathogenesis of the disorder. Reducing the expression of Nr4a2 in the brain might explain certain AS phenotypes, including poor learning/memory, and motor incoordination. In the rat hippocampus, *Nr4a2* knockdown was reported to affect spatial discrimination, learning and memory (140). In the AS mouse model, where Nr4a2 is down-regulated, the mice also show severe long term potentiation and learning impairment (22). In contrast, *Nr4a2* mRNA expression was found to be increased during learning in the rat model (141).

Recently, Nr4a2 has been linked to the establishment and development of the nervous system by interacting with Wnt signaling via beta-catenin (142). More importantly, *Nr4a2* was reported to be critical for induction and survival of dopaminergic neurons (125). $Nr4a2^{+/-}$ mice appeared normal at birth, but develop motor deficit as a result of reduced numbers of dopaminergic neurons (143).

Parkinson's disease patients also show steady degeneration of dopaminergic neurons upon onset of the disease in the absence of another E3 ligase, Parkin. It was suggested that Parkin can mediate ubiquitination of specific cellular substrates required for the survival of dopaminergic neurons (144). This poses a similar situation where AS mice were shown to have reduced numbers of dopamine neurons in a latest report (68). Hence, the motor dysfunction seen in AS patients as a result of loss of maternal Ube3a is likely to be related to the decreased levels of Nr4a2, which mediates the induction and survival of dopaminergic neurons.

Interestingly, the transcription of *Nr4a2* was recently reported to be regulated by *Mc1r*, another gene validated to be down-regulated in the AS mice cerebellum (128). In the brain, Mc1r was shown to prevent inflammation, as well as to provide a neuroprotective effect on the brain cell population (145). However this G-coupled receptor is more widely studied in peripheral tissues such as the skin for its important role in the upstream regulation of pigment production (112). There are three major types of pigment melanin determining skin color, namely the black/brown eumelanin, the yellow/red pheomelanin and the dark neuromelanin. In the human skin, the quantity, ratio and quality of eumelanin and pheomelanin determine the color of the skin and is regulated by Mc1r. There is currently no report of Mc1r regulating the production of neuromelanin, the third type of pigment present predominantly in the brain. Neuromelanin also serves to protect

neurons, in particular against oxidative stress, and is assumed to be involved in the coordination of movement, a major phenotype lacking in AS patients (145,146). This neuro-pigment is associated with the radical aggression and death of substantia nigra neurons seen in Parkinson's disease and its synthesis pathway is still unknown. The fact that Mc1r is expressed in the wildtype mouse brain and this expression is decreased in the AS mouse shows the important role the receptor has on the brain. Further study of Mc1r function in the brain is likely to shed light on how its low expression in AS brain could contribute to the overall development of the disease.

## 5.2: The controversy of hypopigmentation in Angelman syndrome

The effects that UBE3A has on *MC1R* expression suggest an important consequence on the pathogenesis of AS with respect to its hypopigmentation trait. The information gathered in this report may reconcile a current neglected controversy of AS phenotype variation.

A majority of type I AS patient (large deletion of 15q11-q13) exhibit hypopigmentation (~ 90%), which is currently attributed towards the haploinsufficiency of the *OCA2* gene that is often deleted with *UBE3A* along 15q11-q13 (29,121-123). *OCA2* mutation alone causes the autosomal recessive oculocutaneous albinism type II (MIM 203200). However, AS patient with deletion of maternal 15q11-q13 should have another putative functional copy of OCA2 from the paternal allele. Therefore theoretically, these patients should not manifest the phenotype. Few patients have been reported to have mutations in their paternal inherited *OCA2* in addition to the loss of maternal inherited *OCA2* as a result of the microdeletion (122,123).

The diminished Mc1r expression as a result of the loss of Ube3a appears to have an important causative role in the AS hypopigmentation trait. MC1R was previously shown to interact with OCA2 in an epistasis manner and is shown to be able to mask or modify OCA2 phenotype (147). This interaction is presumed to be influencing human pigmentation (148). Pigmentation has always been considered to be a multigenic trait, thus portraying the important interaction network of genes in regulating pigmentation. Since MC1R is an important upstream element regulating melanogenesis, we propose that complete deletion of maternal *UBE3A* in Type I AS patients can cause a decrease in the MC1R expression, which together with a hemizygous *OCA2* will result in a synergistic effect and hypopigmentation phenotype.

The fact that UBE3A regulates *MC1R* expression, via its intrinsic coactivator domain and independent of its ligase function, also provides a possible explanation why 20-50% of AS type IV patients with *UBE3A* mutations exhibit hypopigmentation to a certain extent even though both *OCA2* alleles are supposedly intact (44). The great majority of these AS type IV patients have mutations along the C-terminal of *UBE3A*, leaving a supposedly unaffected N-terminal where the coactivation domain resides (29,36,37). In support of this, analysis of patient genotypes also reveals that most AS type IV patients with only UBE3A mutations have an intact coactivation domain and it was suggested in the

same report that the phenotype observed in this group of patient should arise from the lack of ubiquitin ligase activity (75). Only approximately 20% of patients in this group exhibit hypopigmentation (29). This report shows that the regulation of *MC1R* expression by UBE3A is independent of its ligase function at the C-terminal, which may explain the low occurrence of the hypopigmentation trait seen among type IV AS patients compared to those of type I AS patients. The UBE3A coactivation domain is intact in most of the type IV patients and thus is able to activate *MC1R* expression. The AS mouse model used in this study contains deletion along *Ube3a* exon 2 which causes a translational frameshift, creating a complete destruction of UBE3A function, including its coactivation domain and ligase activity (22). Here we show that the $Ube3a^{(-/-)}$ mice appeared to have mild hypopigmentation in their dorsal skin and foot pad when compared to their wildtype littermates, most likely due to the impaired Ube3a coactivation function that is required for transactivating *Mc1r*.

The mild hypopigmentation observed in the dorsal skin of the $Ube3a^{(-/-)}$ mice described here may be more pronounced in the case of human AS patients. AS patients are exposed to everyday external factors, such as UV irradiation from outdoor activities, over long periods of time that plays an important role in post-natal pigment development. Hence differences in skin color between AS patients who have genetically impaired pigment production and those of their normal peers

will be more pronounced. In contrast, the laboratory mice bred in an indoor environment are not subjected to any of such stimuli and therefore the difference observed may be lesser. Exposure to the sun UV irradiation induces various stresses and stimulate melanin production via the cAMP-dependent pathway (149). In particular, UV stress stimulation triggers the release of signaling molecules including the α-melanocyte-stimulating hormone (α-MSH), the ligand for the MC1R receptor (150). Ligand activation of MC1R leads to the increase in intracellular cAMP levels which leads to induction of expression of melanogenesis-related proteins.

Our finding shows that the lack of UBE3A will affect regular pigment production through the inability to activate *MC1R* expression. Although there has not been any other report showing a direct relationship between UBE3A and pigmentation, there are a few studies showing strong evidence of melanin production regulation by previously identified UBE3A interacting partners. For example, the heat shock protein 70 (HSP70), an interacting partner of UBE3A, was elegantly demonstrated to suppress melanin production under UV-B irradiation (88,151). This study also showed that HSP70 interacts with the microphthalmia-associated transcription factor (MITF) and the two proteins co-localize in the nucleus. It was suggested in the study that HSP70 binds directly to MITF and inhibits its specific binding to target promoters. The fact that UBE3A interacts with HSP70 is relevant to our

findings, such that UBE3A regulates the *MC1R* promoter physically along the E box element of the promoter where MITF was previously shown to bind (133,134). Hence it is plausible that together with MITF, UBE3A activates the *MC1R* promoter, and HSP70 will intercept by binding onto MITF and thus suppressing its activation. UBE3A may then bind to HSP70 as to lift this effect. In addition, HSP70 expression is up-regulated by stressors (88,152). The initial finding of the interaction between HSP70 and UBE3A suggest that UBE3A may function in cellular quality control via stress response (88). Indeed back in 1999, UBE3A was previously identified in a screen for stress-response gene in the *Caenorhabditis elegans* (153). Hence individuals devoid of UBE3A may not respond well in the context of UV stress, and hence the effect of HSP70 melanin production suppression is maximized resulting in hypopigmentation.

Another prominent example of UBE3A's interacting partner directly being involved in pigment regulation is the E3 ligase called HERC2. The interaction indicates that HERC2 stimulates UBE3A ubiquitin-protein ligase activity in vivo (154). HERC2 is also regarded to play a role in iris color determination (155,156). Interestingly HERC2 was shown to interact with both MC1R and OCA2 as well in determination of skin color (148). This displays the complex gene-gene interaction network that is responsible for proper expression and regulation in determining human complex traits (157,158). After all, pigmentation is assumed to be under the

control of at least 120 genes (111). In addition, *HERC2* is located upstream of *OCA2* and approximately 3 Mb from *UBE3A*, all three lying within the deletion hot spot of AS. After the identification of responsible genes, the next step is to elucidate the fine detailed mechanism/s on how their interaction spatially and temporally controls the variation of the pigmentation traits. This contributes not just pharmaceutically to AS or melanoma management, but may also have potential cosmetic applications.

## 5.3: Novel Transcriptional Regulation Target of UBE3A: The Melanocortin-1-Receptor (*MC1R*)

This report shows that alteration of Ube3a level affects *Mc1r* expression and that UBE3A is physically associated with the *MC1R* promoter and regulates its activity in a dosage dependent manner. The induction of the promoter activity does not seem to require UBE3A ligase function, suggesting that the co-activator domain of UBE3A, previously mapped along amino acids 170 and 680, may be responsible. Studies had shown that UBE3A interacts with, and co-activates, steroid receptor transactivites using this co-activation domain on other gene promoters to regulate transcription. For instance, UBE3A was shown to be associated with the p300-CBP/SRC-1 complex along the estrogen-responsive *pS2* promoter in vivo, illustrating its role in regulating hormone-dependent gene expression (159).

Identifying the region that UBE3A exerts it effect along the *MC1R* promoter is important to scrutinize its role in regulating *MC1R* expression. This study shows that *Ube3a* physically associates with the mouse *Mc1r* promoter in a region that is highly homologous to the human *MC1R* minimal promoter which contains a conserved E box element. This E box element was shown to be functional in mouse and human through gel shift assay (133). It was shown that a basic helix-loop-helix

leucine zipper dimeric transcription factor called MITF influences *Mc1r* promoter at this E box (133). Recent report showed that UBE3A exploits the E box element to transactivate gene transcription, such as in the case of the activation of the *hTERT* gene promoter by UBE3A in the presence of the HPV E6 protein (102). Hence, UBE3A is likely to play a similar role along the *MC1R* promoter via the E box. Immediately adjacent to this E box along the *MC1R* minimal promoter is a functional human SP1 (160). SP1 is believed to stabilize initiation complex and multi-component transcriptional factor II D (TFIID) complex. This is even more important in a TATA-less gene promoter, such as in the MC1R promoter, where co-activator was shown to play an important role together with SP1, probably in replacing the TATA box and function to tether the transcription initiation factors (161). Since promoter regulation is usually a complex system that consists of complex combination of protein recruited at a specific time to achieve temporal and spatial control, the role of UBE3A in the *MC1R* promoter, and whether it works in concert with MITF and/or SP1, requires further clarification. In addition, it was suggested that TATA-less promoter are a common characteristic among a group of G-protein coupled receptor promoters including MC1R, D1/D2/D5 dopaminergic receptors, and 5HT1a, 5HT1c and 5HT2a serotonin receptors. Interestingly, our gene profiling of the AS mouse cerebellum shows that lack of maternal UBE3A expression can cause a down-regulation of *Mc1r*, D2 dopaminergic receptor (*Drd2*) and 5HT2a serotonin receptor (*5HT2a*). Hence it is

likely that UBE3A may also regulate these receptors in a manner similar to the way UBE3A regulates *MC1R* promoter as described.

Other than the E box and the SP1 binding sites, the 5' flanking region along the human MC1R promoter region also contains other consensus regulatory elements such as the AP-1 and AP-2 sites (160). These sites in which the mammalian transcription factor, Activator protein-1/2, binds have not been experimentally proven functional on the *MC1R* promoter. The search for such known cis-binding motifs is usually identified via computational methods, such as the TRANSFAC database (162-164). However, these motifs in which transcription factors bind are usually short 6-10 nucleotide sequences, resulting in rather high false-positive identification rates. In addition, many DNA binding proteins have not yet had their cognate DNA binding sequence fully characterized. Therefore there is much to be explored pertaining to the regulation of the *MC1R* promoter and our observation demonstrates how non-DNA binding UBE3A protein can participate in this regulation.

## 5.4: UBE3A: The multi-functional role

Since the initial discovery and cloning of UBE3A more than a decade ago, tremendous numbers of reports on its cellular role has been documented. The areas of study include its conventional role as an E3 ligase, in search of ubiquitination mediated proteosomal degradation targets and its consequences. However in recent years, more studies have unraveled the unorthodox role of UBE3A, showing how it acts diversely as a coactivator for transcription regulation, such as those described in this report, and its suggested role in monoubiquitination of protein for non-proteosomal degradational purposes. This reinforces the relevance of studying UBE3A with respect to its multifunctional cellular importance.

UBE3A was first discovered as an E3 ligase that ubiquitinates the oncogene p53 for unscheduled degradation when interacting with the E6 oncoprotein of the human papillomaviruses, resulting in carcinogenesis (1). Naturally from then on, many non-pathogen related studies have focused on its ubiquitin ligase associated processes. This has produced many high impact findings including the ubiquitination of the polycomb protein Ring1B which modifies nucleosomal histone H2A, as well as the synaptic protein Arc which acts on the internalization of AMPA subtype of glutamate receptors. These findings are highly regarded for their implications towards the pathogenesis of AS (82,83). In addition, data also

suggests that UBE3A can target itself for autoubiquitination proteosomal degradation that occurs in cis and requires UBE3A-UBE3A interaction (165). More interestingly shown in the drosophila, endogenous Dube3a can ubiquitinates ectopically expressed Dube3a (i.e. Dube3a-C/A) in vivo (166). All these examples show the importance of the cellular contribution of the E3 ligase activity and that the conventional direction of studying UBE3A for its E3 ligase implications is still very relevant.

However in recent years, more reports have surfaced indicating the non-ubiquitination role of UBE3A. The first report of a non-ubiquitination associated role of UBE3A was described by Nawaz et al in 1999, after the observation of its ability to coactivate steroid receptors that may potentially have an effect on the expression of other genes (75). However, few subsequent reports have been available to support the idea of an E3 ligase independent role of UBE3A, until recent years. For instance, Ube3a has been reported to regulate the synthesis of monamines via increasing GTP cyclohydrolase I activity that works on a non-ubiquitin ligase mechanism in Drosophila (166). This conclusion coincides with our observation in this report such that UBE3A is able to regulate *MC1R* promoter activity that does not depend on the UBE3A ligase catalytic domain, suggesting that the effect is attributed to the transcriptional coactivation function of UBE3A.

This opens up a new research area, both structurally and biochemically, on the characteristics of the UBE3A protein and the genes that are associated with it.

Another non-proteosomal degradation related role of UBE3A involves the mono-ubiquitination of its targets. It was suggested that the mono-ubiquitination by UBE3A may be associated with the trafficking of synaptic proteins (78,167). It is not clear if the transfer of such ubiquitination involves the same critical residue (i.e. cysteine on the 883$^{rd}$ amino acid), hence suggesting that other important residues may have yet to be discovered. This has an impact on the pathogenesis of diseases like AS, in particularly those of type IV patients (those with *UBE3A* mutations) who show a wide spectrum of mutations across the gene. Accompanying the mutation spectrum is a diverse clinical phenotype of different severity, hence highlighting the need to identify other important domains/residues of the protein.

Other ubiquitin protein E3 ligases that function via a non-ubiquitin ligase dependent mechanism have also been reported. A good example, associated with our protein of interest (i.e. UBE3A,) is a giant protein called the HERC2, another E3 ligase which is also a member of the HECT domain subfamily of E3 ligases, like UBE3A. Interestingly in 2011, Kuhnle et al. reported the physical functional interaction between UBE3A and HERC2 (154). This interaction initiates HERC2 to stimulate the ubiquitin protein ligase activity of UBE3A (154). Importantly, this

process does not depend on the ubiquitin protein ligase activity of HERC2 (154). This strongly supports the multi-functional role of these proteins and hence the need to study potential domains in greater detail. In the case of UBE3A, other than the HECT domain at the C-terminal which is responsible for the E3 ligase activity, the N –terminal contains the previously identified coactivation domain (75). What should be emphasized is that there are three known isoforms of UBE3A generated by differential splicing differing at their N-terminal, but currently no information is available with regards to their unique properties or function. Hence, a closer comparison of the three isoforms and their individual functions, in particularly the differences in their N-termini will reveal more specifically the finer characteristics of the protein.

# Chapter VI: Conclusion

Screening and identification of differentially expressed genes in the AS mice will contribute to the repertoire of knowledge on UBE3A functions, as well as providing a basis for potential genotype-phenotype correlationship and their relevant mechanism/s. The link between UBE3A, MC1R and pigment regulation described in this report is an example of how the information gathered from gene expression profiling can be applied to explain certain disease traits. Establishing the mechanism that describes how UBE3A influences *MC1R* promoter through its coactivation function can provide relief towards the controversy of the AS hypopigmentation phenotype.

Altogether, a genome-wide gene profiling of the AS *Ube3a*$^{(m-/p+)}$ mouse was performed and confirm the differential expression status through a battery of validation including RNAi knockdown and overexpression assays. Pathway analysis shows that these differentially expressed genes are involved in three major networks including cell signaling, nervous system development and cell death. Focusing on the validated *Mc1r* gene, the mechanistic relationship between Ube3a and *Mc1r* expression was further characterized. Ube3a was shown to physically reside and transactivate the *Mc1r* promoter, which does not require Ube3a

ubiquitin ligase function. Transactivation of the *Mc1r* promoter by UBE3A was demonstrated to be dependent on the E box and SP1 response element along the *MC1R* minimal promoter.

I hope that the molecular data gathered in this report can eventually contribute towards the improvement in AS clinical management and a general better appreciation of UBE3A cellular function.

# Chapter VII: Publications

***Low D***, Chen KS: Genome-wide gene expression profiling of the Angelman syndrome mice with *Ube3a* mutation. *European Journal of Human Genetics*. 2010 Nov; 18(11):1228-35

***Low D***, Chen KS: UBE3A regulates MC1R Expression: A link to hypopigmentation in Angelman syndrome. *Pigment Cell & Melanoma Research*. 2011 Oct; 24(5): 944-52

Poster Presentation at the 3rd Korea-Singapore International Conference on Bioscience and Biotechnology

# Chapter VIII: References


1. Scheffner, M., Huibregtse, J.M., Vierstra, R.D. and Howley, P.M. (1993) The Hpv-16 E6 and E6-Ap Complex Functions as a Ubiquitin-Protein Ligase in the Ubiquitination of P53. *Cell*, **75**, 495-505.
2. Kishino, T., Lalande, M. and Wagstaff, J. (1997) UBE3A/E6-AP mutations cause Angelman syndrome. *Nature Genetics*, **15**, 70-73.
3. Ciechanover, A. and Brundin, P. (2003) The ubiquitin proteasome system in neurodegenerative diseases: Sometimes the chicken, sometimes the egg. *Neuron*, **40**, 427-446.
4. Albrecht, U., Sutcliffe, J.S., Cattanach, B.M., Beechey, C.V., Armstrong, D., Eichele, G. and Beaudet, A.L. (1997) Imprinted expression of the murine Angelman syndrome gene, Ube3a, in hippocampal and Purkinje neurons. *Nature Genetics*, **17**, 75-78.
5. Wu, S.C. and Zhang, Y. (2010) Active DNA demethylation: many roads lead to Rome. *Nature Reviews Molecular Cell Biology*, **11**, 607-620.
6. Landers, M., Bancescu, D.L., Le Meur, E., Rougeulle, C., Glatt-Deeley, H., Brannan, C., Muscatelli, F. and Lalande, M. (2004) Regulation of the large (similar to 1000 kb) imprinted murine Ube3a antisense transcript by alternative exons upstream of Snurf/Snrpn. *Nucleic Acids Research*, **32**, 3480-3492.
7. Steffenburg, S., Gillberg, C.L., Steffenburg, U. and Kyllerman, M. (1996) Autism in Angelman syndrome: A population-based study. *Pediatric Neurology*, **14**, 131-136.
8. Petersen, M.B., Brondumnielsen, K., Hansen, L.K. and Wulff, K. (1995) Clinical, cytogenetic, and molecular diagnosis of Angelman syndrome: estimated prevalence rate in a Danish county. *American Journal of Medical Genetics*, **60**, 261-262.
9. Thomson, A.K., Glasson, E.J. and Bittles, A.H. (2006) A long-term population-based clinical and morbidity profile of Angelman syndrome in Western Australia: 1953-2003. *Disability and Rehabilitation*, **28**, 299-305.
10. Williams, C.A., Beaudet, A.L., Clayton-Smith, J., Knoll, J.H., Kyllerman, M., Laan, L.A., Magenis, R.E., Moncla, A., Schinzel, A.A., Summers, J.A. *et al.* (2006) Angelman syndrome 2005: Updated consensus for diagnostic criteria. *American Journal of Medical Genetics Part A*, **140A**, 413-418.
11. Pelc, K., Boyd, S.G., Cheron, G. and Dan, B. (2008) Epilepsy in Angelman syndrome. *Seizure-European Journal of Epilepsy*, **17**, 211-217.
12. Thibert, R.L., Conant, K.D., Braun, E.K., Bruno, P., Said, R.R., Nespeca, M.P. and Thiele, E.A. (2009) Epilepsy in Angelman syndrome: A

questionnaire-based assessment of the natural history and current treatment options. *Epilepsia*, **50**, 2369-2376.

13. King, R.A., Wiesner, G.L., Townsend, D. and White, J.G. (1993) Hypopigmentation in Angelman syndrome. *American Journal of Medical Genetics*, **46**, 40-44.
14. Angelman, H. (1965) 'Puppet' children: a report on three cases. *Developmental Medicine & Child Neurology* **7**, 681-688.
15. Boyd, S.G., Harden, A. and Patton, M.A. (1988) The EEG in early diagnosis of the Angelman (Happy Puppet) syndrome). *European Journal of Pediatrics*, **147**, 508-513.
16. Rubin, D.I., Patterson, M.C., Westmoreland, B.F. and Klass, D.W. (1997) Angelman's syndrome: Clinical and electroencephalographic findings. *Electroencephalography and Clinical Neurophysiology*, **102**, 299-302.
17. Korff, C.M., Kelley, K.R. and Nordli, D.R. (2005) Notched delta, phenotype, and Angelman syndrome. *Journal of Clinical Neurophysiology*, **22**, 238-243.
18. Sandanam, T., Beange, H., Robson, L., Woolnough, H., Buchholz, T. and Smith, A. (1997) Manifestations in institutionalised adults with Angelman syndrome due to deletion. *American Journal of Medical Genetics*, **70**, 415-420.
19. Van Buggenhout, G., Descheemaeker, M.J., Thiry, P., Trommelen, J.C.M., Hamel, B.C.J. and Fryns, J.P. (2000) Angelman syndrome in three adult patients with atypical presentation and severe neurological complications. *Genetic Counseling*, **11**, 363-373.
20. Dan, B. and Boyd, S.G. (2003) Angelman syndrome reviewed from a neurophysiological perspective. The UBE3A-GABRB3 hypothesis. *Neuropediatrics*, **34**, 169-176.
21. Harting, I., Seitz, A., Rating, D., Sartor, K., Zschocke, J., Janssen, B., Ebinger, F. and Wolf, N.I. (2009) Abnormal myelination in Angelman syndrome. *European Journal of Paediatric Neurology*, **13**, 271-276.
22. Jiang, Y.H., Armstrong, D., Albrecht, U., Atkins, C.M., Noebels, J.L., Eichele, G., Sweatt, J.D. and Beaudet, A.L. (1998) Mutation of the angelman ubiquitin ligase in mice causes increased cytoplasmic p53 and deficits of contextual learning and long-term potentiation. *Neuron*, **21**, 799-811.
23. King, R.A., Wiesner, G.L., Townsend, D. and White, J.G. (1991), *2nd North American Conf on Angelman Syndrome*, Orlando, Fl, pp. 40-44.
24. Peters, S.U., Bird, L.M., Kimonis, V., Glaze, D.G., Shinawi, U.M., Bichell, T.J., Barbieri-Welge, R., Nespeca, M., Anselm, I., Waisbren, S. *et al.* Double-Blind Therapeutic Trial in Angelman Syndrome Using Betaine and Folic Acid. *American Journal of Medical Genetics Part A*, **152A**, 1994-2001.

25. Williams, C. and Franco, L. (2009) Angelman syndrome at the synapse: meeting report of the Angelman Syndrome Foundation's 2009 scientific symposium. *Journal of Child Neurology*, **25**, 254-261.
26. Clayton-Smith, J. and Laan, L. (2003) Angelman syndrome: a review of the clinical and genetic aspects. *Journal of Medical Genetics*, **40**, 87-95.
27. Knoll, J.H.M., Nicholls, R.D., Magenis, R.E., Graham, J.M., Lalande, M. and Latt, S.A. (1989) Angelman and Prader-Willi syndromes share a common chromosome-15 deletion but differ in parental origin of the deletion. *American Journal of Medical Genetics*, **32**, 285-290.
28. Pujana, M.A., Nadal, M., Guitart, M., Armengol, L., Gratacos, M. and Estivill, X. (2002) Human chromosome 15q11-q14 regions of rearrangements contain clusters of LCR15 duplicons. *European Journal of Human Genetics*, **10**, 26-35.
29. Lossie, A.C., Whitney, M.M., Amidon, D., Dong, H.J., Chen, P., Theriaque, D., Hutson, A., Nicholls, R.D., Zori, R.T., Williams, C.A. *et al.* (2001) Distinct phenotypes distinguish the molecular classes of Angelman syndrome. *Journal of Medical Genetics*, **38**, 834-845.
30. Nicholls, R.D., Pai, G.S., Khan, T.A. and Gottlieb, W. (1991) Paternal uniparental disomy in Angelman syndrome. *American Journal of Human Genetics*, **49**, 281-281.
31. Buiting, K., Saitoh, S., Gross, S., Dittrich, B., Schwartz, S., Nicholls, R.D. and Horsthemke, B. (1995) Inherited microdeletions in the Angelman and Prader-Willi syndrome define an imprinting center on human chromosome 15. *Nature Genetics*, **9**, 395-400.
32. Chamberlain, S.J. and Lalande, M. (2010) Angelman Syndrome, a Genomic Imprinting Disorder of the Brain. *Journal of Neuroscience*, **30**, 9958-9963.
33. Buiting, K. (2010) Prader-Willi Syndrome and Angelman Syndrome. *American Journal of Medical Genetics Part C-Seminars in Medical Genetics*, **154C**, 365-376.
34. Bielinska, B., Blaydes, S.M., Buiting, K., Yang, T., Krajewska-Walasek, M., Horsthemke, B. and Brannan, C.I. (2000) De novo deletions of SNRPN exon 1 in early human and mouse embryos result in a paternal to maternal imprint switch. *Nature Genetics*, **25**, 74-78.
35. El-Maarri, O., Buiting, K., Peery, E., Kroisel, P.M., Balaban, B.W., K. Urman, B., Heyd, J., Lich, C.B., C.I., Walter, J. and Horsthemke, B. (2001) Maternal methylation imprints on human chromosome 15 are established during or after fertilization. *Nature Genetics*, **27**, 341-344.
36. Malzac, P., Webber, H., Moncla, A., Graham, J.M., Kukolich, M., Williams, C., Pagon, R.A., Ramsdell, L.A., Kishino, T. and Wagstaff, J. (1998) Mutation analysis of UBE3A in Angelman syndrome patients. *American Journal of Human Genetics*, **62**, 1353-1360.

37. Fang, P., Lev-Lehman, E., Tsai, T.F., Matsuura, T., Benton, C.S., Sutcliffe, J.S., Christian, S.L., Kubota, T., Halley, D.J., Meijers-Heijboer, H. *et al.* (1999) The spectrum of mutations in UBE3A causing Angelman syndrome. *Human Molecular Genetics*, **8**, 129-135.
38. Huang, L., Kinnucan, E., Wang, G.L., Beaudenon, S., Howley, P.M., Huibregtse, J.M. and Pavletich, N.P. (1999) Structure of an E6AP-UbcH7 complex: Insights into ubiquitination by the E2-E3 enzyme cascade. *Science*, **286**, 1321-1326.
39. Bottani, A., Robinson, W.P., Delozierblanchet, C.D., Engel, E., Morris, M.A., Schmitt, B., Thunhohenstein, L. and Schinzel, A. (1994) Angelman syndrome due to paternal uniparental disomy of chromosome 15- A milder phenotype. *American Journal of Medical Genetics*, **51**, 35-40.
40. Varela, M.C., Kok, F., Otto, P.A. and Koiffmann, C.P. (2004) Phenotypic variability in Angelman syndrome: comparison among different deletion classes and between deletion and UPD subjects. *European Journal of Human Genetics*, **12**, 987-992.
41. Gillessen-Kaesbach, G., Demuth, S., Thiele, H., Theile, U., Lich, C. and Horsthemke, B. (1999) A previously unrecognised phenotype characterised by obesity, muscular hypotonia, and ability to speak in patients with Angelman syndrome caused by an imprinting defect. *European Journal of Human Genetics*, **7**, 638-644.
42. Moncla, A., Malzac, P., Livet, M.O., Voelckel, M.A., Mancini, J., Delaroziere, J.C., Philip, N. and Mattei, J.F. (1999) Angelman syndrome resulting from UBE3A mutations in 14 patients from eight families: clinical manifestations and genetic counselling. *Journal of Medical Genetics*, **36**, 554-560.
43. Fridman, C., Varela, M.C., Kok, F., Diament, A. and Koiffmann, C.P. (2000) Paternal UPD15: Further genetic and clinical studies in four Angelman syndrome patients. *American Journal of Medical Genetics*, **92**, 322-327.
44. Saitoh, S., Harada, N., Jinno, Y., Hashimoto, K., Imaizumi, K., Kuroki, Y., Fukushima, Y., Sugimoto, T., Renedo, M., Wagstaff, J. *et al.* (1994) Molecular and Clinical-Study of 61 Angelman-Syndrome Patients. *American Journal of Medical Genetics*, **52**, 158-163.
45. Wang, W., Law, H.Y. and Chong, S.S. (2009) Detection and Discrimination between Deletional and Non-Deletional Prader-Willi and Angelman Syndromes by Methylation-Specific PCR and Quantitative Melting Curve Analysis. *Journal of Molecular Diagnostics*, **11**, 446-449.
46. Horsthemke, B. and Wagstaff, J. (2008) Mechanisms of imprinting of the Prader-Willi/Angelman region. *American Journal of Medical Genetics Part A*, **146A**, 2041-2052.

47. Lalande, M. and Calciano, M.A. (2007) Molecular epigenetics of Angelman syndrome. *Cellular and Molecular Life Sciences*, **64**, 947-960.
48. Herzing, L.B.K., Kim, S.J., Cook, E.H. and Ledbetter, D.H. (2001) The human aminophospholipid-transporting ATPase gene ATP10C maps adjacent to UBE3A and exhibits similar imprinted expression. *American Journal of Human Genetics*, **68**, 1501-1505.
49. Meguro, M., Kashiwagi, A., Mitsuya, K., Nakao, M., Kondo, I., Saitoh, S. and Oshimura, M. (2001) A novel maternally expressed gene, ATP10C, encodes a putative aminophospholipid translocase associated with Angelman syndrome. *Nature Genetics*, **28**, 19-20.
50. El-Maarri, O., Buiting, K., Peery, E.G., Kroisel, P.M., Balaban, B., Wagner, K., Urman, B., Heyd, J., Lich, C., Brannan, C.I. *et al.* (2001) Maternal methylation imprints on human chromosome 15 are established during or after fertilization. *Nature Genetics*, **27**, 341-344.
51. Farber, C., Dittrich, B., Buiting, K. and Horsthemke, B. (1999) The chromosome 15 imprinting centre (IC) region has undergone multiple duplication events and contains an upstream exon of SNRPN that is deleted in all Angelman syndrome patients with an IC microdeletion. *Human Molecular Genetics*, **8**, 337-343.
52. Buiting, K., Gross, S., Lich, C., Gillessen-Kaesbach, G., El-Maarri, O. and Horsthemke, B. (2003) Epimutations in Prader-Willi and Angelman syndromes: A molecular study of 136 patients with an imprinting defect. *American Journal of Human Genetics*, **72**, 571-577.
53. Runte, M., Huttenhofer, A., Gross, S., Kiefmann, M., Horsthemke, B. and Buiting, K. (2001) The IC-SNURF-SNRPN transcript serves as a host for multiple small nucleolar RNA species and as an antisense RNA for UBE3A. *Human Molecular Genetics*, **10**, 2687-2700.
54. Chamberlain, S.J. and Brannan, C.I. (2001) The Prader-Willi syndrome imprinting center activates the paternally expressed murine Ube3a antisense transcript but represses paternal Ube3a. *Genomics*, **73**, 316-322.
55. Cavaille, J., Buiting, K., Kiefmann, M., Lalande, M., Brannan, C.I., Horsthemke, B., Bachellerie, J.P., Brosius, J. and Huttenhofer, A. (2000) Identification of brain-specific and imprinted small nucleolar RNA genes exhibiting an unusual genomic organization. *Proceedings of the National Academy of Sciences of the United States of America*, **97**, 14311-14316.
56. de los Santos, T., Schweizer, J., Rees, C.A. and Francke, U. (2000) Small evolutionarily conserved RNA, resembling C/D box small nucleolar RNA, is transcribed from PWCR1, a novel imprinted gene in the Prader-Willi deletion region, which is highly expressed in brain. *American Journal of Human Genetics*, **67**, 1067-1082.
57. Meguro, M., Mitsuya, K., Nomura, N., Kohda, M., Kashiwagi, A., Nishigaki, R., Yoshioka, H., Nakao, M., Oishi, M. and Oshimura, M. (2001)

Large-scale evaluation of imprinting status in the Prader-Willi syndrome region: an imprinted direct repeat cluster resembling small nucleolar RNA genes. *Human Molecular Genetics*, **10**, 383-394.

58. Herzing, L.B.K., Cook, E.H. and Ledbetter, D.H. (2002) Allele-specific expression analysis by RNA-FISH demonstrates preferential maternal expression of UBE3A and imprint maintenance within 15q11-q13 duplications. *Human Molecular Genetics*, **11**, 1707-1718.
59. Navarro, P., Pichard, S., Ciaudo, C., Avner, P. and Rougeulle, C. (2005) Tsix transcription across the Xist gene alters chromatin conformation without affecting Xist transcription: implications for X-chromosome inactivation. *Genes & Development*, **19**, 1474-1484.
60. Heard, E., Lovell-Badge, R. and Avner, P. (1999) Anti-Xistentialism. *Nature Genetics*, **21**, 343-344.
61. Lavorgna, G., Dahary, D., Lehner, B., Sorek, R., Sanderson, C.M. and Casari, G. (2004) In search of antisense. *Trends in Biochemical Sciences*, **29**, 88-94.
62. Rougeulle, C. and Heard, E. (2002) Antisense RNA in imprinting: spreading silence through Air. *Trends in Genetics*, **18**, 434-437.
63. Shibata, S. and Lee, J.T. (2004) Tsix transcription- versus RNA-based mechanisms in Xist repression and epigenetic choice. *Current Biology*, **14**, 1747-1754.
64. Chamberlain, S.J., Chen, P.F., Ng, K.Y., Bourgois-Rocha, F., Lemtiri-Chlieh, F., Levine, E.S. and Lalande, M. (2010) Induced pluripotent stem cell models of the genomic imprinting disorders Angelman and Prader-Willi syndromes. *Proceedings of the National Academy of Sciences of the United States of America*, **107**, 17668-17673.
65. Numata, K., Kohama, C., Abe, K. and Kiyosawa, H. (2010) Highly parallel SNP genotyping reveals high-resolution landscape of mono-allelic Ube3a expression associated with locus-wide antisense transcription. *Nucleic Acids Research*, **39**, 2649-2657.
66. Faghihi, M.A. and Wahlestedt, C. (2009) Regulatory roles of natural antisense transcripts. *Nature Reviews Molecular Cell Biology*, **10**, 637-643.
67. Mabb, A.M., Judson, M.C., Zylka, M.J. and Philpot, B.D. (2011) Angelman syndrome: insights into genomic imprinting and neurodevelopmental phenotypes. *Trends in Neurosciences*, **34**, 293-303.
68. Mulherkar, S.A. and Jana, N.R. (2010) Loss of dopaminergic neurons and resulting behavioural deficits in mouse model of Angelman syndrome. *Neurobiology of Disease*, **40**, 586-592.
69. Miura, K., Kishino, T., Li, E., Webber, H., Dikkes, P., Holmes, G.L. and Wagstaff, J. (2002) Neurobehavioral and electroencephalographic abnormalities in Ube3a maternal-deficient mice. *Neurobiology of Disease*, **9**, 149-159.

70. Gabriel, J.M., Merchant, M., Ohta, T., Ji, Y., Caldwell, R.G., Ramsey, M.J., Tucker, J.D., Longnecker, R. and Nicholls, R.D. (1999) A transgene insertion creating a heritable chromosome deletion mouse model of Prader-Willi and Angelman syndromes. *Proceedings of the National Academy of Sciences of the United States of America*, **96**, 9258-9263.
71. Jiang, Y.H., Pan, Y.Z., Zhu, L., Landa, L., Yoo, J., Spencer, C., Lorenzo, I., Brilliant, M., Noebels, J. and Beaudet, A.L. (2010) Altered Ultrasonic Vocalization and Impaired Learning and Memory in Angelman Syndrome Mouse Model with a Large Maternal Deletion from Ube3a to Gabrb3. *Plos One*, **5**.
72. Wu, M.Y., Chen, K.S., Bressler, J., Hou, A.H., Tsai, T.F. and Beaudet, A.L. (2006) Mouse imprinting defect mutations that model Angelman syndrome. *Genesis*, **44**, 12-22.
73. Wu, Y., Bolduc, F.V., Bell, K., Tully, T., Fang, Y., Sehgal, A. and Fischer, J.A. (2008) A Drosophila model for Angelman syndrome. *Proceedings of the National Academy of Sciences of the United States of America*, **105**, 12399-12404.
74. Lu, Y.B., Wang, F., Li, Y., Ferris, J., Lee, J.A. and Gao, F.B. (2009) The Drosophila homologue of the Angelman syndrome ubiquitin ligase regulates the formation of terminal dendritic branches. *Human Molecular Genetics*, **18**, 454-462.
75. Nawaz, Z., Lonard, D.H., Smith, C.L., Lev-Lehman, E., Tsai, S.Y., Tsai, M.J. and O'Malley, B.W. (1999) The Angelman syndrome-associated protein, E6-AP, is a coactivator for the nuclear hormone receptor superfamily. *Molecular and Cellular Biology*, **19**, 1182-1189.
76. Hershko, A. and Ciechanover, A. (1998) The ubiquitin system. *Annual Review of Biochemistry*, **67**, 425-479.
77. Dindot, S.V., Antalffy, B.A., Bhattacharjee, M.B. and Beaudet, A.L. (2008) The Angelman syndrome ubiquitin ligase localizes to the synapse and nucleus, and maternal deficiency results in abnormal dendritic spine morphology. *Human Molecular Genetics*, **17**, 111-118.
78. Haas, K.F. and Broadie, K. (2008) Roles of ubiquitination at the synapse. *Biochimica Et Biophysica Acta-Gene Regulatory Mechanisms*, **1779**, 495-506.
79. Smith, C.L., DeVera, D.G., Lamb, D.J., Nawaz, Z., Jiang, Y.H., Beaudet, A.L. and O'Malley, B.W. (2002) Genetic ablation of the steroid receptor coactivator-ubiquitin ligase, E6-AP, results in tissue-selective steroid hormone resistance and defects in reproduction. *Molecular and Cellular Biology*, **22**, 525-535.
80. Khan, O.Y., Fu, G.L., Ismail, A., Srinivasan, S., Cao, X.N., Tu, Y.P., Lu, S. and Nawaz, Z. (2006) Multifunction steroid receptor coactivator, E6-

associated protein, is involved in development of the prostate gland. *Molecular Endocrinology*, **20**, 544-559.

81. Shai, A., Pitot, H.C. and Lambert, P.F. (2010) E6-Associated Protein Is Required for Human Papillomavirus Type 16 E6 to Cause Cervical Cancer in Mice. *Cancer Research*, **70**, 5064-5073.
82. Zaaroor-Regev, D., de Bie, P., Scheffner, M., Noy, T., Shemer, R., Heled, M., Stein, I., Pikarsky, E. and Ciechanover, A. (2010) Regulation of the polycomb protein Ring1B by self-ubiquitination or by E6-AP may have implications to the pathogenesis of Angelman syndrome. *Proceedings of the National Academy of Sciences of the United States of America*, **107**, 6788-6793.
83. Greer, P.L., Hanayama, R., Bloodgood, B.L., Mardinly, A.R., Lipton, D.M., Flavell, S.W., Kim, T.K., Griffith, E.C., Waldon, Z., Maehr, R. *et al.* (2010) The Angelman Syndrome Protein Ube3A Regulates Synapse Development by Ubiquitinating Arc. *Cell*, **140**, 704-716.
84. Nasu, J., Murakami, K., Miyagawa, S., Yamashita, R., Ichimura, T., Wakita, T., Hotta, H., Miyamura, T., Suzuki, T., Satoh, T. *et al.* (2010) E6AP Ubiquitin Ligase Mediates Ubiquitin-Dependent Degradation of Peroxiredoxin 1. *Journal of Cellular Biochemistry*, **111**, 676-685.
85. Mishra, A., Godavarthi, S.K. and Jana, N.R. (2009) UBE3A/E6-AP regulates cell proliferation by promoting proteasomal degradation of p27. *Neurobiology of Disease*, **36**, 26-34.
86. Louria-Hayon, I., Alsheich-Bartok, O., Levav-Cohen, Y., Silberman, I., Berger, M., Grossman, T., Matentzoglu, K., Jiang, Y.H., Muller, S., Scheffner, M. *et al.* (2009) E6AP promotes the degradation of the PML tumor suppressor. *Cell Death and Differentiation*, **16**, 1156-1166.
87. Mulherkar, S.A., Sharma, J. and Jana, N.R. (2009) The ubiquitin ligase E6-AP promotes degradation of alpha-synuclein. *Journal of Neurochemistry*, **110**, 1955-1964.
88. Mishra, A., Godavarthi, S.K., Maheshwari, M., Goswami, A. and Jana, N.R. (2009) The Ubiquitin Ligase E6-AP is induced and recruited to aggresomes in response to proteasome inhibition and may be involved in the ubiquitination of Hsp70-bound misfolded proteins. *Journal of Biological Chemistry*, **284**, 10537-10545.
89. Shimoji. T, Murakami. K, Sugiyama. Y, Matsuda. M, Inubushi. S, Nasu, J., Shirakura. M,, Suzuki. T, Wakita. T, Kishino. T, Hotta. H *et al.* (2009) Identification of annexin A1 as a novel substrate for E6AP-mediated ubiquitylation. *Journal of Cellular Biochemistry*, **106**, 1123-1135.
90. Zheng, L., Ding, H.R., Lu, Z.M., Li, Y., Pan, Y.Q., Ning, T. and Ke, Y. (2008) E3 ubiquitin ligase E6AP-mediated TSC2 turnover in the presence and absence of HPV16 E6. *Genes to Cells*, **13**, 285-294.

91. Shirakura, M., Murakami, K., Ichimura, T., Suzuki, R., Shimoji, T., Fukuda, K., Abe, K., Sato, S., Fukasawa, M., Yamakawa, Y. *et al.* (2007) E6AP ubiquitin ligase mediates ubiquitylation and degradation of hepatitis C virus core protein. *Journal of Virology*, **81**, 1174-1185.
92. Reiter, L.T., Seagroves, T.N., Bowers, M. and Bier, E. (2006) Expression of the Rho-GEF Pbl/ECT2 is regulated by the UBE3A E3 ubiquitin ligase. *Human Molecular Genetics*, **15**, 2825-2835.
93. Nuber, U., Schwarz, S.E. and Scheffner, M. (1998) The ubiquitin-protein ligase E6-associated protein (E6-AP) serves as its own substrate. *European Journal of Biochemistry*, **254**, 643-649.
94. Kumar, S., Kao, W.H. and Howley, P.M. (1997) Physical interaction between specific E2 and Hect E3 enzymes determines functional cooperativity. *Journal of Biological Chemistry*, **272**, 13548-13554.
95. Oda, H., Kumar, S. and Howley, P.M. (1999) Regulation of the Src family tyrosine kinase Blk through E6AP-mediated ubiquitination. *Proceedings of the National Academy of Sciences of the United States of America*, **96**, 9557-9562.
96. Kumar, S., Talis, A.L. and Howley, P.M. (1999) Identification of HHR23A as a substrate for E6-associated protein-mediated ubiquitination. *Journal of Biological Chemistry*, **274**, 18785-18792.
97. Daniels, P.R., Sanders, C.M., Coulson, P. and Maitland, N.J. (1997) Molecular analysis of the interaction between HPV type 16 E6 and human E6-associated protein. *Febs Letters*, **416**, 6-10.
98. Ramamoorthy, S. and Nawaz, Z. (2008) E6-associated protein (E6-AP) is a dual function coactivator of steroid hormone receptors. *Nuclear Receptor Signaling*, **6**.
99. Rotin, D. and Kumar, S. (2009) Physiological functions of the HECT family of ubiquitin ligases. *Nature Reviews Molecular Cell Biology*, **10**, 398-409.
100. Talis, A.L., Huibregtse, J.M. and Howley, P.M. (1998) The role of E6AP in the regulation of p53 protein levels in human papillomavirus (HPV)-positive and HPV-negative cells. *Journal of Biological Chemistry*, **273**, 6439-6445.
101. Crinelli, R., Bianchi, M., Menotta, M., Carloni, E., Giacomini, E., Pennati, M. and Magnani, M. (2008) Ubiquitin over-expression promotes E6AP autodegradation and reactivation of the p53/MDM2 pathway in HeLa cells. *Molecular and Cellular Biochemistry*, **318**, 129-145.
102. Liu, X.F., Yuan, H., Fu, B.J., Disbrow, G.L., Apolinario, T., Tomaic, V., Kelley, M.L., Baker, C.C., Huibregtse, J. and Schlegel, R. (2005) The E6AP ubiquitin ligase is required for transactivation of the hTERT promoter by the human papillomavirus E6 oncoprotein. *Journal of Biological Chemistry*, **280**, 10807-10816.

103. Yashiro, K., Riday, T.T., Condon, K.H., Roberts, A.C., Bernardo, D.R., Prakash, R., Weinberg, R.J., Ehlers, M.D. and Philpot, B.D. (2009) Ube3a is required for experience-dependent maturation of the neocortex. *Nature Neuroscience*, **12**, 777-U132.
104. Sato, M. and Stryker, M.P. (2010) Genomic imprinting of experience-dependent cortical plasticity by the ubiquitin ligase gene Ube3a. *Proceedings of the National Academy of Sciences of the United States of America*, **107**, 5611-5616.
105. Mardirossian, S., Rampon, C., Salvert, D., Fort, P. and Sarda, N. (2009) Impaired hippocampal plasticity and altered neurogenesis in adult Ube3a maternal deficient mouse model for Angelman syndrome. *Experimental Neurology*, **220**, 341-348.
106. Bischofberger, J. (2007) Young and excitable: new neurons in memory networks. *Nature Neuroscience*, **10**, 273.
107. Heck, D.H., Zhao, Y., Roy, S., LeDoux, M.S. and Reiter, L.T. (2008) Analysis of cerebellar function in Ube3a-deficient mice reveals novel genotype-specific behaviors. *Human Molecular Genetics*, **17**, 2181-2189.
108. Williams, K., Irwin, D.A., Jones, D.G. and Murphy, K.M. (2010) Dramatic loss of Ube3A expression during aging of the mammalian cortex. *Frontiers in aging neuroscience*, **2**, 1.
109. van Woerden, G.M., Harris, K.D., Hojjati, M.R., Gustin, R.M., Qiu, S.F., Freire, R.D.A., Jiang, Y.H., Elgersma, Y. and Weeber, E.J. (2007) Rescue of neurological deficits in a mouse model for Angelman syndrome by reduction of alpha CaMKII inhibitory phosphorylation. *Nature Neuroscience*, **10**, 280-282.
110. Pathak, M.A., Jimbow, K. and Fitzpatrick, T. (1980), *Phenotypic Expression in Pigment Cells*. University of Tokyo Press, pp. 655-670.
111. Bennett, D.C. and Lamoreux, M.L. (2003) The color loci of mice - A genetic century. *Pigment Cell Research*, **16**, 333-344.
112. Abdel-Malek, Z., Suzuki, I., Tada, A., Im, S. and Akcali, C. (1998) In Luger, T. A., Paus, R., Lipton, J. M. and Slominski, A. T. (eds.), *Conference on Cutaneous Neuroimmunomodulation - The Proopiomelanocortin System*, Munster, Germany, pp. 117-133.
113. Rosemblat, S., Durhampierre, D., Gardner, J.M., Nakatsu, Y., Brilliant, M.H. and Orlow, S.J. (1994) Identification of a melanosome membrane protein encoded by the pink-eyed dilution (Type II oculocutananeous albinism) gene. *Proceedings of the National Academy of Sciences of the United States of America*, **91**, 12071-12075.
114. Prota, G. (1980) Recent advances in the chemistry of melanogenesis in mammals. *Journal of Investigative Dermatology*, **75**, 122-127.

115. Mountjoy, K.G., Robbins, L.S., Mortrud, M.T. and Cone, R.D. (1992) The cloning of a family of genes that encode the Melanocortin receptors. *Science*, **257**, 1248-1251.
116. Slominski, A., Wortsman, J., Luger, T., Paus, R. and Solomon, S. (2000) Corticotropin releasing hormone and proopiomelanocortin involvement in the cutaneous response to stress. *Physiological Reviews*, **80**, 979-1020.
117. Lin, J.Y. and Fisher, D.E. (2007) Melanocyte biology and skin pigmentation. *Nature*, **445**, 843-850.
118. Garcia-Borron, J.C., Sanchez-Laorden, B.L. and Jimenez-Cervantes, C. (2005) Melanocortin-1 receptor structure and functional regulation. *Pigment Cell Research*, **18**, 393-410.
119. Rouzaud, F., Annereau, J.P., Valencia, J.C., Costin, G.E. and Hearing, V.J. (2003) Regulation of melanocortin 1 receptor expression at the mRNA and protein levels by its natural agonist and antagonist. *Faseb Journal*, **17**, 2154-+.
120. Rees, J.L. (2003) Genetics of hair and skin color. *Annual Review of Genetics*, **37**, 67-90.
121. Spritz, R.A., Bailin, T., Nicholls, R.D., Lee, S.T., Park, S.K., Mascari, M.J. and Butler, M.G. (1997) Hypopigmentation in the Prader-Willi syndrome correlates with P gene deletion but not with haplotype of the hemizygous P allele. *American Journal of Medical Genetics*, **71**, 57-62.
122. Fridman, C., Hosomi, N., Varela, M.C., Souza, A.H., Fukai, K. and Koiffmann, C.P. (2003) Angelman syndrome associated with oculocutaneous albinism due to an intragenic deletion of the P gene. *American Journal of Medical Genetics Part A*, **119A**, 180-183.
123. Saitoh, S., Oiso, N., Wada, T., Narazaki, O. and Fukai, K. (2000) Oculocutaneous albinism type 2 with a P gene missense mutation in a patient with Angelman syndrome. *Journal of Medical Genetics*, **37**, 392-394.
124. Ravid, K. and Freshney, R.I. (1998), *DNA Transfer to Cultured Cells*, pp. 111-124.
125. Saucedo-Cardenas, O., Quintana-Hau, J.D., Le, W.D., Smidt, M.P., Cox, J.J., DeMayo, F., Burbach, J.P.H. and Conneely, O.M. (1998) Nurr1 is essential for the induction of the dopaminergic phenotype and the survival of ventral mesencephalic late dopaminergic precursor neurons. *Proceedings of the National Academy of Sciences of the United States of America*, **95**, 4013-4018.
126. Apparsundaram, S., Ferguson, S.M., George, A.L. and Blakely, R.D. (2000) Molecular cloning of a human, hemicholinium-3-sensitive choline transporter. *Biochemical and Biophysical Research Communications*, **276**, 862-867.

127. Yue, Y., Chen, Z.Y., Gale, N.W., Blair-Flynn, J., Hu, T.J., Yue, X., Cooper, M., Crockett, D.P., Yancopoulos, G.D., Tessarollo, L. *et al.* (2002) Mistargeting hippocampal axons by expression of a truncated Eph receptor. *Proceedings of the National Academy of Sciences of the United States of America*, **99**, 10777-10782.
128. Smith, A.G., Luk, N., Newton, R.A., Roberts, D.W., Sturm, R.A. and Muscat, G.E.O. (2008) Melanocortin-1 receptor signaling markedly induces the expression of the NR4A nuclear receptor subgroup in melanocytic cells. *Journal of Biological Chemistry*, **283**, 12564-12570.
129. Low, D. and Chen, K.S. (2010) Genome-wide gene expression profiling of the Angelman syndrome mice with Ube3a mutation. *European Journal of Human Genetics*, **18**, 1228-1235.
130. Huibregtse, J.M., Scheffner, M., Beaudenon, S. and Howley, P.M. (1995) A family of proteins structurally and functionally related to the E6-AP ubiquitin protein ligase. *Proceedings of the National Academy of Sciences of the United States of America*, **92**, 2563-2567.
131. Scheffner, M., Nuber, U. and Huibregtse, J.M. (1995) Protein ubiquitination involving an E1-E2-E3 enzyme ubiquitin thioester cascade. *Nature*, **373**, 81-83.
132. Moro, O., Ideta, R. and Ifuku, O. (1999) Characterization of the promoter region of the human melanocortin-l receptor(MC1R) gene. *Biochemical and Biophysical Research Communications*, **262**, 452-460.
133. Adachi, S., Morii, E., Kim, D.K., Ogihara, H., Jippo, T., Ito, A., Lee, Y.M. and Kitamura, Y. (2000) Involvement of mi-transcription factor in expression of alpha-melanocyte-stimulating hormone receptor in cultured mast cells of mice. *Journal of Immunology*, **164**, 855-860.
134. Aoki, H. and Moro, O. (2002) Involvement of microphthalmia-associated transcription factor (MITF) in expression of human melanocortin-1 receptor (MC1R). *Life Sciences*, **71**, 2171-2179.
135. Quevedo, W.C. and Holstein, T.J. (1998) *General biology of mammalian pigmentation*. Oxford University Press.
136. Colosi, D.C., Martin, D., More, K. and Lalande, M. (2006) Genomic organization and allelic expression of UBE3A in chicken. *Gene*, **383**, 93-98.
137. Kirstein, L. and Silfverskiold, B.P. (1958) A Family with Emotionally Precipitated Drop Seizures. *Acta Psychiatrica Et Neurologica*, **33**, 471-476.
138. Chahrour, M., Jung, S.Y., Shaw, C., Zhou, X.B., Wong, S.T.C., Qin, J. and Zoghbi, H.Y. (2008) MeCP2, a key contributor to neurological disease, activates and represses transcription. *Science*, **320**, 1224-1229.
139. Urdinguio, R.G., Lopez-Serra, L., Lopez-Nieva, P., Alaminos, M., Diaz-Uriarte, R., Fernandez, A.F. and Esteller, M. (2008) Mecp2-Null Mice Provide New Neuronal Targets for Rett Syndrome. *Plos One*, **3**.

140. Colon-Cesario, W.I., Martinez-Montemayor, M.M., Morales, S., Felix, J., Cruz, J., Adorno, M., Pereira, L., Colon, N., Maldonado-Vlaar, C.S. and de Ortiz, S.P. (2006) Knockdown of Nurr1 in the rat hippocampus: Implications to spatial discrimination learning and memory. *Learning & Memory*, **13**, 734-744.
141. de Ortiz, S.P., Maldonado-Vlaar, C.S. and Carrasquillo, Y. (2000) Hippocampal expression of the orphan nuclear receptor gene hzf-3/nurr1 during spatial discrimination learning. *Neurobiology of Learning and Memory*, **74**, 161-178.
142. Kitagawa, H., Ray, W.J., Glantschnig, H., Nantermet, P.V., Yu, Y.J., Leu, C.T., Harada, S.I., Kato, S. and Freedman, L.P. (2007) A regulatory circuit mediating convergence between Nurr1 transcriptional regulation and Wnt signalingv. *Molecular and Cellular Biology*, **27**, 7486-7496.
143. Jiang, C.T., Wan, X.H., He, Y., Pan, T.H., Jankovic, J. and Le, W.D. (2005) Age-dependent dopaminergic dysfunction in Nurr1 knockout mice. *Experimental Neurology*, **191**, 154-162.
144. Moore, D.J. (2006) Parkin: a multifaceted ubiquitin ligase. *Biochemical Society Transactions*, **34**, 749-753.
145. Catania, A. (2008) Neuroprotective actions of melanocortins: a therapeutic opportunity. *Trends in Neurosciences*, **31**, 353-360.
146. Nicolaus, B.J.R. (2005) A critical review of the function of neuromelanin and an attempt to provide a unified theory. *Medical Hypotheses*, **65**, 791-796.
147. King, R.A., Willaert, R.K., Schmidt, R.M., Pietsch, J., Savage, S., Brott, M.J., Fryer, J.P., Summers, C.G. and Oetting, W.S. (2003) MC1R mutations modify the classic phenotype of oculocutaneous albinism type 2 (OCA2). *American Journal of Human Genetics*, **73**, 638-645.
148. Branicki, W., Brudnik, U. and Wojas-Pelc, A. (2009) Interactions Between HERC2, OCA2 and MC1R May Influence Human Pigmentation Phenotype. *Annals of Human Genetics*, **73**, 160-170.
149. Busca, R. and Ballotti, R. (2000) Cyclic AMP a key messenger in the regulation of skin pigmentation. *Pigment Cell Research*, **13**, 60-69.
150. Edwards, E.K., Frank, B.L. and Rosen, L.B. (1986) The effect of an ultraprotective sunscreen on Langerhans cell alteration induced by ultraviolet-light in human skin. *International Journal of Dermatology*, **25**, 327-329.
151. Hoshino, T., Matsuda, M., Yamashita, Y., Takehara, M., Fukuya, M., Mineda, K., Maji, D., Ihn, H., Adachi, H., Sobue, G. *et al.* (2010) Suppression of Melanin Production by Expression of HSP70. *Journal of Biological Chemistry*, **285**, 13254-13263.
152. Morris, S.D. (2002) Heat shock proteins and the skin. *Clinical and Experimental Dermatology*, **27**, 220-224.

153. Yanase, S. and Ishi, N. (1999) Cloning of the oxidative stress-responsive genes in Caenorhabditis elegans. *Journal of Radiation Research*, **40**, 39-47.
154. Kuehnle, S., Kogel, U., Glockzin, S., Marquardt, A., Ciechanover, A., Matentzoglu, K. and Scheffner, M. (2011) Physical and Functional Interaction of the HECT Ubiquitin-protein Ligases E6AP and HERC2. *Journal of Biological Chemistry*, **286**, 19410-19416.
155. Kayser, M., Liu, F., Janssens, A., Rivadeneira, F., Lao, O., van Duijn, K., Vermeulen, M., Arp, P., Jhamai, M.M., van Ijcken, W.F.J. *et al.* (2008) Three genome-wide association studies and a linkage analysis identify HERC2 as a human iris color gene. *American Journal of Human Genetics*, **82**, 411-423.
156. Sturm, R.A., Duffy, D.L., Zhao, Z.Z., Leite, F.P.N., Stark, M.S., Hayward, N.K., Martin, N.G. and Montgomery, G.W. (2008) A single SNP in an evolutionary conserved region within intron 86 of the HERC2 gene determines human blue-brown eye color. *American Journal of Human Genetics*, **82**, 424-431.
157. Moore, J.H. (2003) The ubiquitous nature of epistasis in determining susceptibility to common human diseases. *Human Heredity*, **56**, 73-82.
158. Carlborg, O. and Haley, C.S. (2004) Epistasis: too often neglected in complex trait studies? *Nature Reviews Genetics*, **5**, 618-U614.
159. Reid, G., Hübner, M.R., Métivier, R., Brand, H., Denger, S., Manu, D., Beaudouin, J., Ellenberg, J. and Gannon, F. (2003) Cyclic, proteasome-mediated turnover of unliganded and liganded ERalpha on responsive promoters is an integral feature of estrogen signaling. *Molecular and Cell*, **3**, 695-707.
160. Moro, O., Ideta, R. and Ifuku, O. (1999) Characterization of the promoter region of the human melanocortin-1 receptor (MC1R) gene. *Biochemical and Biophysical Research Communication.* , **262**, 452-460.
161. Pugh, B.F. and Tjian, R. (1990) Mechanism of transcriptional activation by SP1 - Evidence for coactivators. *Cell*, **61**, 1187-1197.
162. Wingender, E., Dietze, P., Karas, H. and Knuppel, R. (1996) TRANSFAC: A database on transcription factors and their DNA binding sites. *Nucleic Acids Research*, **24**, 238-241.
163. Wingender, E., Kel, A.E., Kel, O.V., Karas, H., Heinemeyer, T., Dietze, P., Knuppel, R., Romaschenko, A.G. and Kolchanov, N.A. (1997) TRANSFAC, TRRD and COMPEL: Towards a federated database system on transcriptional regulation. *Nucleic Acids Research*, **25**, 265-268.
164. Pennacchio, L.A. and Rubin, E.M. (2001) Genomic strategies to identify mammalian regulatory sequences. *Nature Reviews Genetics*, **2**, 100-109.
165. Nuber, U., Schwarz, S., Kaiser, P., Schneider, R. and Scheffner, M. (1996) Cloning of human ubiquitin-conjugating enzymes UbcH6 and UbcH7 (E2-

F1) and characterization of their interaction with E6-AP and RSP5. *Journal of Biological Chemistry*, **271**, 2795-2800.

166. Ferdousy, F., Bodeen, W., Summers, K., Doherty, O., Wright, O., Elsisi, N., Hilliard, G., O'Donnell, J.M. and Reiter, L.T. (2010) Drosophila Ube3a regulates monoamine synthesis by increasing GTP cyclohydrolase I activity via a non-ubiquitin ligase mechanism. *Neurobiology of Disease*, **41**, 669-677.
167. Hicke, L. (2001) Protein regulation by monoubiquitin. *Nature Reviews Molecular Cell Biology*, **2**, 195-201.